UNCLASSIFIED

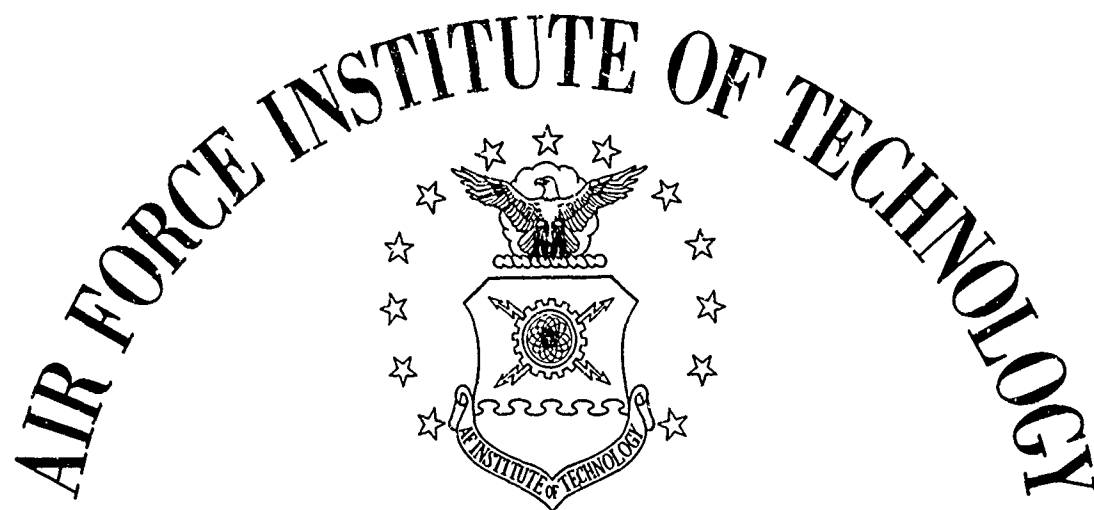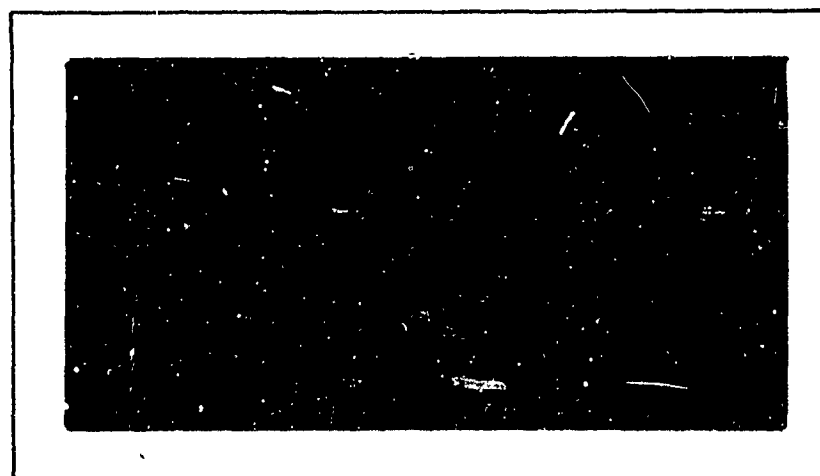## AD NUMBER

AD860095

NEW LIMITATION CHANGE

TO

Approved for public release, distribution
unlimited

FROM

Distribution authorized to U.S. Gov't.
agencies and their contractors; Critical
Technology; JUN 1969. Other requests shall
be referred to Air Force Institute of
Technology, AFIT-SE, Wright-Patterson AFB,
OH 45433.

AUTHORITY

afit memo, 22 jul 1971

THIS PAGE IS UNCLASSIFIED

AD 860095

AIR FORCE INSTITUTE OF TECHNOLOGY

AIR UNIVERSITY
UNITED STATES AIR FORCE

SCHOOL OF ENGINEERING

WRIGHT—PATTERSON AIR FORCE BASE, OHIO

232

MANUAL ASTRONAUT NAVIGATION

THESIS

GA/AE/69-1

Roger C. Horrigan   Richard C. Walsh
Major   USAF   Captain   USAF

MANUAL ASTRONAUT NAVIGATION

THESIS

Presented to the Faculty of the School of Engineering
of the Air Force Institute of Technology

Air University

in Partial Fulfillment of the

Requirements for the Degree of

Master of Science

by

Roger C. Horrigan, B.S.M.E.
Major   USAF

and

Richard C. Walsh, B.S.
Captain   USAF

Graduate Astronautical Engineering

June   1969

Preface

Our original aspiration with regard to "Manual Astronaut Navigation" was to prepare a set of charts, tables, and simplified procedures the astronaut could use in solving the orbit determination problem. But we soon learned that a great deal of background theory needed development or refinement before such a flight manual approach could be justified. Our original plan of attack was therefore changed from preparing a flight manual to research and presentation of a variety of theoretical approaches to the manual space navigation problem. Our thesis more closely resembles a textbook approach rather than the originally intended flight manual.

We have incorporated and presented the theoretical development of a number of topics applicable to the problem of "Manual Space Navigation." We claim no truly original ideas or significant "breakthroughs." In fact, most of the concepts we have built upon have been known for centuries. Only recently, though, has man found himself making observations from the vehicle for which the orbit is desired. In the past, the observation point has been rigidly constrained to the surface of the earth. With the new and exciting viewpoint, many of the classical orbit determination methods assume new and interesting possibilities. We hope our research points out some of the many advantages the astronaut has in his position as an observer aboard the spacecraft.

GA/AE/69-1

Contents

Contents

Contents

Contents

List of Figures

List of Figures

List of Figures

List of Tables

List of Symbols

Symbol	Definition
A	Earth's angular diameter as viewed from spacecraft (degrees), or
	Earth-moon angle as viewed from the spacecraft, as specified in text (degrees).
A_{x1} through C_{z3}	Constants resulting from inversion of three-star fix equations.
B	Angle between earth-vehicle line and earth-moon line (degrees).
C	Angle between vehicle-moon line and earth-moon line (degrees).
$C_{a,r}$	Semimajor axis range error coefficient (NM/NM range error).
$C_{a,t}$	Semimajor axis timing error coefficient (NM/MIN timing error).
$C_{E,r}$	Eccentric anomaly range error coefficient (degrees/NM range error).
$C_{E,t}$	Eccentric anomaly timing error coefficient (degrees/MIN timing error).
$C_{e,r}$	Eccentricity range error coefficient (NM range error).
$C_{e,t}$	Eccentricity timing error coefficient (NM range error)$^{-1}$.
D	Angle between vehicle-star line and its projection in earth-moon-vehicle plane (degrees).
E	Eccentric Anomaly (degrees or radians) measured from perifocus or peripoint, or,
	Angle between projection of vehicle-star line and vehicle-earth line, as specified in text (degrees).
E_r	Absolute value of maximum error of the subscripted variable.

xii

Symbol	Definition
F	Hyperbolic anomaly $= \sqrt{-1}\, E$, or, Angle between vehicle-star line and vehicle-earth line, as specified in text (degrees).
$\hat{I}$	Unit vector in direction of line-of-sight to a star--geocentric equatorial coordinates.
M	Mean anomaly (degrees or radians).
P	Orbital period--alternate designation τ (units of time).
$\hat{P}, \hat{Q}, \hat{W}$	Orbital unit vectors: $\hat{P}$ directed toward perifocus, $\hat{W}$ perpendicular to orbit plane in direction of angular momentum vector, $\hat{Q}$ directed to form orthonormal set.
R	General planet radius (NM or KM).
$R_{\oplus}$	Radius of earth (NM or appropriate units).
$\dot{S}$	Magnitude of vehicle velocity vector $= \lvert \dot{\vec{r}} \rvert$ (units of $\dot{\vec{r}}$).
V	Total velocity (scalar) (NM/time unit or KM/time unit).
a	Semimajor axis (nautical miles or kilometers).
e	Eccentricity (dimensionless).
h	Altitude above surface of earth (NM).
i	Inclination of orbital plane (degrees).
$\hat{i}, \hat{j}, \hat{k}$	Unit vectors in positive x,y,z directions-- geocentric equatorial coordinate system.
k	Coefficient, as specified in text.
ℓ	Semilatus rectum (nautical miles or kilometers).
ℓ, m, n	Direction cosines with respect to x,y,z axes.
n	Mean angular velocity, or mean motion (radians/unit time).

Symbol	Definition
r	Radial distance of vehicle from center of attracting body (nautical miles or kilometers).
r_p	Perifocus, or peripoint, distance (NM or KM).
$\dot{r}$	Radial velocity of vehicle (distance unit/time unit--normally NM/MIN).
$\ddot{r}$	Radial acceleration (distance unit/time unit^2--normally NM/MIN^2).
$\bar{r}$	Vehicle position vector (geocentric equatorial coordinates).
$\hat{r}$	Vehicle unit position vector $= \bar{r}/r$.
$\dot{\bar{r}}$	Velocity vector of vehicle (NM/MIN or appropriate units).
r_x, r_y, r_z	Components of vehicle unit position vector, i.e., direction cosines of vehicle.
t	Time (sec, min, or hours), or, Time from perifocus or peripoint.
x, y, z	Geocentric equatorial coordinates--rectangular.

Greek Symbols

Symbol	Definition
Δ	Incremental change or determinate of coefficients.
ΔA	Difference between actual angle A and reference angle A (radians).
ΔB	Difference between actual angle B and reference angle B (radians).
ΔF	Difference between actual angle F and reference angle F (radians).
$\Delta H1$	Change of altitude, or range, between 1 and 2 (NM).
$\Delta H2$	Change of altitude, or range, between 2 and 3 (NM).

Symbol	Definition
Δr	Difference between an actual range and a reference range (KM).
Δt	Timing interval between altitude, or range, measurements (Minutes).
ψ	Star-earth center-vehicle angle--earth at vertex (degrees).
Ω	Longitude of ascending node (more correctly, right ascension of ascending node in geocentric equatorial coordinates)(degrees).
τ	Orbital period--alternate designation P (units of time).
α	Right ascension--geocentric equatorial coordinate system (degrees).
γ	Star-vehicle-earth horizon angle--vehicle at vertex (degrees).
δ	Declination--geocentric equatorial coordinate system (degrees).
ε	Range measurement error.
θ	True anomaly measured from perifocus (degrees or radians).
μ	Earth gravitational constant--product of universal gravitational constant and mass of the earth (62750.717 NM^3/SEC^2).
σ	Standard deviation (KM).
ω	Argument of perifocus, or peripoint (degrees).

Subscripts

1	Subscript 1,2 . . . generally denotes the order (in time). Thus, r_1 precedes r_2 in time, etc.
$\circ$	Various definitions as defined in supporting text. Denotes: perifocus, epoch, minimum.
$\oplus$	Associates variable with earth. Thus, $R_\oplus$ denotes radius of the earth.

Symbol	Definition
v	Associates variable with vehicle. Thus, α_v denotes right ascension of vehicle.
x1 through z3	Used as subscript notation for three-star fix data. x denotes that constant is used in computing r_x; 1 denotes that the constant multiplies $\cos(\gamma_1 + A/2)$.

Superscripts

3	Number without parentheses denotes exponent.
(5)	Number in parenthesis denotes order of differentiation. Thus, (5) denotes fifth derivative.
-1	Generally denotes mathematical inverse. Thus, $\sin^{-1} x$ denotes "the angle whose sine is x."

Notation

$|\ \ |$	Absolute value.
$\cdot$	Dot above variable--denotes first derivative with respect to time (two dots denote second derivative, etc.).
	Dot between vector variables denotes dot product.
$f(x,y)$	Functional notation: The function f with arguments x and y.
$\dfrac{\partial f}{\partial x}$	Partial derivative of the function f with respect to the independent variable x.
$\wedge$	Unit vector notation. $\hat{r}$ identifies r as a unit vector $= \bar{r}/r$.

Symbol	Definition
$-$	Vector notation. $\bar{r}$ identifies r as a vector.
x	Vector cross product.

Abstract

Manual Astronaut Navigation, onboard orbit determination independent of primary system computers, must be developed to insure the safety of future manned space flight. This report presents selected methods, procedures, and equipment that form a basis from which a flexible operational manual navigation system may eventually be developed.

The Delta-H method of graphically determining eccentricity is simple and potentially accurate. Prepared charts are entered with two changes in altitude, or "Delta-H's," and eccentricity is read directly. An estimate of the size of the orbit, as represented by the major axis, must be made to allow selection of the correct chart.

The geometric elements of the orbit can be obtained by use of numerical differentiation of a series of range measurements to obtain radial velocity and radial acceleration. This procedure is limited by the effects of truncation and measurement errors. Differential correction of the orbital elements can be made if a back-up computer is available to handle the computational load.

The three-dimensional position fix opens the door to many orbit determination possibilities. Three fixes input to the Gibbs method is the most promising investigated. This procedure may be performed by hand or with a small back-up computer.

If the geometric elements are known, the orientation elements may be obtained without resorting to lengthy iterative techniques. Knowledge of angular positions at two times coupled with the true anomaly at one of those times is all that is required.

Accurate ranging is essential in most orbit determination schemes. A reference trajectory may be employed with linear perturbation techniques to obtain a good estimate of spacecraft range. Linearization is valid for relatively large deviations from the reference trajectory. For midcourse trajectories, this method is vastly superior to methods incorporating angular diameter measurements.

Orbit determination procedures exist that do not depend upon range measurements. The complete orbit may be obtained through knowledge of three angular positions and three true anomaly rates.

To date, very little has been done in the area of manual navigation equipment design. "Aids" to manual navigation such as back-up inertial platforms, hand-held mechanical calculators, and battery operated, hand-held computers are necessary to optimize the performance of future manual navigation systems.

The manual navigation problem can be solved by combining the proper methods, procedures, and equipment.

MANUAL ASTRONAUT NAVIGATION

I. Introduction

Background

The dramatic success of the Apollo 8 lunar mission has brought
this nation to the threshold of an age of interplanetary space travel.
The earth orbits of projects Mercury and Gemini, once considered with
awe, are now classified as simple "parking" orbits from which manned
vehicles, such as Apollo, will depart upon long midcourse trajecto-
ries to the moon and planets. As in the flight of Apollo 8, the
success of these missions will depend heavily upon accurate and
reliable navigation and guidance. In the event of primary system
failure, an adequate back-up system must be available to allow a safe
return to earth. Manual navigation and guidance procedures should be
provided to eliminate all dependence on primary system computers.
Such procedures would involve use of equipment such as the space
stadimeter, a space sextant, prepared tables and charts, and hand-held
computing devices.

The Problem

This report is intended to be a continuation of the work accom-
plished by Captains Richard R. Schehr and Patrick J. Smith in their
thesis, "Manual Astronaut Navigation: Apollo Mission Applications,"
(Ref 17). The term "navigation" is defined as the determination of
any six independent parameters which specify uniquely the geometric
qualities of an orbit, or trajectory, and its orientation in inertial

1

space. "Guidance" is defined as the subsequent determination of the velocity correction vector necessary to insure the arrival of the spacecraft at a predetermined point. "Manual" navigation, the problem attacked in this thesis, is defined as the onboard determination of the orbital parameters using procedures and equipment totally independent of the primary system computer.

Scope

The previous thesis dealt with manual navigation in low altitude, near-circular earth and lunar orbits. This thesis will explore general manual navigation techniques applicable to midcourse trajectories such as the translunar phase of the Apollo mission. No attempt is made to consolidate the procedures described in an operational "flight manual" presentation, as was done by Captains Schehr and Smith. The principal objectives are to extend and improve upon their methods, and to investigate other promising manual navigation techniques. Sources of error are discussed, and some error analyses are presented. Numerical examples are provided, wherever possible, to enhance the theoretical development.

Assumptions

The primary assumption made in this thesis is that of restricted two-body motion. This implies that:

1. The mass of the vehicle is negligible when compared to the mass of the attracting body.

2. The gravity field of the attracting body is ideal, inverse-square, and central.

The only other assumption made is that all measurements indicated can be performed.

The first assumption allows all orbits and trajectories to be considered as conic sections. This assumption is valid for near planet orbits and the major part of midcourse trajectories. The second assumption is, of course, a practical necessity in any theoretical discussion of manual navigation.

The reader is assumed familiar with the basics of astrodynamics and celestial mechanics.

Organization

Each of Chapters II through VII in this report deals with an independent method of obtaining one or more of the six orbital parameters necessary for solution of the manual navigation problem. These parameters, or elements, are divided into two sets: the geometric parameters,

e - eccentricity

a - semimajor axis

t - time from perifocus

and the orientation parameters,

i - inclination of the orbital plane

Ω - longitude of the ascending node

ω - argument of perifocus

Chapter VIII deals with an improved method of optical ranging, and Chapter IX is a discussion of certain "aids" to manual navigation such as battery operated, hand-held computers.

Discussion

As stated previously, this is not a "flight manual." No "best" set of procedures is determined. It will be seen that this determination depends upon the answers to several questions. Most important are:

1. What back-up computational tools are available?

2. What types of measurements are possible?

3. How much time is allowable for the completion of the procedures?

4. What is the required accuracy?

This thesis forms a basis from which an operational flight manual may eventually be developed once the above questions have been answered.

II. The Delta-H Method

Introduction

The cornerstone of the geometric parameters determination for low eccentricity elliptical orbits in the thesis, "Manual Astronaut Navigation: Apollo Mission Applications," by Captains Schehr and Smith, is what they labeled the "Delta-H" method of obtaining orbital eccentricity. This is the first of three independent geometric elements obtained in their approach to the manual navigation problem. The other two parameters are the time from peripoint and the period. In their scheme, once eccentricity is determined it is used to obtain graphically the ratio of time from peripoint to period. The period is also determined graphically by a comparison with a zero eccentricity, or circular, orbit.

As will be seen, the Delta-H method of obtaining orbital eccentricity, original to the aforementioned thesis, is relatively simple and can be sufficiently accurate. For this reason, and because the Delta-H concept was not fully developed due to lack of time, this chapter is devoted primarily to an investigation of this method of obtaining orbital eccentricity. Particularly, an extension of the previous work to highly eccentric geocentric ellipses such as the translunar phase of the Apollo mission is accomplished as a follow-on to the original low eccentricity development.

5

Background

The Delta-H method of eccentricity determination involves the measurement of three consecutive altitudes (or ranges) separated by equal time intervals. The second altitude (range) is subtracted from the first, and the third from the second, to give two changes in altitude, or "Delta-H's." By definition

$$\Delta H1 \;=\; h_1 - h_2 \tag{2-1}$$

and

$$\Delta H2 \;=\; h_2 - h_3 \tag{2-2}$$

In their investigation, Captains Schehr and Smith discovered that if the changes in altitude were taken in pairs successively along the ellipse and plotted as ordinate and abscissa in an orthogonal axis system, curves of constant eccentricity resulted (Ref 17:18). Figure 1 is an example of one of their Delta-H plots. To obtain eccentricity, the plot is entered with $\Delta H1$ and $\Delta H2$ and eccentricity is read directly. The curves were generated for time intervals of 5 and 15 minutes along geocentric and selenocentric orbits. Only very low eccentricities were considered; from .002 to .016 in geocentric orbit, and from .01 to .08 in selenocentric orbit. Most importantly, for the range of major axes considered, i.e., from planet radius plus 80 nautical miles to planet radius plus 170 nautical miles, the curves appeared to be invariant. This has since been confirmed by the authors of this thesis as well as by the Universal Technology Corporation working under Air Force contract. The apparent insensitivity to the size of the orbit,

6

as represented by the major
axis, means that relatively
few plots are necessary to
cover a sizable range of
orbits. This advantage
makes the Delta-H method
more practical than the
previously developed graph-
ical approaches (Ref 17:18).
Operationally, the accuracy
of the Delta-H method de-
pends upon the accuracies

Fig. 1

Typical Low Eccentricity, Low
Altitude Delta-H Plot
(From Ref 17:126)

of timing and altitude (or
range) measurement. These,
in turn, depend upon the
hardware available, the skill of the user, and the inherent accuracy
of the measurement procedure.

Within the scope of the problem defined, the Delta-H method
appeared to Captains Schehr and Smith to be a simple, direct, and
potentially accurate approach to obtaining orbital eccentricity man-
ually. Motivated by their work, the rest of this chapter deals with
the generation of Delta-H plots, an investigation of their properties,
and a discussion of the possibilities of using them in a high eccen-
tricity manual navigation scheme.

Data Generation

A double-precision computer program was written to provide accurate reference data for use in investigating the Delta-H method and other manual navigation techniques to be described in later chapters. The computer graphs the Delta-H data via a tape-driven digital plotter. Details are provided here to minimize the amount of backtracking necessary in future follow-on work.

Theory. As stated in Chapter I, a two-body approach is taken in this thesis. The equations used in the development of the computer program are

$$n = \frac{\mu^{1/2}}{a^{3/2}} \qquad (2\text{-}3)$$

$$\tau = \frac{2\pi}{n} \qquad (2\text{-}4)$$

$$V^2 = \mu\left(\frac{2}{r} - \frac{1}{a}\right) \qquad (2\text{-}5)$$

$$h = r - R \qquad (2\text{-}6)$$

$$M = nt = E - e \sin E \qquad (2\text{-}7)$$

$$r = a(1 - e \cos E) \qquad (2\text{-}8)$$

where

n = mean motion

μ = gravitational constant

a = semimajor axis

τ = period

V = total velocity

8

e   =   eccentricity

r   =   radial distance

h   =   altitude

M   =   mean anomaly

t   =   time from peripoint

E   =   eccentric anomaly measured from peripoint

R   =   planet radius

It is desired to have the computer solve for altitude as a function of semimajor axis, eccentricity, and time from peripoint. This involves the solution of Eq (2-7) for eccentric anomaly as a function of the same three variables, and then Eq (2-8) for radial distance. Altitude is then obtained from Eq (2-6). Difficulties arise because Eq (2-7), Kepler's equation, is transcendental in eccentric anomaly. This problem is not serious for low eccentricities since many excellent approximate solutions have been formulated (Ref 4:41). Most of these solutions are in the form of series expansions. Captains Schehr and Smith used the first three terms of a series expansion in powers of eccentricity about the mean anomaly (Ref 17:17). This series diverges for values of eccentricity above .662743 (Ref 11:II-5). Consequently, to investigate orbits with eccentricities above .9, a different approach had to be formulated. Further research disclosed that all series expansions for eccentric anomaly diverge in this region, so it was decided to employ an iterative procedure based upon the Newton method of approximations. Rearranging Eq (2-7)

$$\sin(E) = \frac{1}{e}(E - M) \qquad\qquad (2\text{-}7a)$$

9

or

$$f(E) = \sin E - \frac{1}{e}(E - M) \tag{2-7b}$$

When Eq (2-7) is satisfied, f(E) is identically zero. An estimate of eccentric anomaly is made to start the iteration. Then, the Newton method is employed to obtain a better estimate, or second approximation.

$$E_2 = E_1 - \left. \frac{f(E)}{\frac{d\ f(E)}{dE}} \right]_1 \tag{2-9}$$

or

$$E_2 = E_1 - \frac{\sin E_1 - \frac{1}{e}(E_1 - M)}{\cos E_1 - \frac{1}{e}} \tag{2-9a}$$

This procedure is repeated until f(E) is zero. The Newton method is generalized in the text "Astrodynamics--Advanced Topics and Applications," by Baker (Ref 3:26). Since the altitude computations start at the peripoint, the initial value of eccentric anomaly is zero. Altitudes are to be computed for every 2.5 minutes thereafter. This short time interval makes the final value of eccentric anomaly at one time an excellent initial value for the next. Also, once the desired altitudes are obtained, they can be combined in pairs to give Delta-H's for timing intervals of any integral multiple of 2.5 minutes. Thus, the effect of the timing interval can be investigated and the number of iterations for convergence is kept small.

The Computer Program. The computer program mentioned at the begin-
ning of this section is reproduced in Appendix A. The statements
required for automatic plotting are not included since they complicate
the program considerably and are not essential for an understanding of
the logic involved. Input to the program are semimajor axis, eccen-
tricity, and time from peripoint. The output includes period, altitude,
ΔH1, ΔH2, eccentric anomaly, and the ratio of velocity to the velocity
at peripoint.

High Eccentricity Delta-H Plots

The translunar phase of the Apollo mission is a geocentric ellipse
with a typical eccentricity of .9668 and an apogee distance of approxi-
mately 60 earth radii (Ref 1). These figures are used as a point of
departure in this section.

The computer was programmed to generate geocentric Delta-H plots
for seven values of eccentricity for each of seven values of semimajor
axis. Thus, the effect of the semimajor axis can be isolated and
studied. The eccentricity was initialized at .9068 and incremented by
.0100 until the .9668 value was attained. The semimajor axis was
initialized at 105,000 nautical miles and incremented by 1,000 nautical
miles until a final value of 111,000 nautical miles was attained. This
set of values for eccentricity and semimajor axis gives a minimum
apogee distance of approximately 58 earth radii and a maximum of
approximately 63 earth radii, since at apogee

$$r = a(1 + e) \tag{2-10}$$

from Eq (2-8). The timing interval was set at 15 minutes with the

first altitude determined at perigee and the last 3.5 hours from perigee.
From the point of view of the Apollo mission, this represents the
portion of the translunar coast phase prior to the first scheduled
midcourse correction (Ref 1). To insure a sufficient number of data
points for accurate curve plotting, the Delta-H pairs were computed
using 2.5 minute displacements of the three altitudes, i.e., the first
pair consists of altitudes computed at times 0, 15, and 30 minutes; the
second pair consists of altitudes computed at times 2.5, 17.5, and
32.5 minutes, and so on. Figure 2 is one of the resulting Delta-H
plots. (To keep the data points in the first quadrant, $-\Delta H1$ is plotted
versus $-\Delta H2$.) The apparent overlapping observed is highly undesirable
since it produces ambiguity for certain combinations of $\Delta H1$ and $\Delta H2$.
Clearly, the curves of constant eccentricity must be distinct every-
where for these plots to have any real value in a manual navigation
scheme. (NOTE: THE COMPUTER SCALES AUTOMATICALLY AND USES THE
NOTATION X 10^1 TO MEAN MULTIPLY THE NUMBER ON THE AXIS BY TEN. THIS
MUST BE KEPT IN MIND SINCE IT IS THE OPPOSITE OF WHAT IS USUALLY SEEN
IN ENGINEERING PRACTICE. THE LIBRARY SUBROUTINE WAS NOT ALTERED DUE
TO THE PROHIBITIVE COST OF RERUNNING THE PLOTS REFERRED TO IN THIS
CHAPTER.)

The Effect of the Timing Interval. Intuitively, it was felt that
perhaps the timing interval was too short to allow adequate "sampling"
of the trajectories in the region of ambiguity. Working on this possi-
bility, the program was altered by increasing the timing interval from
15 minutes to 30 minutes. Figure 3 is the resulting plot for the same
semimajor axis as in Fig. 2. Some improvement is noted in that the
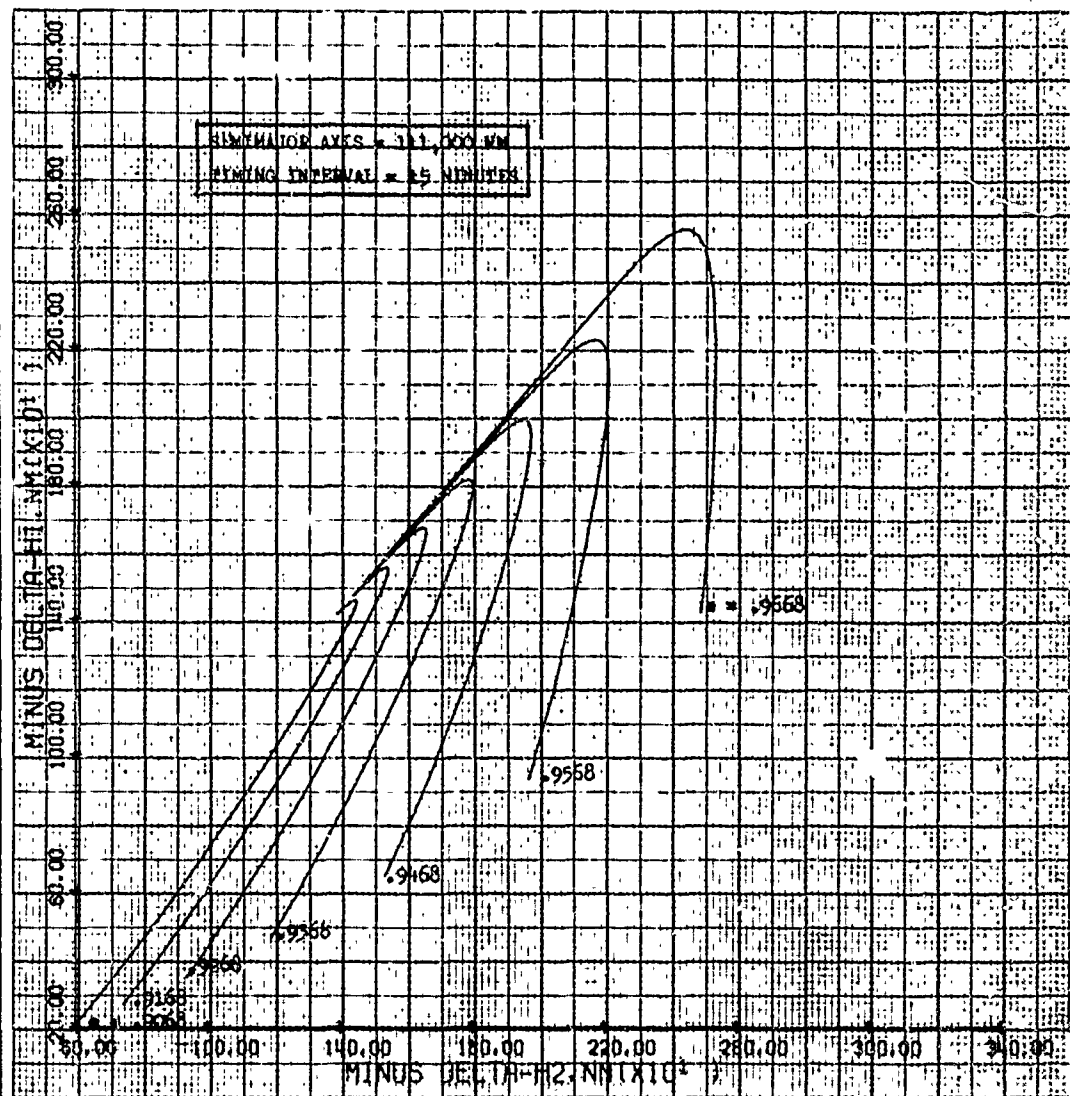
Fig. 2

High Eccentricity Delta-H Plot for
a = 111,000 NM With Δt = 15 Minutes
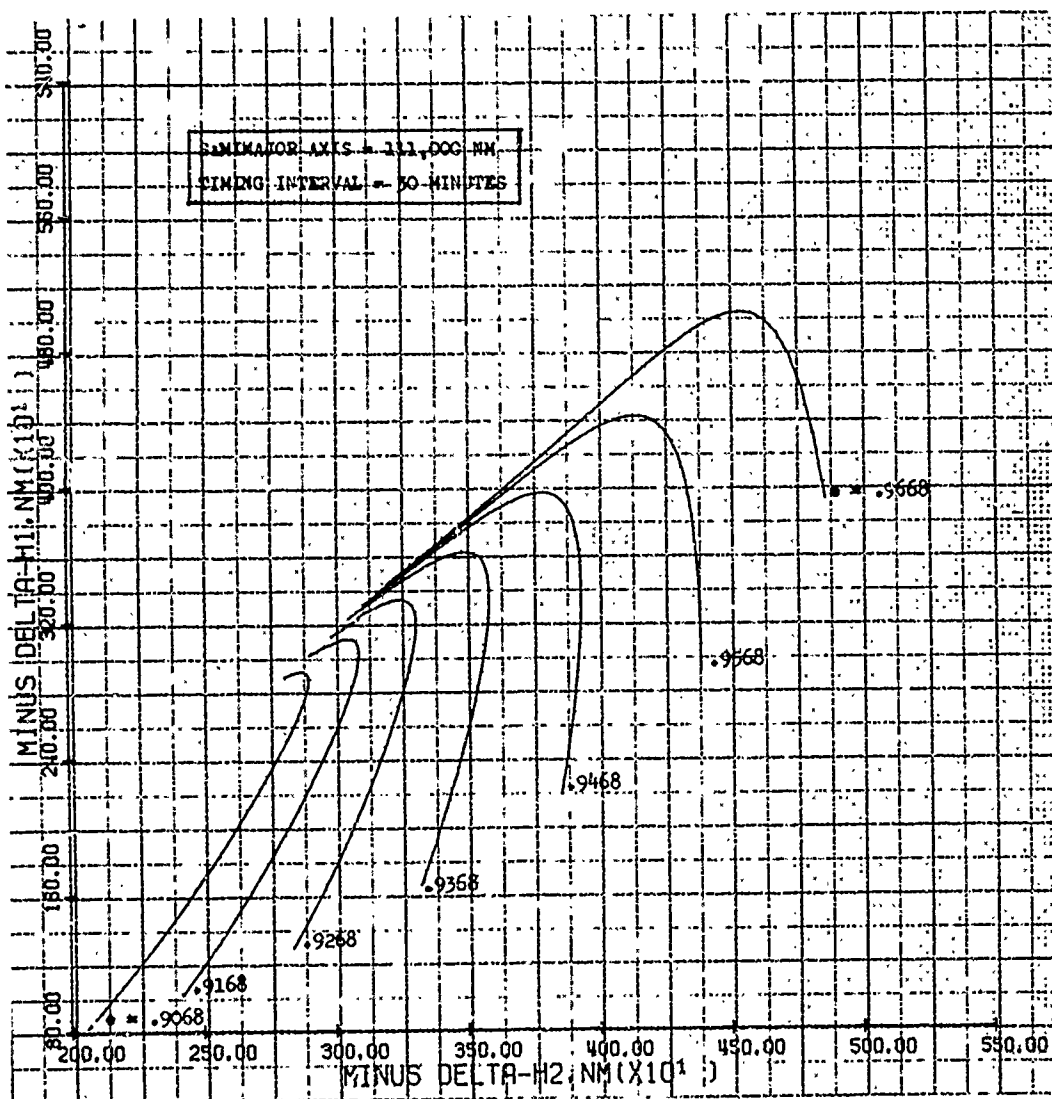
Fig. 3

High Eccentricity Delta-H Plot for
a = 111,000 NM With Δt = 30 Minutes
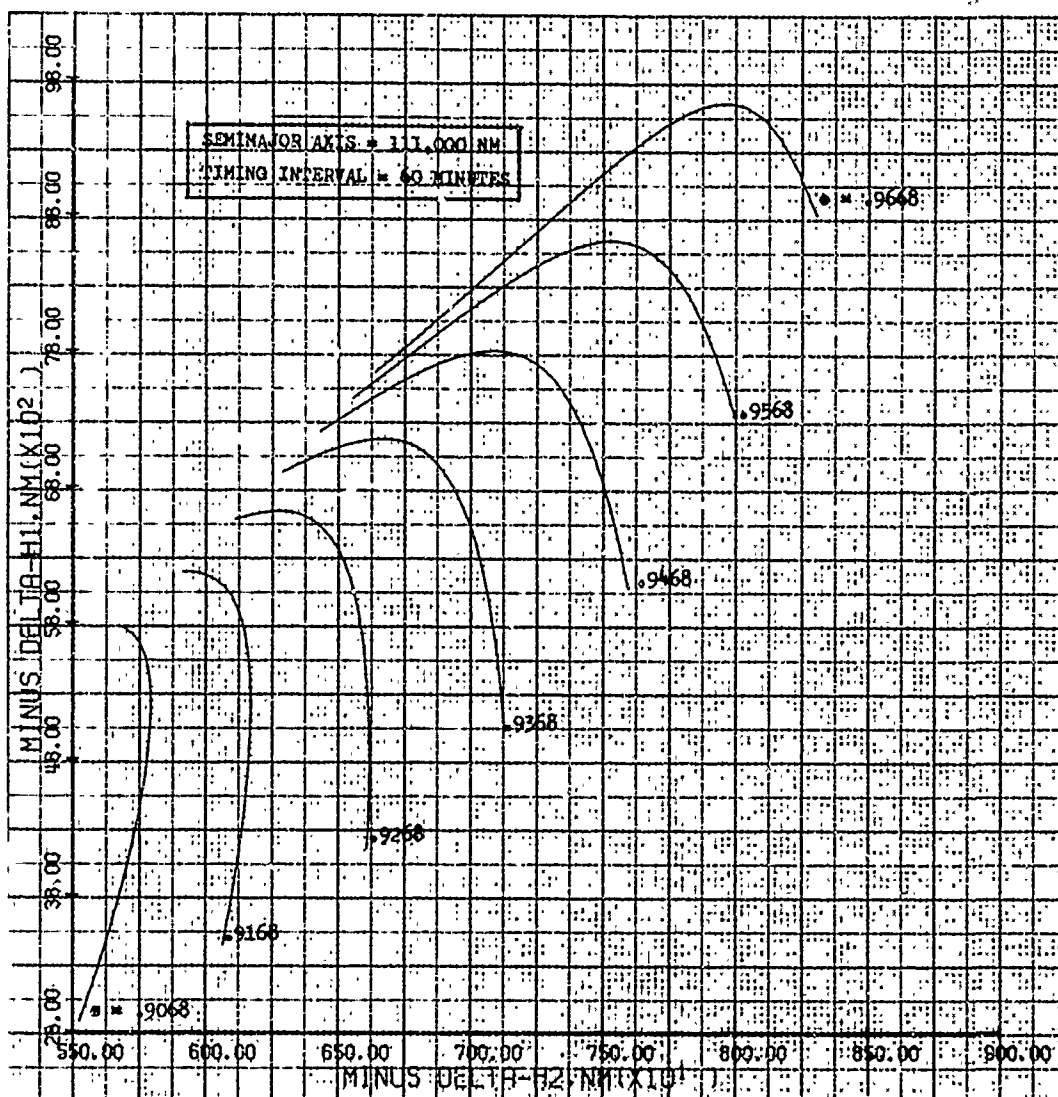
Fig. 4

High Eccentricity Delta-H Plot for
a = 111,000 NM With Δt = 60 Minutes

curves are generally better separated than those in the previous plot.
The timing interval was changed to 60 minutes with the result shown
in Fig. 4. Complete separation is attained, which indicates that
regions of ambiguity can be eliminated by simply increasing the
timing interval. The effect of the timing interval on the high
eccentricity Delta-H plots, then, is to increase or decrease the rela-
tive curve separation as the timing interval is made correspondingly
larger or smaller.

The Effect of the Major Axis. As mentioned previously, Captains
Schehr and Smith found that their constant eccentricity curves appeared
to be invariant. However, the high eccentricity curves considered
here shift slowly as the major axis is changed. This is made apparent
by comparison of the plots in Figs. 5, 5a, and 5b with Fig. 4. As
the major axis is decreased, the curves shift slowly upward and to
the right. It is probable that Captains Schehr and Smith did not
encounter this dependence upon the major axis because of the limited
range of values investigated. In the present case, there must be a
change of 2,000 nautical miles in the major axis to materially affect
the Delta-H plots.

To help in establishing the general effect of the major axis on
these high eccentricity plots, several computer runs were made with
a variety of values of major axis. The conclusion drawn upon
examination of the results is that for high eccentricity ellipses
(e above .9), a variation of more than 1 per cent in the major axis
above or below a particular value is necessary to displace the
constant eccentricity curves a significant amount. The Delta-H

16
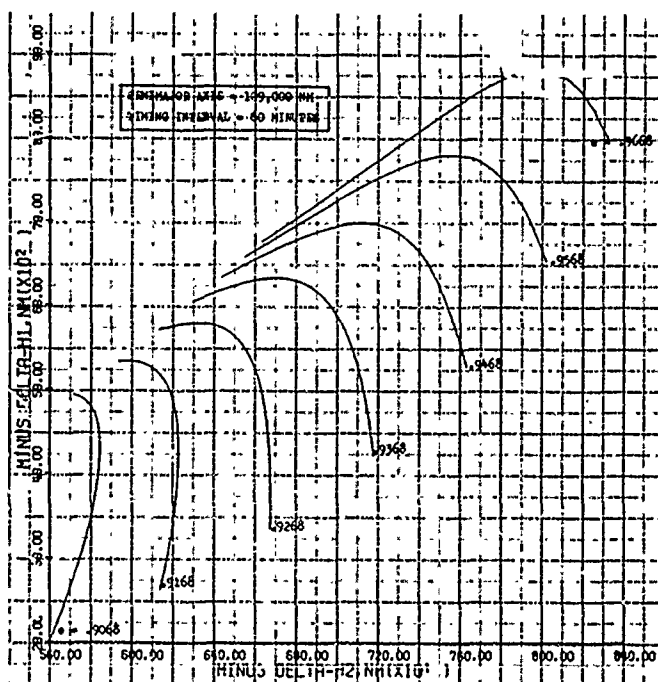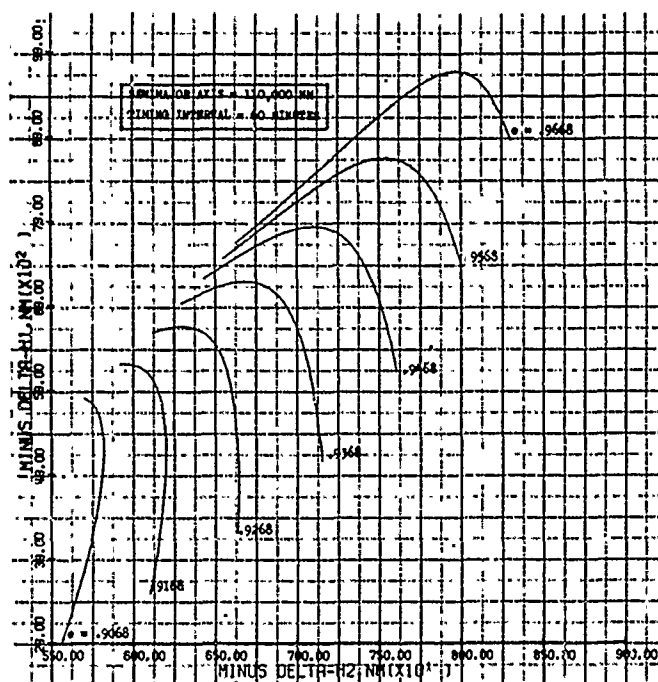
Fig. 5

High Eccentricity Delta-H Plots for a = 110,000 NM
and a = 109,000 NM With Δt = 60 Minutes
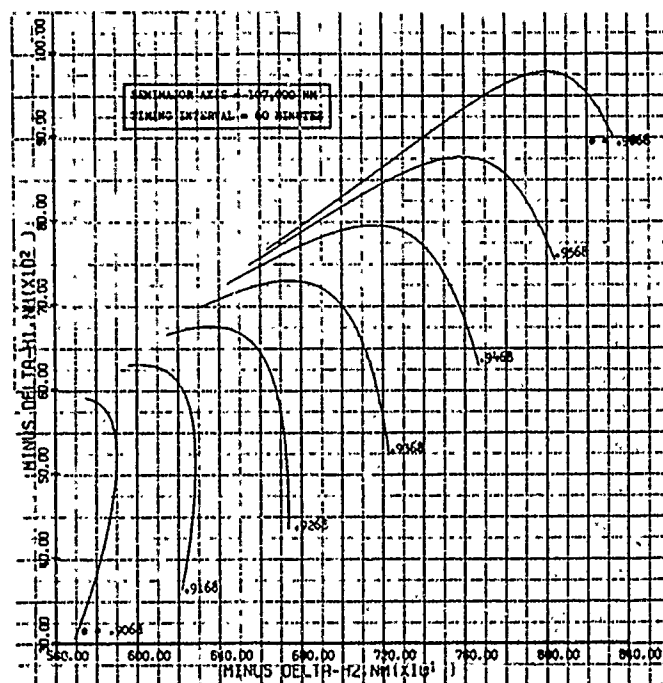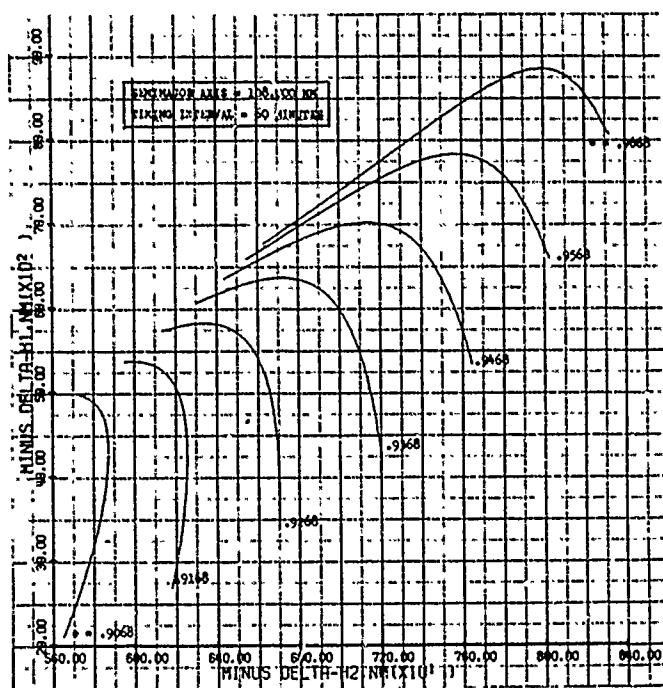
Fig. 5a

High Eccentricity Delta-H Plots for a = 108,000 NM
and a = 107,000 NM With Δt = 60 Minutes
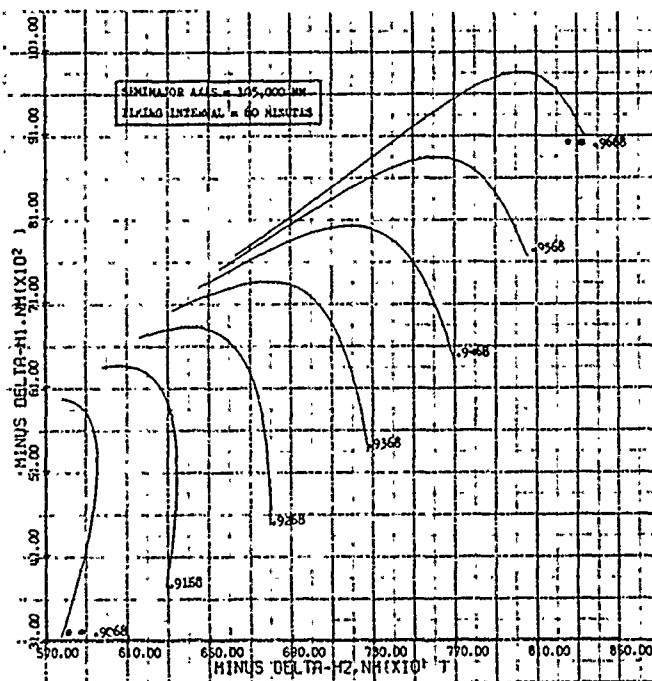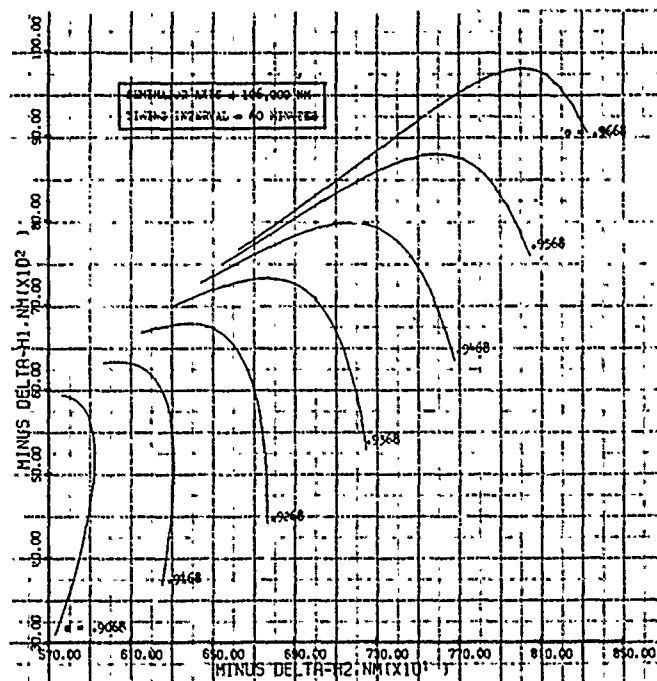
Fig. 5b

High Eccentricity Delta-H Plots for a = 106,000 NM
and a = 105,000 NM With Δt = 60 Minutes

plots shown in Figs 2 through 5b are considered typical.

The Analytic Approach

Attempts have been made to analyze and predict the behavior of the Delta-H curves mathematically. A general expression (valid for any eccentricity less than 1) relating the changes in altitude directly to the major axis, timing interval, and the eccentricity such as

$$\Delta H1 = f(\Delta H2, a, \Delta t, e) \tag{2-11}$$

or

$$\Delta H2 = f(\Delta H1, a, \Delta t, e) \tag{2-11a}$$

has been sought, but all attempts at formulating such an expression have failed due to the transcendental nature of Kepler's equation which links time to altitude via Eqs (2-6) through (2-8). With these equations plus Eqs (2-1) and (2-2), it can be shown that, for altitudes 1, 2, and 3

$$\Delta H1 = ae(\cos E_3 - \cos E_1) - \Delta H2 \tag{2-12}$$

If a, e, Δt, and $\Delta H2$ are specified, E_1 and E_3 can be obtained from the simultaneous solution of

$$\Delta H2 = ae(\cos E_3 - \cos E_2) \tag{2-13}$$

and

$$n\Delta t = (E_3 - E_2) - e(\sin E_3 - \sin E_2) \tag{2-14}$$

which yields E_2 and E_3, and then the solution of either

$$n\Delta t = (E_2 - E_1) - e(\sin E_2 - \sin E_1) \qquad (2\text{-}15)$$

or

$$2n\Delta t = (E_3 - E_1) - e(\sin E_3 - \sin E_1) \qquad (2\text{-}16)$$

which yields E_1. Therefore, Eq (2-12) can be solved for $\Delta H1$ given $\Delta H2$, a, Δt, and e. First, however, E_1, E_2, and E_3 must be obtained by iteration. The necessity of taking this intermediate step seems to preclude the possibility of obtaining an explicit relation such as Eq (2-11) or (2-11a) for use in a mathematical analysis. An empirical approach has, therefore, been taken in this chapter. The computer program provides an implicit solution of Eq (2-12) so the individual effects of varying a, e, and Δt can be observed.

General Characteristics of the Delta-H Plot

To determine some general characteristics of the Delta-H plot, 15 computer runs were made for intermediate (.50 to .75) and low (.01 to .10) values of eccentricity. Both regions were examined for sensitivity to changes in the timing interval and the major axis.

Figure 6 is a plot for eccentricities ranging from .50 to .56 in increments of .01. The timing interval is 15 minutes and the semimajor axis is 106,000 nautical miles. Figures 7, 7a, and 7b are a set of plots for the same values of eccentricity, but with a 60 minute timing interval. The major axis differs from plot to plot by 2,000 nautical miles. These plots display typical intermediate eccentricity characteristics. Their behavior is very similar to
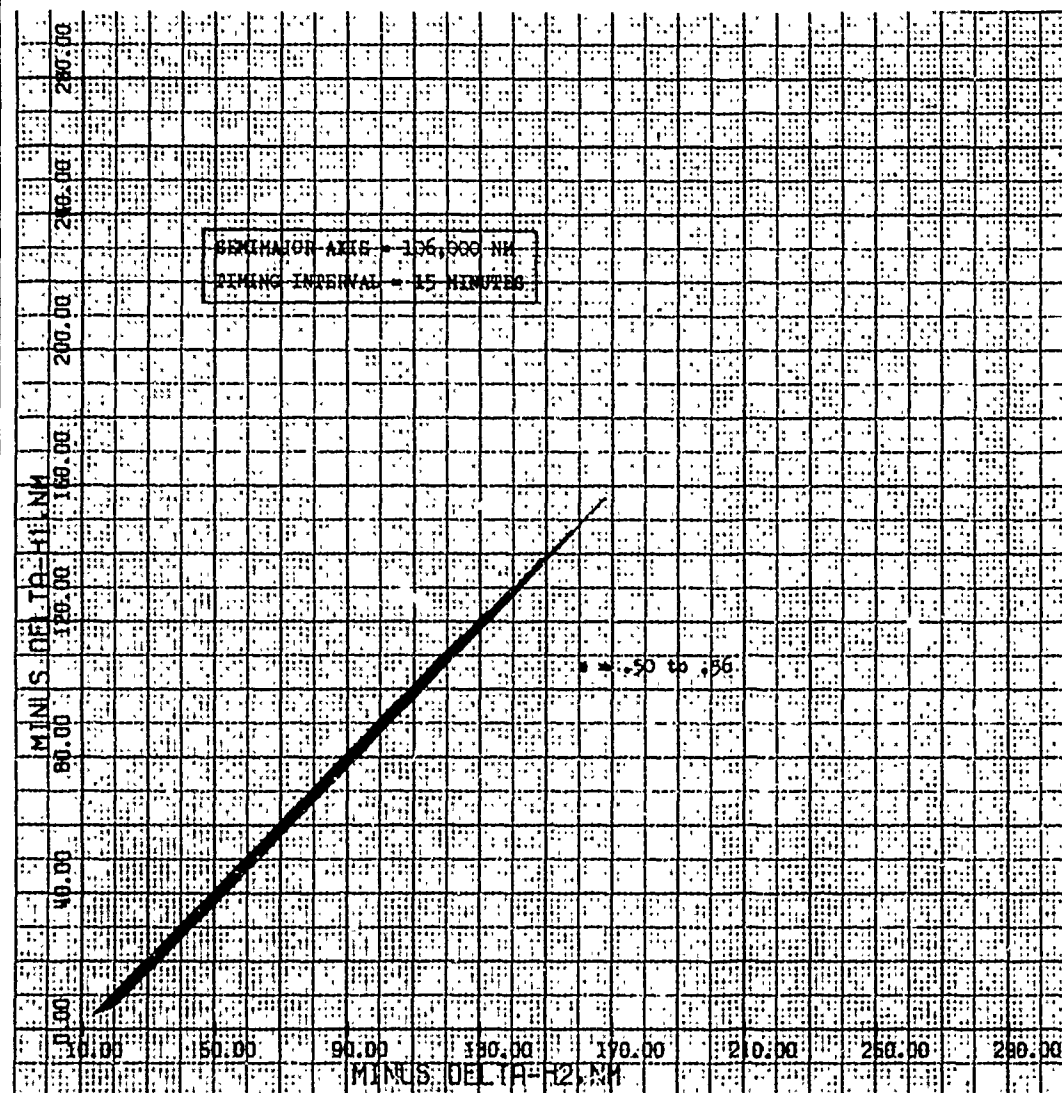
Fig. 6

Intermediate Eccentricity Delta-H Plot for
a = 106,000 NM With Δt = 15 Minutes
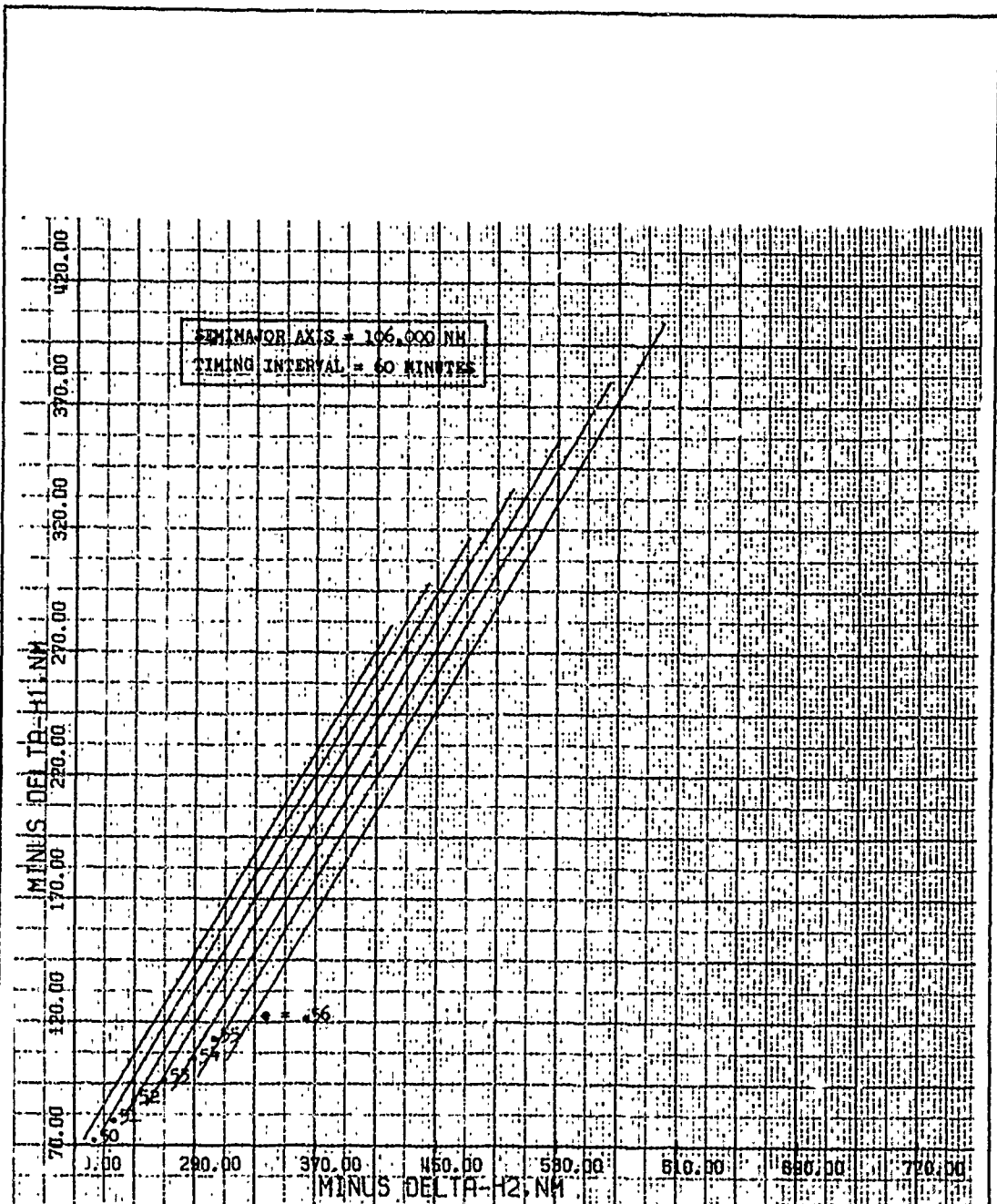
Fig. 7

Intermediate Eccentricity Delta-H Plot for
a = 106,000 NM With Δt = 60 Minutes
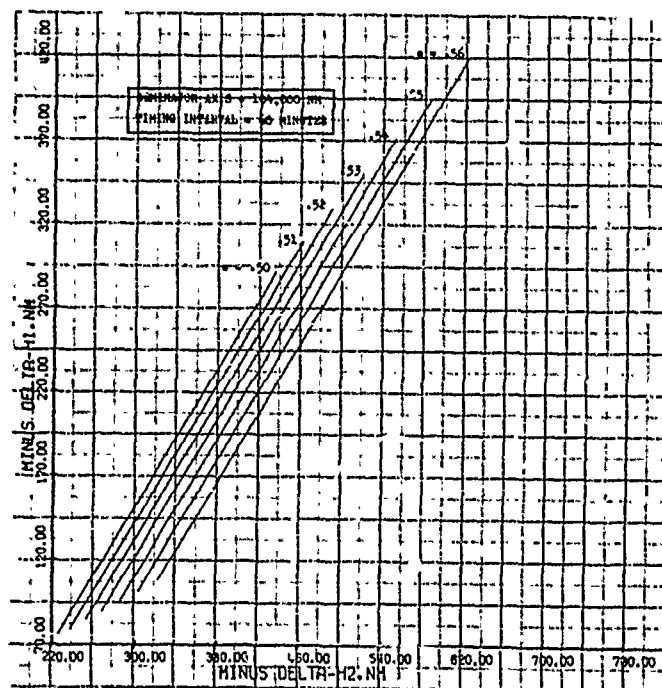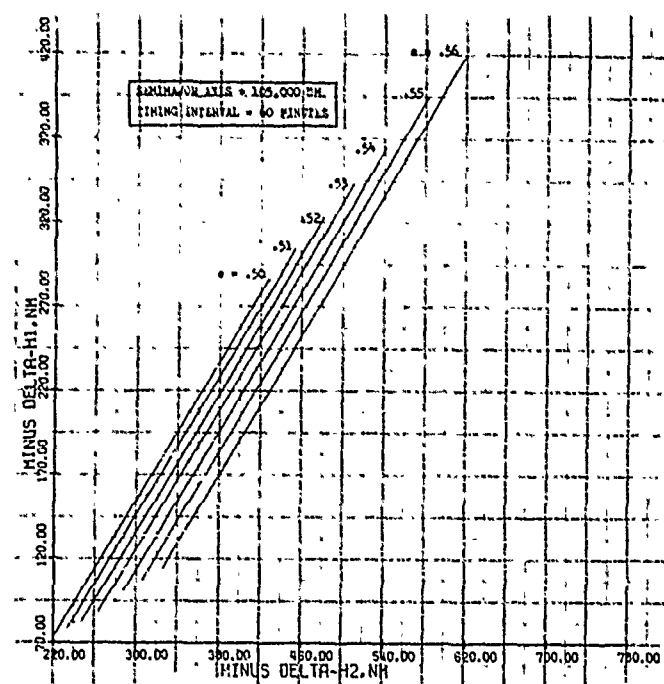
Fig. 7a

Intermediate Eccentricity Delta-H Plots for a = 105,000 NM
and a = 104,000 NM With Δt = 60 Minutes
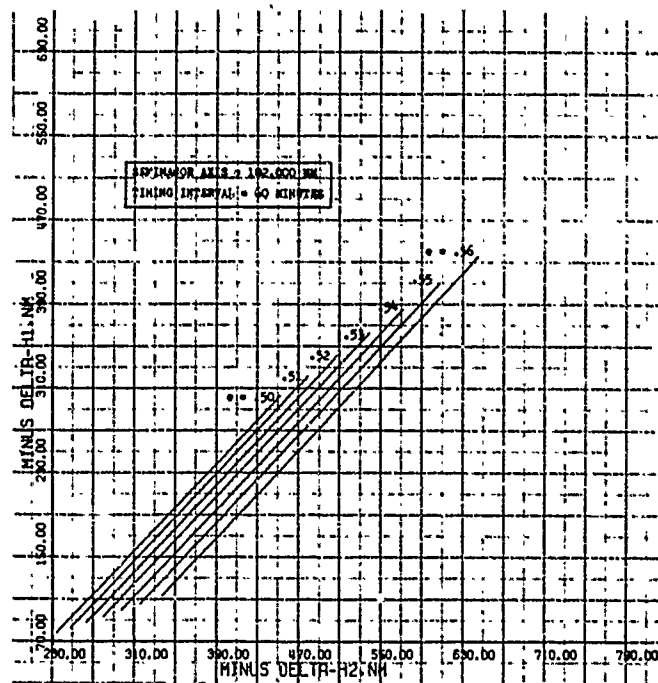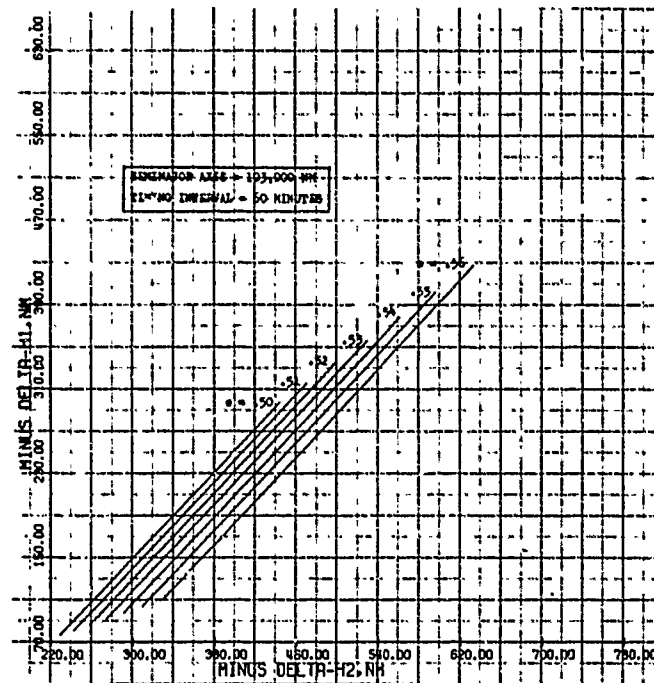
Fig. 7b

Intermediate Eccentricity Delta-H Plots for a = 103,000 NM
and a = 102,000 NM With Δt = 60 Minutes

that noted in the high eccentricity region.

Figures 8, 8a, and 8b are a typical set of low eccentricity plots. Separation was again attained with a 60 minute timing interval. A notable difference in the behavior of these plots lies in the lessened effect of changes in the major axis. A change of more than 3 per cent appears necessary to displace the curves a significant amount.

Conclusions. The general conclusions drawn are:

1. Curve separation for all eccentricities can be controlled by changing the timing interval.

2. Sensitivity to changes in the major axis is variable. It appears that at low eccentricities, a change of more than 3 per cent is necessary for significant displacement, and in the high and intermediate regions, a change of more than 1 per cent is necessary.

Conclusion 2 tends to confirm the supposition that Captains Schehr and Smith failed to encounter the dependence upon the major axis due to the limited range of values investigated. They considered low eccentricities and a maximum change of approximately 2 1/2 per cent in the major axis.

While this has not been a comprehensive analysis of the Delta-H plot characteristics (since such an analysis is beyond the scope of this thesis), two important trends have been discovered in the effects of the timing interval and the major axis. These trends will be used as a basis for fitting the Delta-H method of eccentricity determination into a high eccentricity manual navigation scheme.
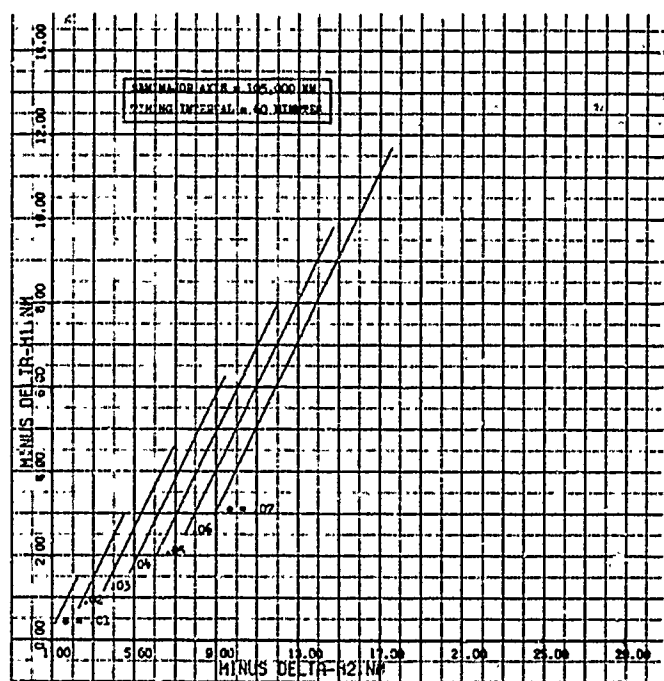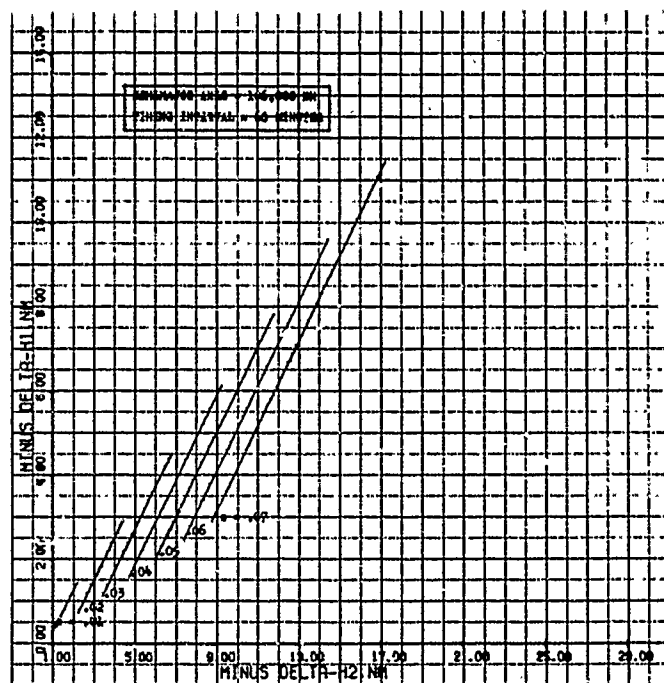
Fig. 8

Low Eccentricity Delta-H Plots for a = 106,000 NM
and a = 105,000 NM With Δt = 60 Minutes
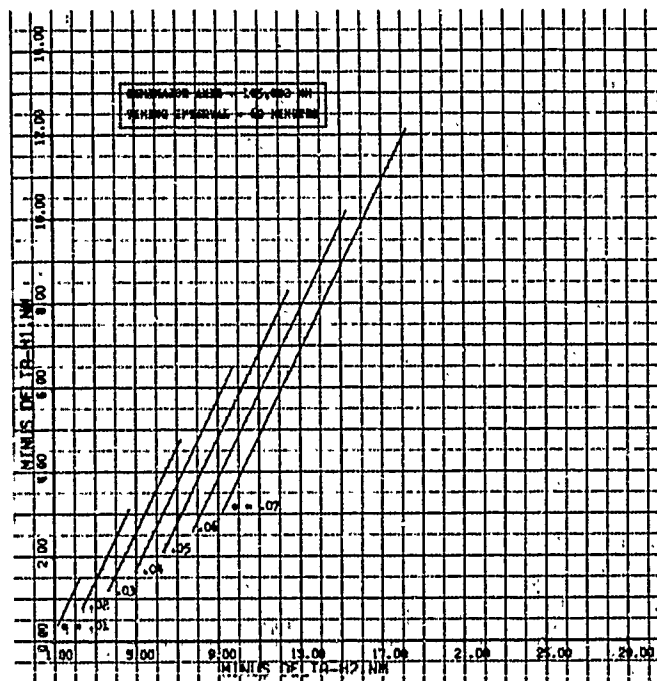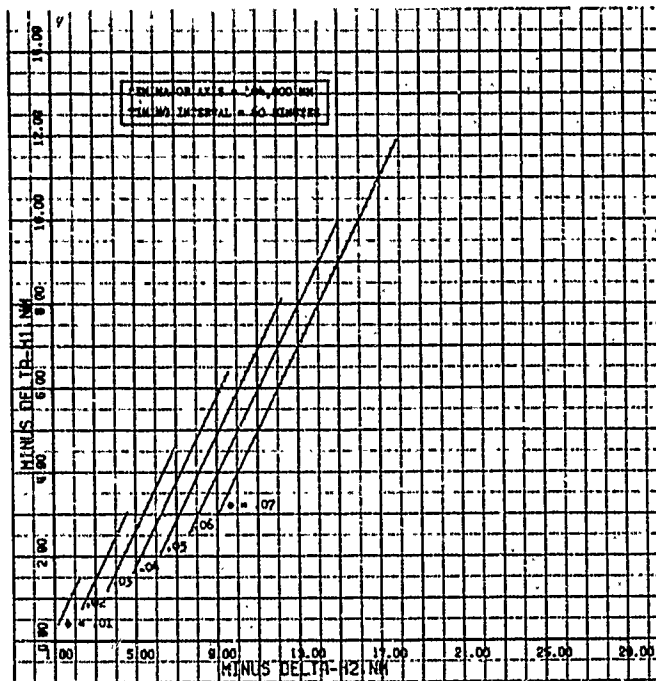
Fig. 8a

Low Eccentricity Delta-H Plots for a = 104,000 NM
and a = 103,000 NM With Δt = 60 Minutes
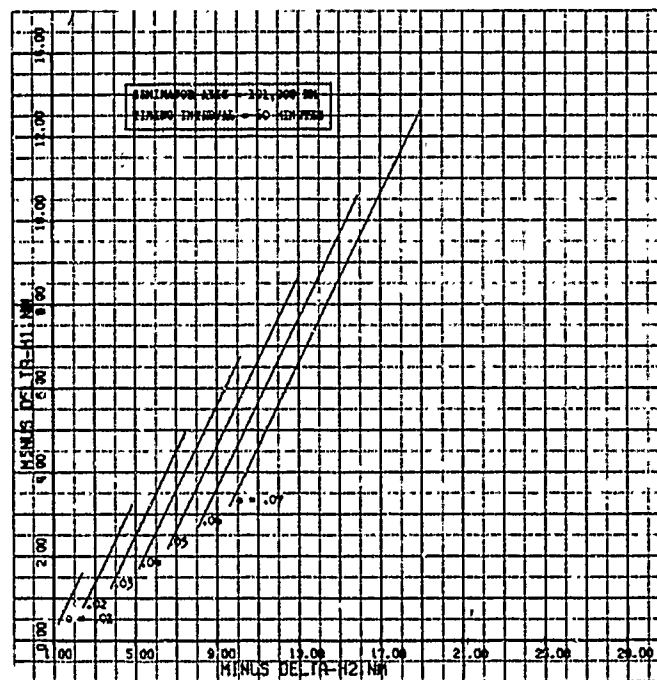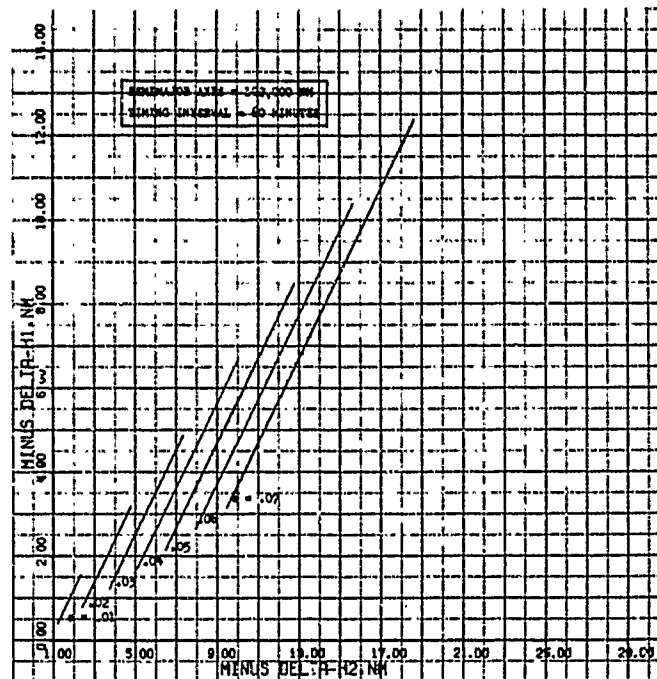
Fig. 8b

Low Eccentricity Delta-H Plots for a = 102,000 NM
and a = 101,000 NM With Δt = 60 Minutes

Discussion

It has been seen that the Delta-H plots are sensitive to changes in the timing interval and the major axis. These sensitivities must be taken into account and used to best advantage if the method is to be extended beyond near circular parking orbits to midcourse trajectories such as the translunar phase of the Apollo mission.

It would be unrealistic to l. 'it the Apollo midcourse problem by assuming a small (± 1 per cent) variation in the major axis so that only one Delta-H plot is necessary to cover each set of possible eccentricities. An inflight emergency involving only moderate deviations from the planned injection velocity could easily place the actual major axis outside this range; see Eq (2-5). Therefore, a practical manual scheme incorporating the Delta-H method would have to include several plots for each set of eccentricities to assure adequate coverage for such a contingency. A set such as the plots in Figs. 4 through 5b would suffice for a 12,000 nautical mile range of major axes, and additional plots could be carried to increase this coverage. The astronaut would have to know the major axis to within 2,000 nautical miles to choose the correct plot for accurate determination of the orbital eccentricity. Larger errors in the major axis are tolerable if some uncertainty in the eccentricity is acceptable. Careful inspection of Figs. 4 through 5b shows that if the major axis is known to within plus or minus 6,000 nautical miles (about ± 3 per cent), the uncertainty in the eccentricity is no greater than approximately .003. This can be demonstrated by assuming a combination of $\Delta H1$ and $\Delta H2$ and then entering each of the seven plots for an

estimate of the eccentricity. (If the central, or fourth, plot is considered to be the correct plot, then this set represents a ± 3 per cent variation from the actual major axis.) The difference between the highest or lowest estimate and the true eccentricity is in no case greater than .003. Therefore, this represents an upper bound on the uncertainty in the eccentricity given that the error in the major axis is within 6,000 nautical miles.

The errors assumed in the previous paragraph are considered to be the result of inaccuracies in the method used to determine the major axis. This does not include the effect of measurement errors. Measurement errors, of course, affect both the determination of the major axis and the two changes in altitude. It is essential that the range (or altitude) measurements be as accurate as possible. However, it is evident from the relatively large changes in altit $\cdot$ noted in Figs. 4 through 5b that small errors can be absorbe ch little affect on the eccentricity determination as long as the major axis is known to within the limits prescribed above. Also, an advantage of the Delta-H method lies in the elimination of measurement errors due to human bias. These errors tend to be self-canceling (Ref 17:27).

The major axis can be obtained from knowledge of the orbital period; see Eq (2-14). The method used by Captains Schehr and Smith is not applicable in this case since it assumes eccentricities close to zero. More flexible methods of determining the major axis are discussed later in this thesis. Once the major axis and the eccentricity are obtained, they can be used to find the final

31

geometric parameter, the time from peripoint to one of the measurements from

$$t = \frac{E - e \sin E}{n} \tag{2-17}$$

where

$$E = \cos^{-1} \frac{a - r}{ae} \tag{2-18}$$

and r is the range at the time of interest. If the cosine of E is positive and the range is increasing, then E is less than 90 degrees. If the range is decreasing, the angle is greater than 270 degrees, and so on.

The curve separating effect of increasing the timing interval can be used to generate Delta-H plots for eccentricity increments of .001 or smaller, thereby improving the accuracy with which the graphs may be read. Figure 9 is a plot for a 90 minute timing interval, and Fig. 10 is a portion of the same plot with .001 increments.

Sample Problem. The following is a sample calculation of the eccentricity and time from peripoint on a known ellipse. The calculations were performed with a slide rule, standard trigonometric tables, and a scratch pad. The errors introduced are assumed typical for the measurements and methods involved.

On the known ellipse (exact values)

a = 105,000 NM (NM for all distances)

e = .9568

h_1 = 7245.584 at 50 minutes from perigee
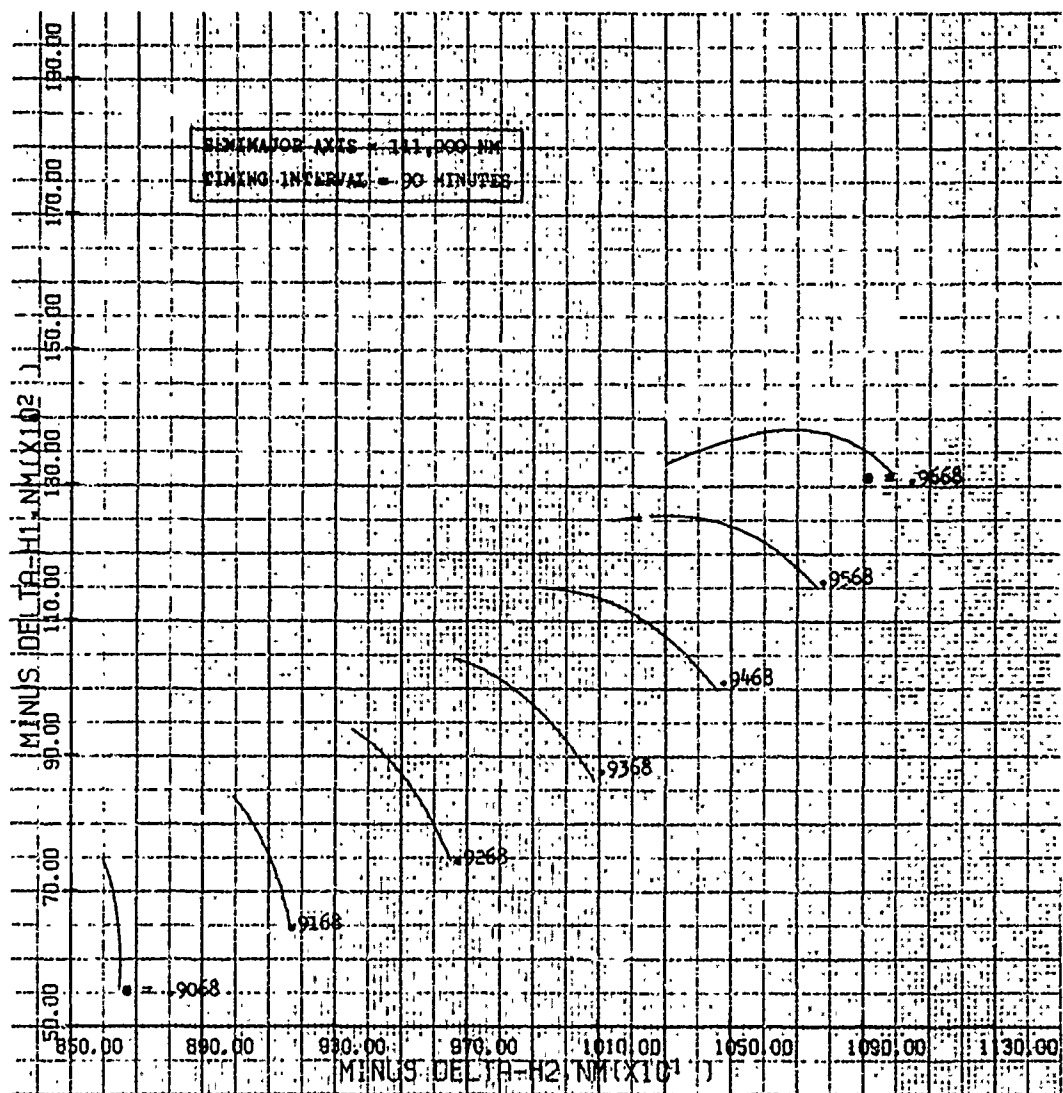
Fig. 9

High Eccentricity Delta-H Plot for a = 111,000 NM
With Δt = 90 Minutes

33
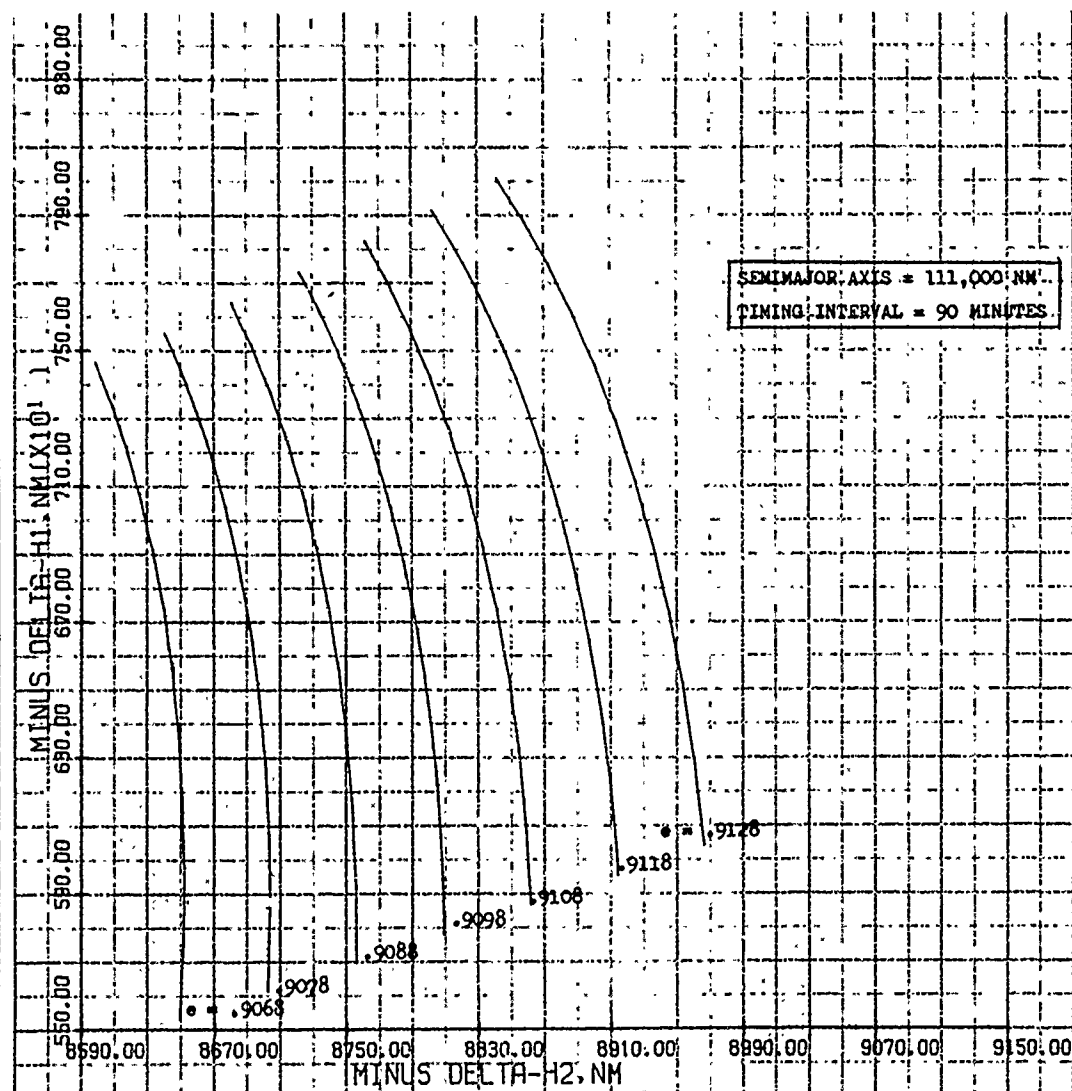
Fig. 10

High Eccentricity Delta-H Plot for a = 111,000 NM With
Δt = 90 Minutes and .001 Eccentricity Increments

34

h_2 = 15540.412 at 110 minutes from perigee

h_3 = 22629.467 at 170 minutes from perigee

The <u>assumed</u> <u>measurements</u>, <u>with</u> <u>errors</u>, are

h_1 = 7300

h_2 = 15650

h_3 = 22750

Δt = 60 minutes

The <u>assumed</u> <u>calculated</u> <u>major</u> <u>axis</u> <u>is</u> <u>108,000</u> <u>nautical</u> <u>miles</u>.
With this input data

$\Delta H1$ = $h_1 - h_2$ = -8350

$\Delta H2$ = $h_2 - h_3$ = -7100

Entering the ΔH plot for <u>a</u> = <u>108,000</u> <u>NM</u> <u>yields</u>

<u>e = .9598</u>

Then

$$E_1 = \cos^{-1} \frac{a - r_1}{ae}$$

$a - r_1$ = 97260

ae = 103658

$$E_1 = \cos^{-1} (.9382)$$

35

$$E_1 = 20° \ 15' = .3534 \text{ radians (range increasing)}$$

$$\sin E_1 = .34612$$

$$n = .0254$$

$$t_1 = \frac{.3534 - .3322}{.0254} \text{ minutes}$$

$$t_1 = (.8346)(60) = \underline{50.07 \text{ minutes from perigee}}$$

Summary. The positive and negative aspects of using the Delta-H method in a high eccentricity scheme may be summarized as follows:

Positive Aspects

1. The computations required are simple.

2. An uncertainty of no more than about .003 in the eccentricity is possible with a ± 3 per cent error in the estimate of the major axis.

3. Small measurement errors can be absorbed with little adverse affect as long as the estimate of the major axis is within the limits prescribed.

4. Human bias as a source of error is eliminated.

5. If an increased timing interval is acceptable, the Delta-H curves can be separated enough to allow eccentricity increments of .001 or smaller.

Negative Aspects

1. A sufficient number of plots must be carried to assure adequate coverage of possible orbits.

2. The major axis must be known to within ± 1 per cent of the actual value for accurate eccentricity determination.

36

3. Measurement inaccuracies can give totally erroneous estimates of the eccentricity through errors in a, ΔH1 and ΔH2.

4. The timing interval must be large enough to eliminate ambiguity. Therefore, it may take two or more hours to obtain ΔH1 and ΔH2.

All of these factors must be weighed before inclusion of the Delta-H method in a high eccentricity manual navigation scheme.

III. Geometric Parameters from Numerical Differentiation

Introduction

The following geometric properties of an orbit can be obtained from a set of timed range (or altitude) measurements:

1. the semimajor axis – a

2. the eccentricity   – e

3. the eccentric anomaly E associated with a position and time.

The range r is the vehicle's distance from the center of the earth. The computation method considered in this chapter involves a numerical differentiation to obtain the radial components of velocity and acceleration $\dot{r}$ and $\ddot{r}$. Once these quantities have been obtained, the geometric elements may be computed from the two-body orbital equations. A block diagram outlining the general procedure is shown in Fig. 11.

Knowledge of the eccentric anomaly E at a specific time t is sufficient to relate position to time through Kepler's equation

$$E - e \sin E = M = (t - t_0) \sqrt{\frac{\mu}{a^3}} \qquad (3\text{-}1)$$

where M is the mean anomaly, t_0 the perifocus time, and μ the earth's gravitational constant. In this chapter, the eccentric anomaly at its associated time will be considered as one of the orbital elements, thus simplifying portions of the presentation.
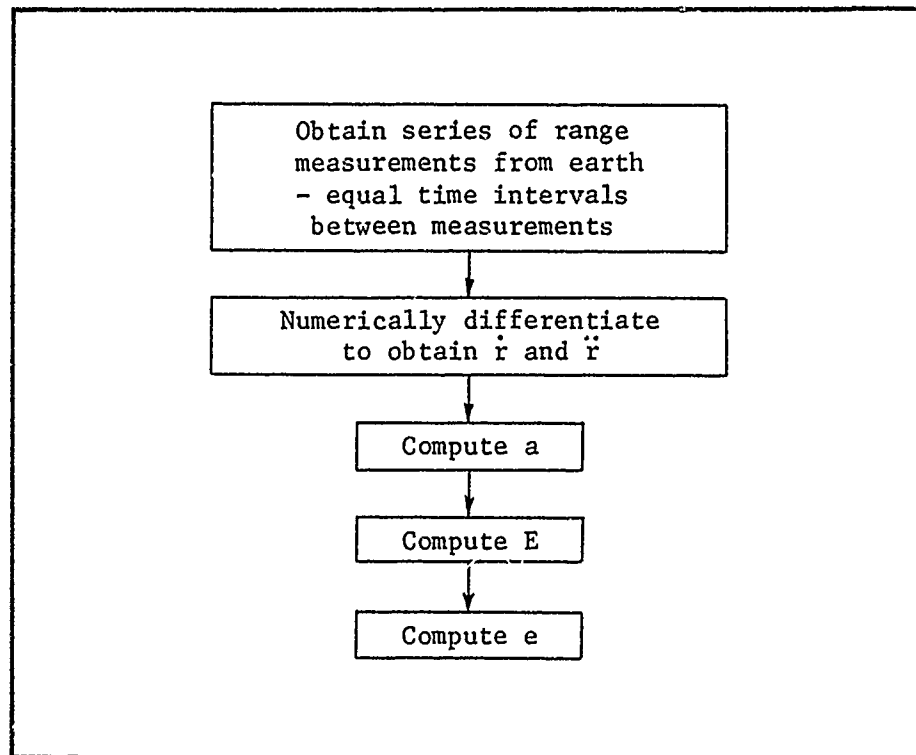
Fig. 11

Determination of Geometric
Orbital Parameters

Numerical Differentiation for $\dot{r}$ and $\ddot{r}$

The radial velocity and radial acceleration can be obtained by
numerically differentiating a set of range measurements. Development
and tabulation of numerical differentiation formulas can be found in
any text on numerical analysis. In general, numerical differentiation
is achieved by using the first few terms of a series not wholly unlike
the familiar Taylor series. Table I is presented as a summary of
numerical differentiation formulas available for sets of range
measurements having up to seven readings. The time interval between
readings is denoted by t.

Table I

Tabulation of Numerical Differentiation Formulas

Number of Readings	Equation for $\dot{r}$	Equation for $\ddot{r}$
3	$\dot{r}_2 = \dfrac{r_3 - r_1}{2t}$	$\ddot{r}_2 = \dfrac{r_1 + r_3 - 2r_2}{t^2}$
4	$\dot{r}_2 = \dfrac{3(2r_3 - r_2) - (2r_1 + r_4)}{6t}$	$\ddot{r}_2 = \dfrac{r_1 + r_3 - 2r_2}{t^2}$
5	$\dot{r}_3 = \dfrac{(r_1 - r_5) - 8(r_2 - r_4)}{12t}$	$\ddot{r}_3 = \dfrac{-(r_1 + r_5) + 16(r_4 + r_2) - 30r_3}{12\,t^2}$
7	$\dot{r}_4 = \dfrac{45(r_5 - r_3) + 9(r_2 - r_6) + (r_7 - r_1)}{60t}$	$\ddot{r}_4 = \dfrac{810(r_5 + r_3) - 81(r_6 + r_2) + 6(r_7 + r_1) - 1470r_1}{540\,t^2}$

Orbit Determination - Geometric Elements

The following notation is introduced:

$r = |\bar{r}| = $ vehicle distance from earth center

$\mu = $ earth gravitational constant

$a = $ semimajor axis

$E = $ eccentric anomaly

$e = $ eccentricity

$\theta = $ true anomaly

The geometric elements are determined from r, $\dot{r}$, and $\ddot{r}$ through three relatively simple equations. For an elliptic orbit

$$a = \frac{\mu}{(\mu/r) - \dot{r}^2 - r\ddot{r}} \qquad (3-2)$$

$$e \cos E = 1 - \frac{r}{a} \qquad (3-3)$$

$$e \sin E = \frac{r\dot{r}}{\sqrt{\mu a}} \qquad (3-4)$$

If the trajectory is hyperbolic, a is negative. The equations for the geometric elements become

$$a = \frac{\mu}{(\mu/r) - \dot{r}^2 - r\ddot{r}} \qquad (3-5)$$

$$e \cosh F = 1 - \frac{r}{a} \qquad (3-6)$$

$$e \sinh F \ = \ \frac{r \ \dot{r}}{\sqrt{- \ \mu a}} \tag{3-7}$$

The hyperbolic functions result from the substitution of iF for E in the elliptic orbit equations (Ref 2:89).

In the unlikely event the orbit is exactly parabolic, then

$$a \ = \ \infty \quad \text{i.e.} \quad \frac{\mu}{r} - \dot{r}^2 - r \ \ddot{r} \ = \ 0 \tag{3-8}$$

$$e \ = \ 1 \tag{3-9}$$

$$\cos \theta \ = \ \frac{r^2 \ \ddot{r}}{\mu} \tag{3-10}$$

A derivation of these equations is presented in Appendix B. There are no approximations involved in the derivations. The numerical determination of $\dot{r}$ and $\ddot{r}$ involves some approximation.

Example Problems - Geometric Element Determination

Example Problem 3-1 - Low Eccentricity. Liftoff from Cape Kennedy was normal, but before parking orbit insertion, the spacecraft was besieged with a series of emergencies. The present situation is complete communication failure coupled with unreliable operation of the navigation computer. The immediate problem is determination of the safety of the orbit.

Solution:

The astronauts obtain the following altitudes at time intervals of five minutes:

$$h_1 \quad = \quad 166.8 \text{ NM*}$$

$$h_2 \quad = \quad 158.7 \text{ NM}$$

$$h_3 \quad = \quad 147.8 \text{ NM}$$

The expressions for $\dot{r}_2$ and $\ddot{r}_2$ become

$$\dot{r}_2 \quad = \quad \frac{h_3 - h_1}{2t} \quad = \quad \frac{147.8 - 166.8}{2(5)} \quad = \quad - 1.9 \text{ NM/MIN}$$

$$\ddot{r}_2 \quad = \quad \frac{h_1 + h_3 - 2h_2}{t^2} \quad = \quad \frac{166.8 + 147.8 - 2(158.7)}{(5)(5)}$$

$$= \quad - 0.112 \text{ NM/MIN}^2$$

For the earth, μ and $\sqrt{\mu}$ are

$$\mu \quad = \quad 225.90258 \times 10^6 \text{ NM}^3/\text{MIN}^2$$

$$\sqrt{\mu} \quad = \quad 15.03005598 \times 10^3 \text{ (NM}^3/\text{MIN}^2)^{1}/2$$

The radial distance from the earth's center is obtained by adding the earth's radius $R_\oplus$ to the altitude reading h_2

$$r_2 \quad = \quad h_2 + R_\oplus \quad = \quad 158.7 + 3440.2 \quad = \quad 3599 \text{ NM}$$

The semimajor axis a is

$$a \quad = \quad \frac{\mu}{\left(\mu/r\right) - \dot{r}^2 - r \ddot{r}} \quad = \quad \frac{(225.9) \ 10^6}{\dfrac{(225.9) \ 10^6}{(3599)} - (1.9)^2 + (3599)(.112)}$$

*These data are identical to Example Problem One in Ref 17:65.

43

and using a slide rule

$$a = 3575 \text{ NM} \quad \text{and} \quad \sqrt{a} = 59.79$$

The period of the orbit can now be determined, if desired, from

$$P = 2\pi\sqrt{\frac{a^3}{\mu}} = (4.180413) \, 10^{-4} \, a \, \sqrt{a}$$

and

$$P = (4.180) \, 10^{-4} \, (3575)(59.79) = 89.3 \text{ min}$$

The eccentric anomaly at r_2 is obtained from

$$\tan E_2 = \frac{r_2 \, \dot{r}_2 \, \sqrt{a}}{\sqrt{\mu} \, (a - r_2)} = \frac{(3599)(-1.9)(59.79)}{(15.03) \, 10^3 \, (3575 - 3599)}$$

then

$$\tan E_2 = 1.133, \quad E_2 = 228.58° \quad \text{and}$$

$$\sin E_2 = -0.7499$$

The eccentric anomaly is greater than 180° since the radial distance is decreasing. The orbital eccentricity is given by

$$e = \frac{r_2 \, \dot{r}_2}{\sqrt{\mu} \, \sqrt{a} \, \sin E} = \frac{(3599)(-1.9)}{(15.03) \, 10^3 \, (59.79)(-.7499)} = .01015$$

44

With the geometric elements determined, the perigee altitude is given
by

$$h_p = a(1 - e) - R_\oplus = 3575(1 - .0101) - 3440$$

$$h_p = 99 \text{ NM}$$

Therefore, the safety of the orbit is established and the astronauts
can then direct their attention to other aspects of the emergency.

The time from perigee of the second range measurement is obtained
from the "easy solution" of Kepler's equation

$$t - t_o = \frac{1}{n} [E - e \sin E] \qquad (3-11)$$

where $n = 2\pi/P$. Then

$$t_2 - t_o = \frac{89.3}{6.283} \left[(228.6)(.01745) + (.0101)(.7499) \right]$$

and

$$t_2 - t_o = 56.8 \text{ min}$$

The iterative computer solution to this example problem is
presented in Ref 17:67. Table II is a comparison of the numerical
differentiation and computer solutions. Note that identical input
data were used and these data were assumed perfect. Therefore, at
this point, no claim can be made regarding the ability to handle
altitude measurements containing normal measurement error.

Table II Comparison of Computer and Numerical Differentiation Solutions of Example Problem 3-1		
Orbital Parameter	Numerical Differentiation Solution	Computer Solution
a	3575 NM	3575.9 NM
e	0.0101	0.0100
$t_2 - t_o$	56.8 min	57.43 min
Period	89.3 min	89.40 min

Example Problem 3-2. The translunar injection burn has been

catastrophic. In addition to premature engine shutdown, the space-

craft tumbled during the burn. The result is that the present

spacecraft orbit is completely unknown. Other emergencies dictate

that the orbit must be determined manually.

Solution:

The following altitudes are obtained at 30 minute

intervals:

$$h_1 = 7232.8 \text{ NM}$$

$$h_2 = 9078.8 \text{ NM}$$

$$h_3 = 10373.2 \text{ NM}$$

These altitudes are known to be slightly in error. The actual altitudes are:

$$(h_1)_{ACT} = 7195.833 \text{ NM}$$

$$(h_2)_{ACT} = 9031.767 \text{ NM}$$

$$(h_3)_{ACT} = 10348.165 \text{ NM}$$

but the astronauts must use their only information--the measured altitudes. The expressions for $\dot{r}$ and $\ddot{r}$ become

$$\dot{r}_2 = \frac{h_3 - h_1}{2t} = \frac{10373.2 - 7232.8}{2(30)} = 52.34 \text{ NM/MIN}$$

$$\ddot{r}_2 = \frac{h_1 + h_3 - 2h_2}{t^2} = \frac{7232 + 10373 - 2(9078)}{30^2}$$

$$= -0.6138 \text{ NM/MIN}^2$$

For the earth, μ and $\sqrt{\mu}$ are

$$\mu = 225.90258 \times 10^6 \text{ NM}^3/\text{MIN}^2$$

$$\sqrt{\mu} = 15.03005 \times 10^3 \ (\text{NM}^3/\text{MIN}^2)^{1/2}$$

The radial distance from the earth's center is obtained by adding

47

the earth's radius $R_\oplus$ to the altitude reading h_2

$$r_2 = h_2 + R_\oplus = 9079 + 3440 = 12,519 \text{ NM}$$

The semimajor axis a is

$$a = \frac{\mu}{\dfrac{\mu}{r_2} - \dot{r}_2{}^2 - r_2\ddot{r}_2} = \frac{(225.9)\ 10^6}{\dfrac{(225.9)\ 10^6}{12519} - (52.34)^2 + (12519)(.6138)}$$

$$a = \frac{(225.9)\ 10^6}{(22980)} = \underline{9830 \text{ NM}}$$

The period of the orbit is

$$P = 2\pi\sqrt{\frac{a^3}{\mu}} = \frac{(4.180)\ 10^{-4}\ (9830)(99.15)}{(60)} = \underline{6.79 \text{ hr}}$$

The eccentric anomaly at r_2 is obtained from

$$\tan E_2 = \frac{r_2\ \dot{r}_2\ \sqrt{a}}{\sqrt{\mu}\ (a - r_2)} = \frac{(12519)(52.34)(99.15)}{(15.03)\ 10^3\ (9830 - 12519)} = -1.607$$

$$E_2 = \underline{121.88°}$$

The eccentric anomaly is less than $180°$ since the radial distance is increasing. The orbital eccentricity is given by

$$e = \frac{r_2\ \dot{r}_2}{\sqrt{\mu}\ \sqrt{a}\ \sin E_2} \qquad \frac{(12519)(52.34)}{(15.03)\ 10^3\ (99.15)(.8491)} = 0.517$$

The actual orbit, the computed orbit using perfect range measurements, and the approximate orbit using the measured values of range are shown in Table III.

Table III

Comparison of Geometric Parameters
of Example Problem 3-2

	Actual Orbit	Computed Orbit Using Perfect Range Values	Computed Orbit Using Measured Values of Range
a	10,000 NM	10,017 NM	9831.5 NM
e	0.5000	0.4998	0.5177
E_2	119.629°	119.364°	121.88°

Example Problem 3-2 was selected to illustrate two points:

1. Measurement error is always present.
2. Comparison of computer versus manual solutions where the same input data is used is meaningless when measurement error is present. The important question is: How far is the manual solution from the _real_ orbit?

The adverse effect of measurement error will be examined further in the next section.

Summary

The geometric elements can be obtained quite easily by obtaining a series of successive range measurements at equal time intervals. Numerical differentiation of these measurements yields the radial velocity and radial acceleration at one of the range readings. With knowledge of range, radial velocity, and radial acceleration, the geometric elements a, e, and E are readily determined from fairly simple equations. A block diagram outlining the steps required to obtain the geometric parameters is shown below.

$$\boxed{\begin{array}{c}\text{Obtain set of range measurements}\\ \text{from attracting center}\end{array}}$$

$$\downarrow$$

$$\boxed{\begin{array}{c}\text{Numerically differentiate to}\\ \text{obtain } \dot{r} \text{ and } \ddot{r}\end{array}}$$

$$\downarrow$$

$$\boxed{\text{Compute a from } a = \frac{\mu}{\dfrac{\mu}{r} - \dot{r}^2 - r\,\ddot{r}}}$$

$$\downarrow$$

$$\boxed{\text{Compute E from } \tan E = \frac{r\,\dot{r}\,\sqrt{a}}{\sqrt{\mu}\,(a - r)}}$$

$$\downarrow$$

$$\boxed{\text{Compute e from } e \sin E = \frac{r\,\dot{r}}{\sqrt{\mu}\,\sqrt{a}}}$$
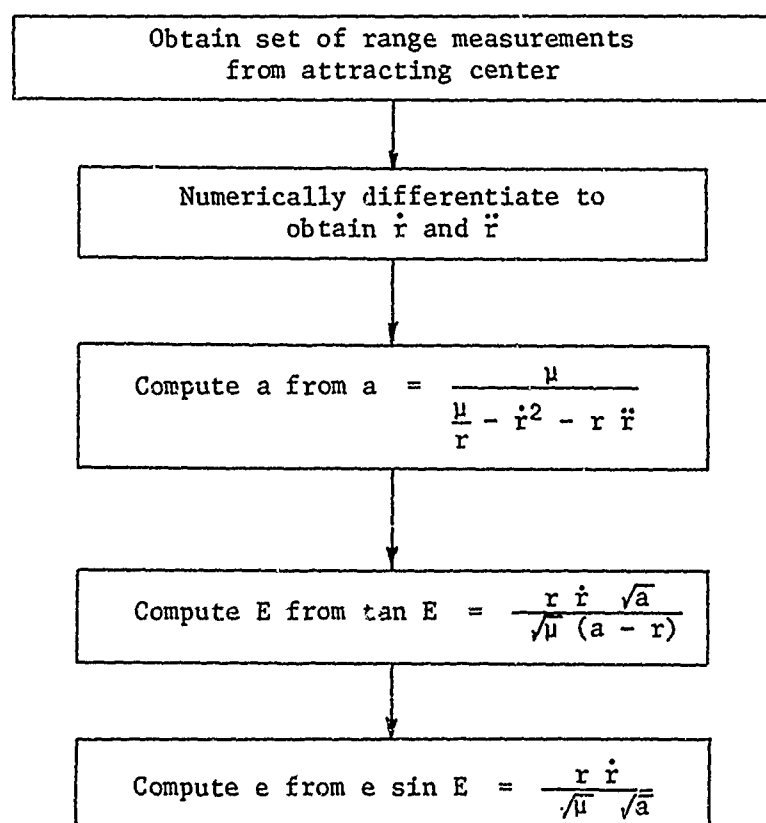
Preliminary Error Analysis

Introduction. Before any orbit determination scheme can be presented in "flight manual" form, it must be determined if the method will, in fact, yield the desired results. Example Problem 3-2 illustrated that measurement error cannot be ignored.

This section is a preliminary error analysis of the numerical differentiation method of orbit determination. The word "preliminary" is used since a statistical approach is not used. Rather, the role of measurement error is studied by determining the worst effect it could produce. The general results and conclusions from either type of error analysis are similar.

The trajectory considered is that which tests manual navigation capability to the utmost--the high eccentricity ellipse. Although this will highlight the shortcomings of the numerical differentiation scheme, readers should deduce that as eccentricity is lowered, the effect of measurement error is somewhat reduced.

The major error sources in the numerical differentiation technique of orbit determination are:

1. numerical differentiation truncation error

2. range measurement error

3. timing measurement error.

Each of these error sources will be discussed.

Truncation Error Effect. Truncation error results from using numerical differentiation to obtain radial velocity and radial acceleration. Using five tabulations, the truncation error for the

first derivative is given by

$$y'(x_0) - p'(x_0) = \frac{h^4}{30} y^{(5)}(\xi) \qquad (3\text{-}12)$$

where

$$y'(x_0) = \text{actual derivative}$$

$$p'(x_0) = \text{approximate derivative}$$

$$h = x_1 - x_0 \text{ (the tabular interval)}$$

$$\xi = \text{some value of } x, \text{ generally} \\ \text{indeterminate, within the range} \\ \text{of values of } x \text{ under consideration.}$$

A derivation of this equation may be found in Ref 16:101. Applied to the orbit determination problem

$$\dot{r}_{3\,(\text{Actual})} - \dot{r}_{3\,(\text{Approx})} = \frac{t^4}{30} r^{(5)}(\xi) \qquad (3\text{-}13)$$

for five range measurements. The presence of t^4 in the numerator suggests that t, the time interval between readings of range, should be small if truncation error is to be minimized. A similar conclusion holds for the second derivative. For three range measurements, the expression for truncation error for $\ddot{r}_2$ is

$$\ddot{r}_{2\,(\text{Actual})} - \ddot{r}_{2\,(\text{Approx})} = \frac{-t^2}{12} r^{(4)}(\xi) \qquad (3\text{-}14)$$

Since determination of truncation error using the formulas above is only an estimate, the effect of truncation error on the orbit determination scheme was obtained in a slightly different manner. Accurate

values of range at equal time intervals were obtained by computer for a representative high eccentricity trajectory. Then the actual orbital parameters were compared with those obtained from the formulas involving numerical differentiation. The results are presented graphically in Figs. 12, 13, and 14. Note that in all cases, truncation error, as expected, increases as the time interval between range measurements is increased.

Range and Timing Measurement Error. Inaccurate values of range are a major source of error in the numerical determination of $\dot{r}$ and $\ddot{r}$. In addition to its effect through the numerical differentiation process, an inaccurate range measurement also directly affects the values of the orbital elements through the value of r itself (since the equations for a, e, and E each contain an explicit value of range). Therefore, it is necessary to consider the effect of errors in range measurement on the orbit determination method being considered. Another error source is that of timing between measurements. The following presentation will begin with a brief discussion of how range measurement error affects the numerical differentiation process. Then the effect of range and timing measurement error will be investigated for each of the orbital parameters being considered.

Measurement Error Effect - Numerical Differentiation. A major step in the orbit determination method being considered is the numerical determination of $\dot{r}$ and $\ddot{r}$ from a set of range measurements. A brief discussion of how inaccurate range measurements can affect these derivatives is thus in order. The cumulative effect of
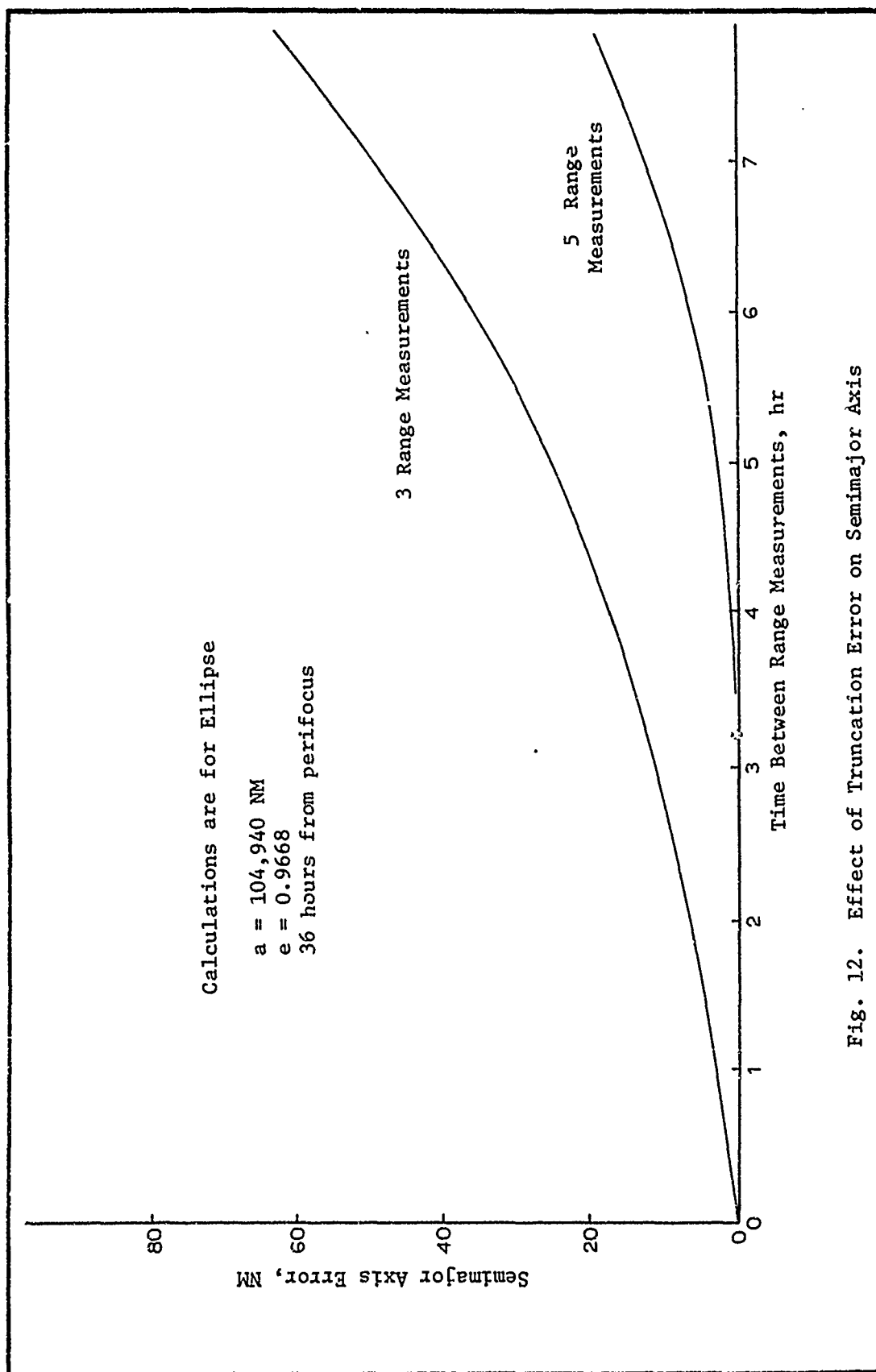
Fig. 12. Effect of Truncation Error on Semimajor Axis

Calculations are for Ellipse

a = 104,940 NM
e = 0.9668
36 hours from perifocus

3 Range Measurements

5 Range Measurements

Time Between Range Measurements, hr

Semimajor Axis Error, NM
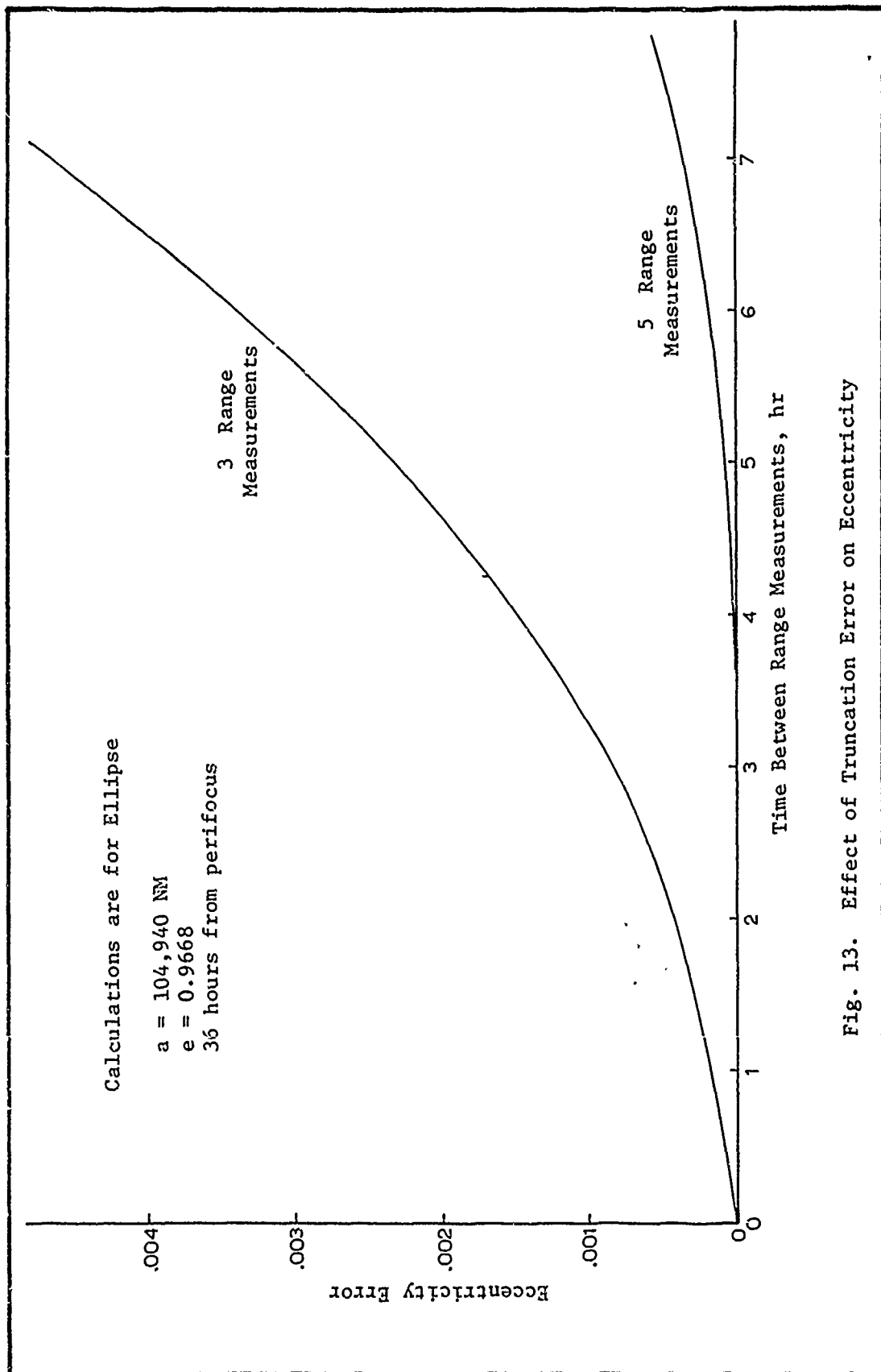
Fig. 13. Effect of Truncation Error on Eccentricity
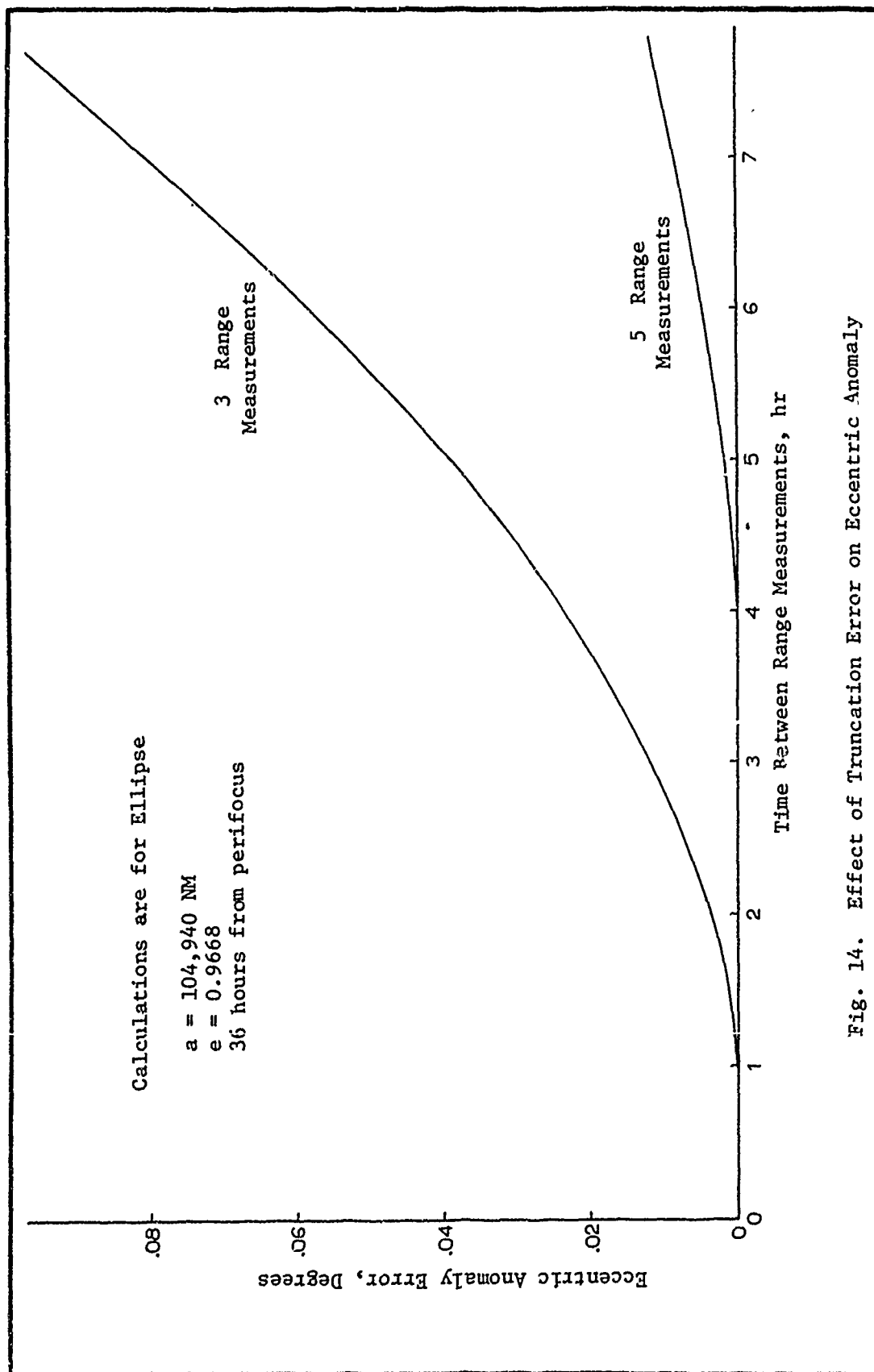
Fig. 14. Effect of Truncation Error on Eccentric Anomaly

measurement errors on the final output--the orbital parameters--will be treated in a later section.

Assume that ϵ_1, ϵ_2, --- ϵ_5 represent the errors associated with each measurement of range and that R_1, R_2, --- R_5 are the actual range values that should be observed. Then

$$R_1 = r_1 + \epsilon_1 \tag{3-15}$$

where r_1 represents the observed range. Then using this definition in the five-measurement differentiation formula, the error in output due to input inaccuracy is

$$\frac{(R_1 - R_5) - 8(R_2 - R_4)}{12t} - \frac{(r_1 - r_5) - 8(r_2 - r_4)}{12t}$$

$$= \frac{(\epsilon_1 - \epsilon_5) - 8(\epsilon_2 - \epsilon_4)}{12t} \tag{3-16}$$

If ϵ_1, . . . ϵ_5 do not exceed ϵ_{max} in magnitude, the output error is, at worst

$$\begin{array}{l}\text{Maximum output error in} \\ \dot{r}_3 \text{ due inaccurate data}\end{array} = \frac{18\epsilon_{max}}{12t} = \frac{3\epsilon_{max}}{2t} \tag{3-17}$$

A small time interval t generally associated with high accuracy (i.e., small truncation error) thus magnifies the effect of measurement error--many times making the trouble of minimizing truncation error pointless.

By similar analysis, the maximum error for the second derivative

(using five measurements again) is

$$\text{Maximum output error in } \dddot{r}_3 \text{ due inaccurate data} = \frac{16\varepsilon_{max}}{3t^2} \qquad (3\text{-}18)$$

This shows that higher derivatives become increasingly inaccurate as
the time interval is reduced. Note, however, the particular arrange-
ment of measurement errors such that $\dot{r}$ and $\ddot{r}$ both exhibit their
maximum errors at the same time cannot occur. Nevertheless, the adverse
effect of measurement error on numerical differentiation is severe.
Long time intervals between measurements act to reduce this adverse
effect.

The cumulative effect of measurement errors (thus including
numerical differentiation) on the final output--the orbital parameters--
is the topic of the next section.

Estimate of the Error in Determining a, e, and E. The orbit
determination scheme, as developed so far, involves the measurement of
several values of range at equal time intervals. These observations
are numerically differentiated to yield $\dot{r}$ and $\ddot{r}$ for the central
measurement and then the geometric orbital elements are obtained from
the three equations

$$a = \frac{\mu}{\frac{\mu}{r} - \dot{r}^2 - r\ddot{r}} \qquad (3\text{-}2)$$

$$\tan E = \frac{r\,\dot{r}\,\sqrt{a}}{\sqrt{\mu}\,(a - r)} \qquad (3\text{-}19)$$

$$e \sin E = \frac{r\,\dot{r}}{\sqrt{\mu}\,\sqrt{a}} \qquad (3\text{-}4)$$

The error arising from numerical differentiation has been briefly discussed. It remains to determine the overall effect of measurement errors on the values of a, ϵ, and E obtained through the use of these approximate data in the three equations listed above.

In general, the maximum error E_u in the value of a function is given by

$$E_u = \left|\frac{\partial f}{\partial x}\right|_{\substack{x = a \\ y = b}} E_a + \left|\frac{\partial f}{\partial y}\right|_{\substack{x = a \\ y = b}} E_b \tag{3-20}$$

where

$$E_a = \left|\text{Max error in function argument } a\right|$$

$$E_b = \left|\text{Max error in function argument } b\right|$$

A derivation of this expression is shown in Appendix C. This expression will be used to examine the possible errors in orbital parameters due to measurement errors.

Error in Major Axis Determination. For the following analysis, it is assumed that truncation error in the determination of $\dot{r}$ and $\ddot{r}$ is negligible (a valid assumption if a sufficient number of range measurements are used). Then the maximum error in a, due to range

measurement and timing error, is

$$E_a = \left|\frac{\partial a}{\partial r_1}\right| E_{r_1} + \left|\frac{\partial a}{\partial r_2}\right| E_{r_2} + \left|\frac{\partial a}{\partial r_3}\right| E_{r_3} + \left|\frac{\partial a}{\partial r_4}\right| E_{r_4}$$

$$+ \left|\frac{\partial a}{\partial r_5}\right| E_{r_5} + \left|\frac{\partial a}{\partial t}\right| E_t \qquad (3-21)$$

for five measurements of range. Assuming $E_{r_1} = E_{r_2} \cdots E_{r_5}$ then

$$E_a = \left[\left|\frac{\partial a}{\partial r_1}\right| + \left|\frac{\partial a}{\partial r_2}\right| + \left|\frac{\partial a}{\partial r_3}\right| + \left|\frac{\partial a}{\partial r_4}\right| + \left|\frac{\partial a}{\partial r_5}\right| \right] E_r$$

$$+ \left|\frac{\partial a}{\partial t}\right| E_t \qquad (3-22)$$

The equation for a is

$$a = \frac{\mu}{\frac{\mu}{r} - \dot{r}^2 - r\,\ddot{r}} \qquad (3-2)$$

and for five measurements,

$$\frac{\partial a}{\partial x} = \mu \left(\frac{\mu}{r_3} - \dot{r}_3{}^2 - r_3\,\ddot{r}_3\right)^{-2} \left(\frac{\mu}{r_3{}^2}\frac{\partial r_3}{\partial x} + 2\dot{r}_3\frac{\partial \dot{r}_3}{\partial x} + r_3\frac{\partial \ddot{r}_3}{\partial x}\right.$$

$$\left. + \ddot{r}_3\frac{\partial r_3}{\partial x}\right) \qquad (3-23)$$

where x is taken to successively represent r_1, r_2, $\cdots$ r_5, and t.
The partial derivatives of $\dot{r}$ and $\ddot{r}$ may be obtained by differentiating
the approximate differentiation formulas. For convenience, let $C_{a,r}$
represent the coefficient of E_r and $C_{a,t}$ the coefficient of E_t. Then

$$E_a = C_{a,r} E_r + C_{a,t} E_t \tag{3-24}$$

where

$$C_{a,r} = \left|\frac{\partial a}{\partial r_1}\right| + \left|\frac{\partial a}{\partial r_2}\right| + \left|\frac{\partial a}{\partial r_3}\right| + \left|\frac{\partial a}{\partial r_4}\right| + \left|\frac{\partial a}{\partial r_5}\right| \tag{3-25}$$

and $C_{a,t} = \left|\partial a/\partial t\right|$. Then by examining the behavior of $C_{a,r}$ and
$C_{a,t}$ the steps required to minimize the effect of range measurement
error can be determined.

A computer program was written to evaluate the coefficients $C_{a,r}$
and $C_{a,t}$ for various values of t and for a high eccentricity trajectory
similar to the initial translunar coast portion of a moon mission. The
results are presented graphically in Figs. 15 and 16. It should be
noted that Figs. 15 and 16 yield the behavior of the maximum error--not
the actual or rms error.

Error in Eccentric Anomaly Determination. Eccentric anomaly error
can be investigated using the same procedure as was followed in examining
the error in major axis determination. The equation for eccentric
anomaly is

$$E = \tan^{-1} \frac{r \; \dot{r} \; \sqrt{a}}{\sqrt{\mu} \; (a - r)} \tag{3-19}$$

61
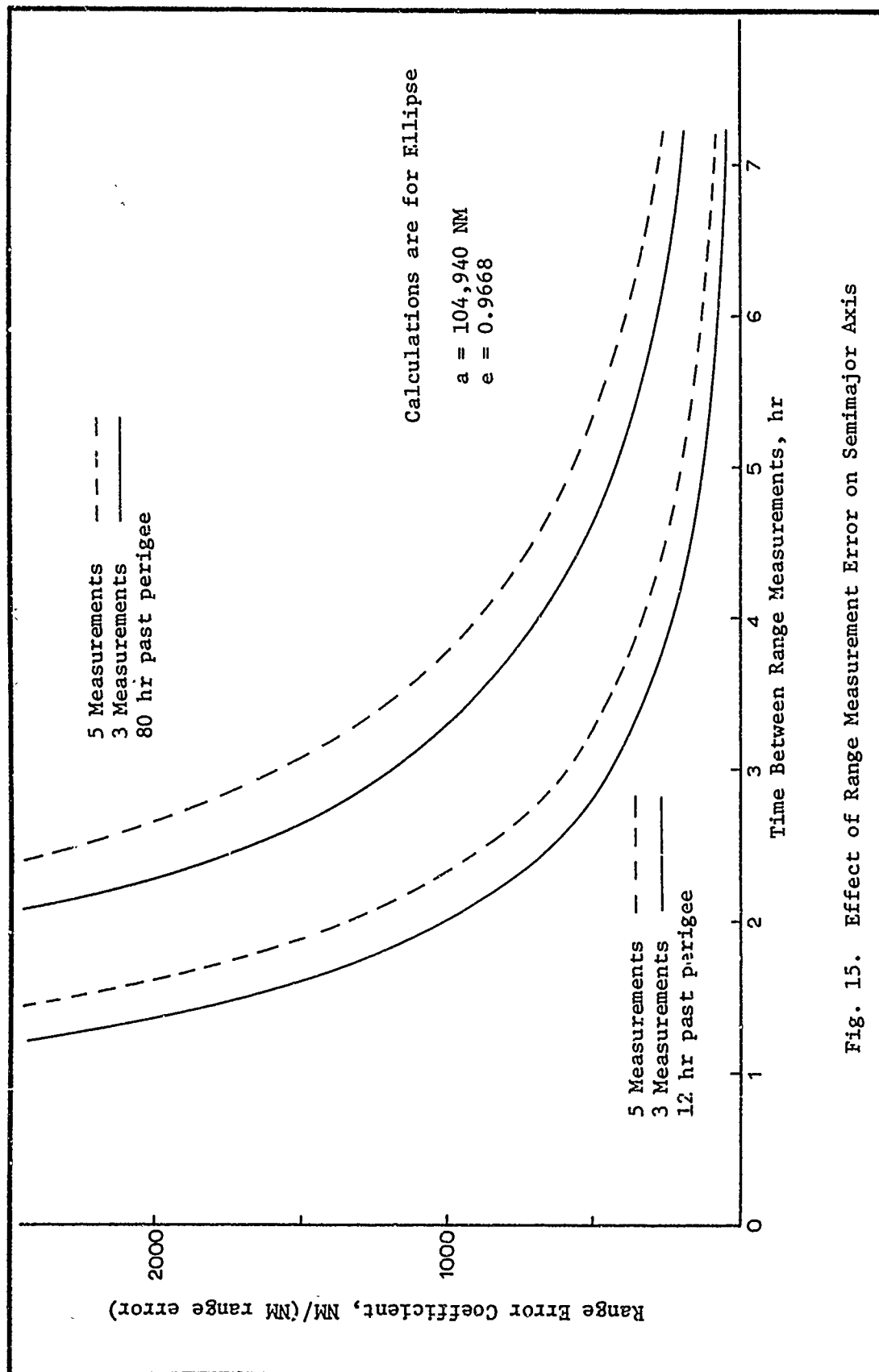
Fig. 15. Effect of Range Measurement Error on Semimajor Axis
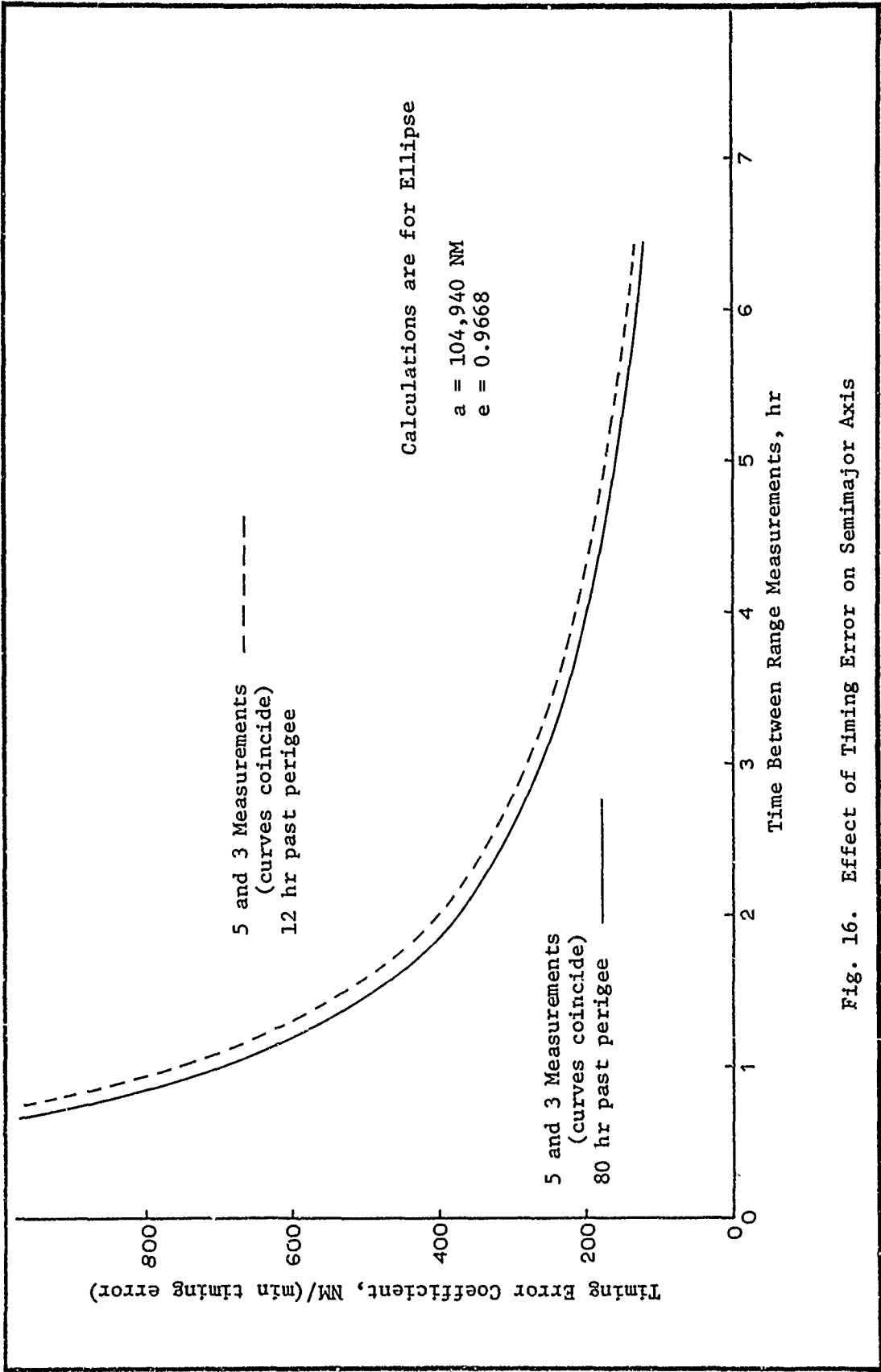
Fig. 16. Effect of Timing Error on Semimajor Axis

and substituting for a, this equation becomes

$$E = \tan^{-1} \frac{\dot{r} \left(\frac{\mu}{r} - \dot{r}^2 - r\ddot{r}\right)^{1/2}}{(\dot{r}^2 + r\ddot{r})} \tag{3-26}$$

For simplication, let

$$u = \dot{r}$$

$$v = \left(\frac{\mu}{r} - \dot{r}^2 - r\ddot{r}\right)^{1/2} \tag{3-27}$$

$$w = (\dot{r}^2 + r\ddot{r})$$

then

$$E = \tan^{-1} \frac{uv}{w} \tag{3-28}$$

Taking partial derivatives as before,

$$\frac{\partial E}{\partial x} = \frac{1}{1 + \frac{u^2 v^2}{w^2}} \cdot \frac{w \left(u \frac{\partial v}{\partial x} + v \frac{\partial u}{\partial x}\right) - u v \frac{\partial w}{\partial x}}{w^2} \tag{3-29}$$

(the independent variable x is again taken to successively represent r_1, r_2, $\cdots$ r_n, t). The maximum error in E (E_E) due to range measurement and timing errors is then

$$E_E = \left|\frac{\partial E}{\partial r_1}\right| E_{r_1} + \left|\frac{\partial E}{\partial r_2}\right| E_{r_2} + \cdots + \left|\frac{\partial E}{\partial r_n}\right| E_{r_n} + \left|\frac{\partial E}{\partial t}\right| E_t \tag{3-30}$$

where n denotes the number of range measurements taken. Again assuming $E_{r_1} = E_{r_2} = \ldots E_{r_n}$

$$E_E = \left[\left| \frac{\partial E}{\partial r_1} \right| + \left| \frac{\partial E}{\partial r_2} \right| + \ldots + \left| \frac{\partial E}{\partial r_n} \right| \right] E_r + \left| \frac{\partial E}{\partial t} \right| E_t \qquad (3\text{-}31)$$

or

$$E_E = C_{E,r} E_r + C_{E,t} E_t \qquad (3\text{-}32)$$

where $C_{E,r}$ and $C_{E,t}$ represent the coefficients of E_r and E_t respectively. Again, $C_{E,r}$ and $C_{E,t}$ can be examined and the steps required to minimize the effect of measurement errors can be determined.

Figures 17 and 18 are the graphical results of a computer program written to evaluate $C_{E,r}$ and $C_{E,t}$ for a typical trajectory.

Error in Eccentricity Determination. The effect of measurement error on the calculation of eccentricity can be examined in the same manner as for the major axis and eccentric anomaly. The expression for eccentricity is

$$e = \frac{a - r}{a \cos E} \qquad (3\text{-}33)$$

Differentiating as before

$$\frac{\partial e}{\partial x} = \frac{(a \cos E)\left[\frac{\partial a}{\partial x} - \frac{\partial r}{\partial x} \right] - (a - r)\left[(- a \sin E) \frac{\partial E}{\partial x} + (\cos E) \frac{\partial a}{\partial x} \right]}{a^2 \cos^2 E} \qquad (3\text{-}34)$$
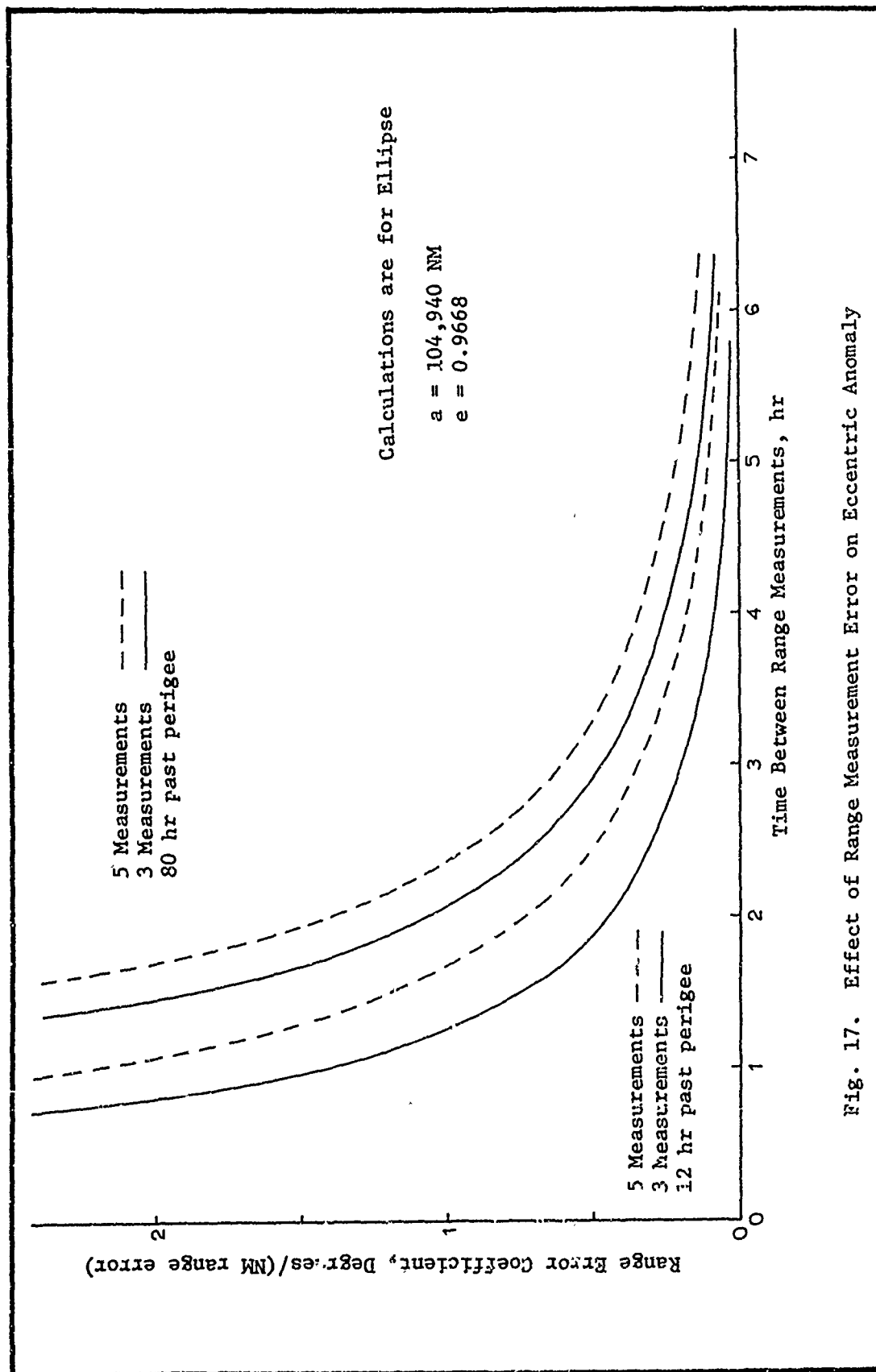
Fig. 17. Effect of Range Measurement Error on Eccentric Anomaly
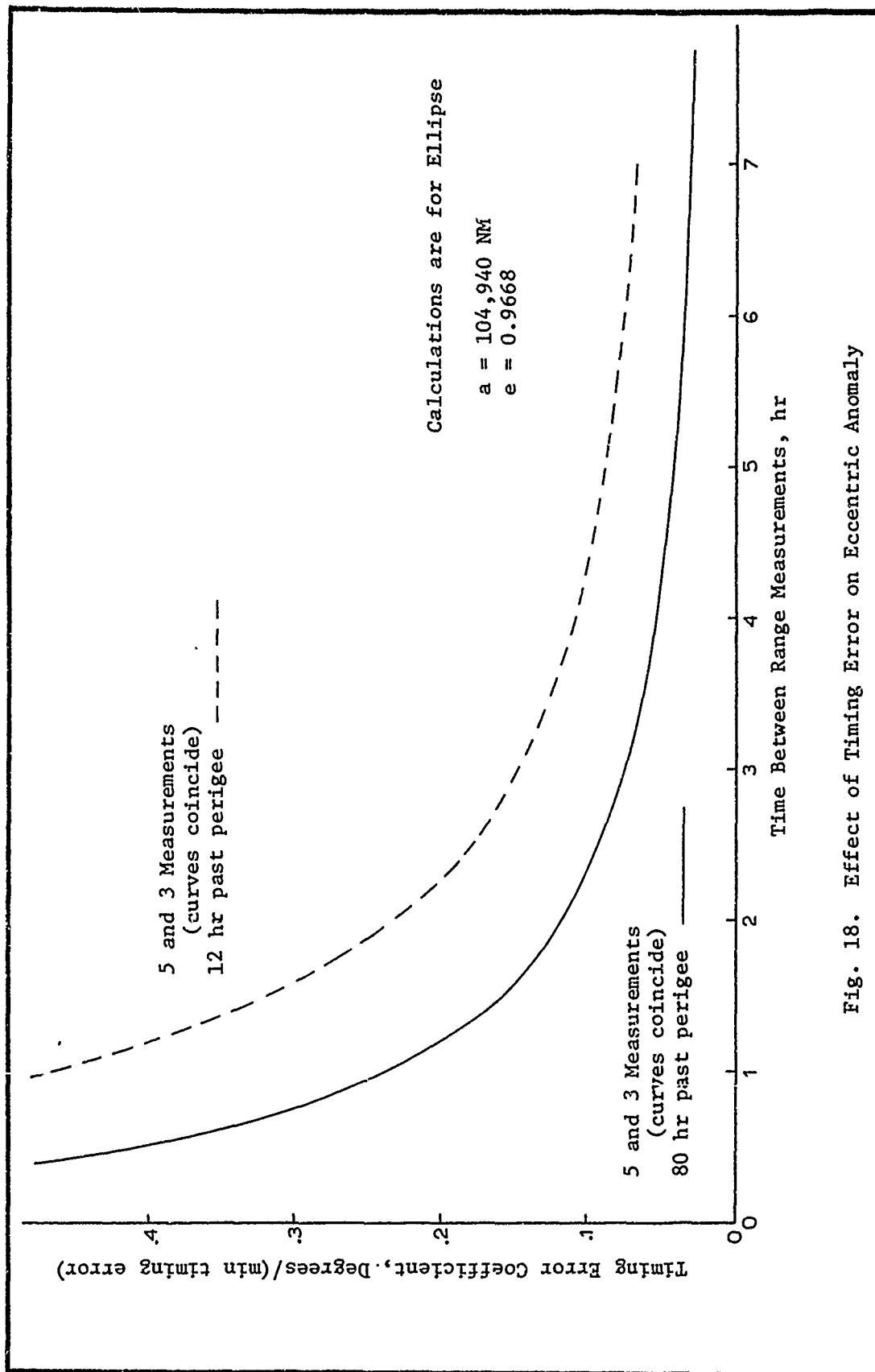
Fig. 18. Effect of Timing Error on Eccentric Anomaly

where the independent variable x is again taken successively as r_1, r_2, ... r_n, and t. The maximum error in e is then approximately

$$E_e = \left[\left[\left| \frac{\partial e}{\partial r_1} \right| + \left| \frac{\partial e}{\partial r_2} \right| + \ldots + \left| \frac{\partial e}{\partial r_n} \right| \right] \right] E_r + \left| \frac{\partial e}{\partial t} \right| E_t \qquad (3-35)$$

or

$$E_e = C_{e,r} E_r + C_{e,t} E_t \qquad (3-36)$$

where E_e is the maximum error in eccentricity and $C_{e,r}$ and $C_{e,t}$ represent the coefficients of range measurement error E_r and timing error E_t respectively.

Figures 19 and 20 are the graphical results of a computer program written to evaluate $C_{e,r}$ and $C_{e,t}$ for a typical trajectory.

Accuracy of Range Measurement. Measurement of the earth's angular diameter is assumed the primary means of determining distance from the earth. The geometry of the measurement is shown in Fig. 21.
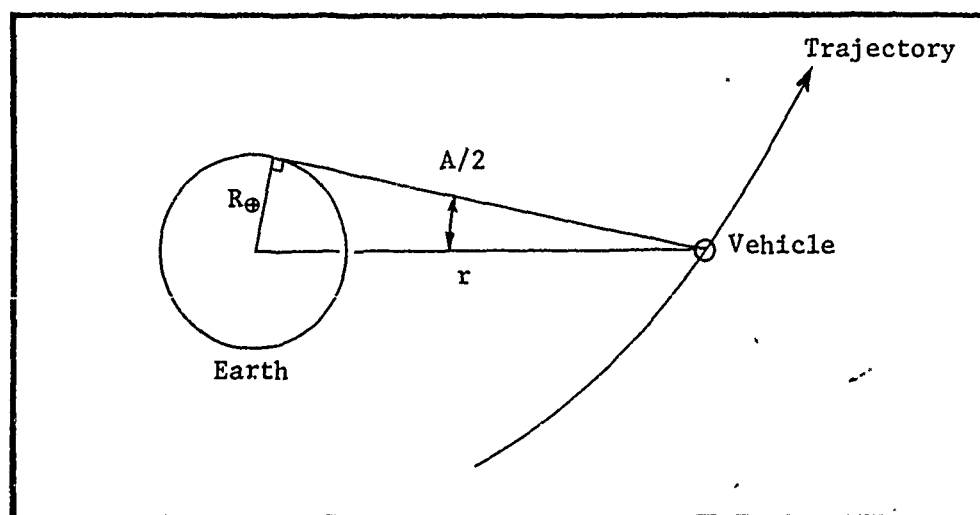
Fig. 21

Range Measurement Geometry

68
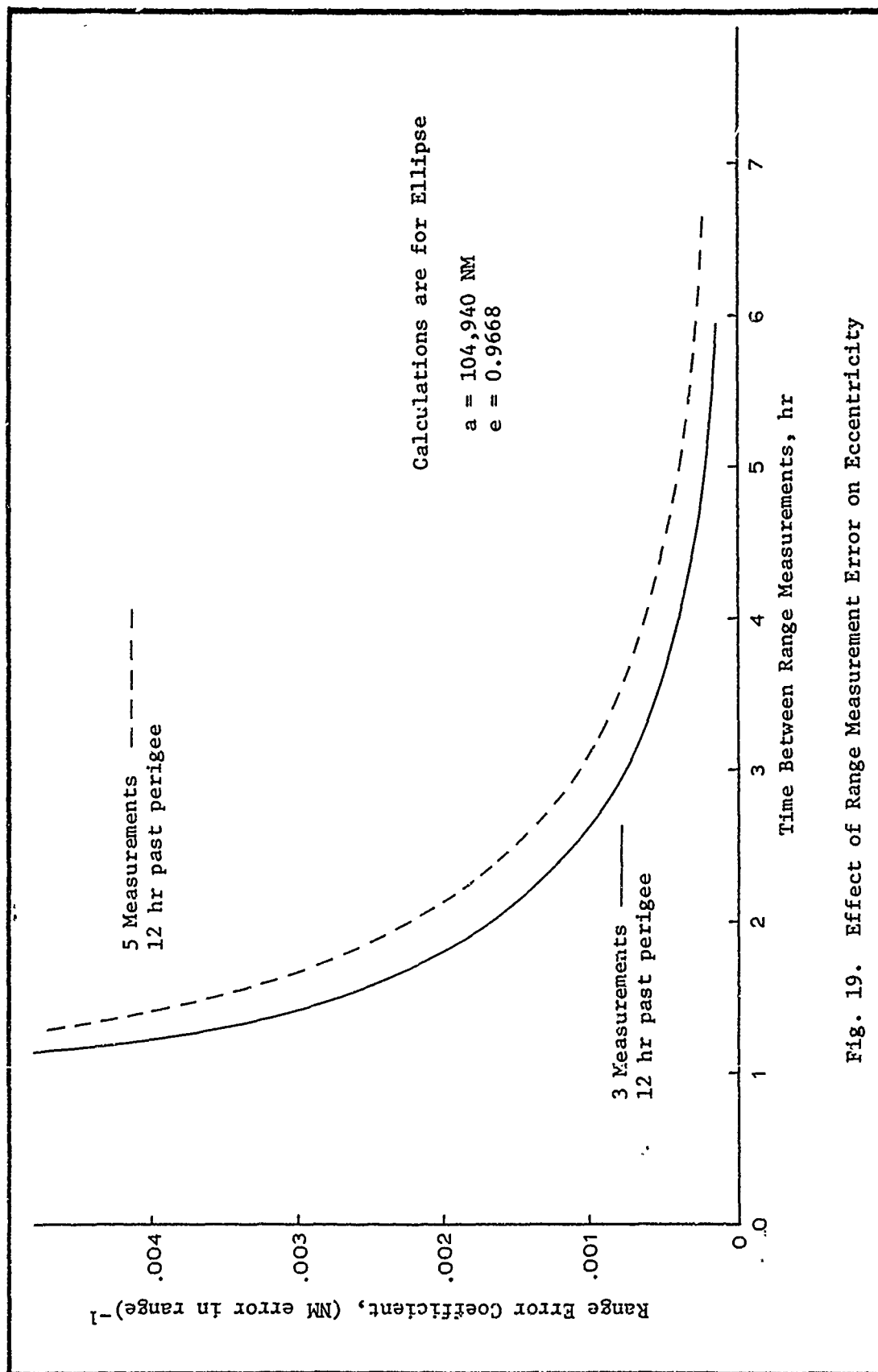
Fig. 19. Effect of Range Measurement Error on Eccentricity
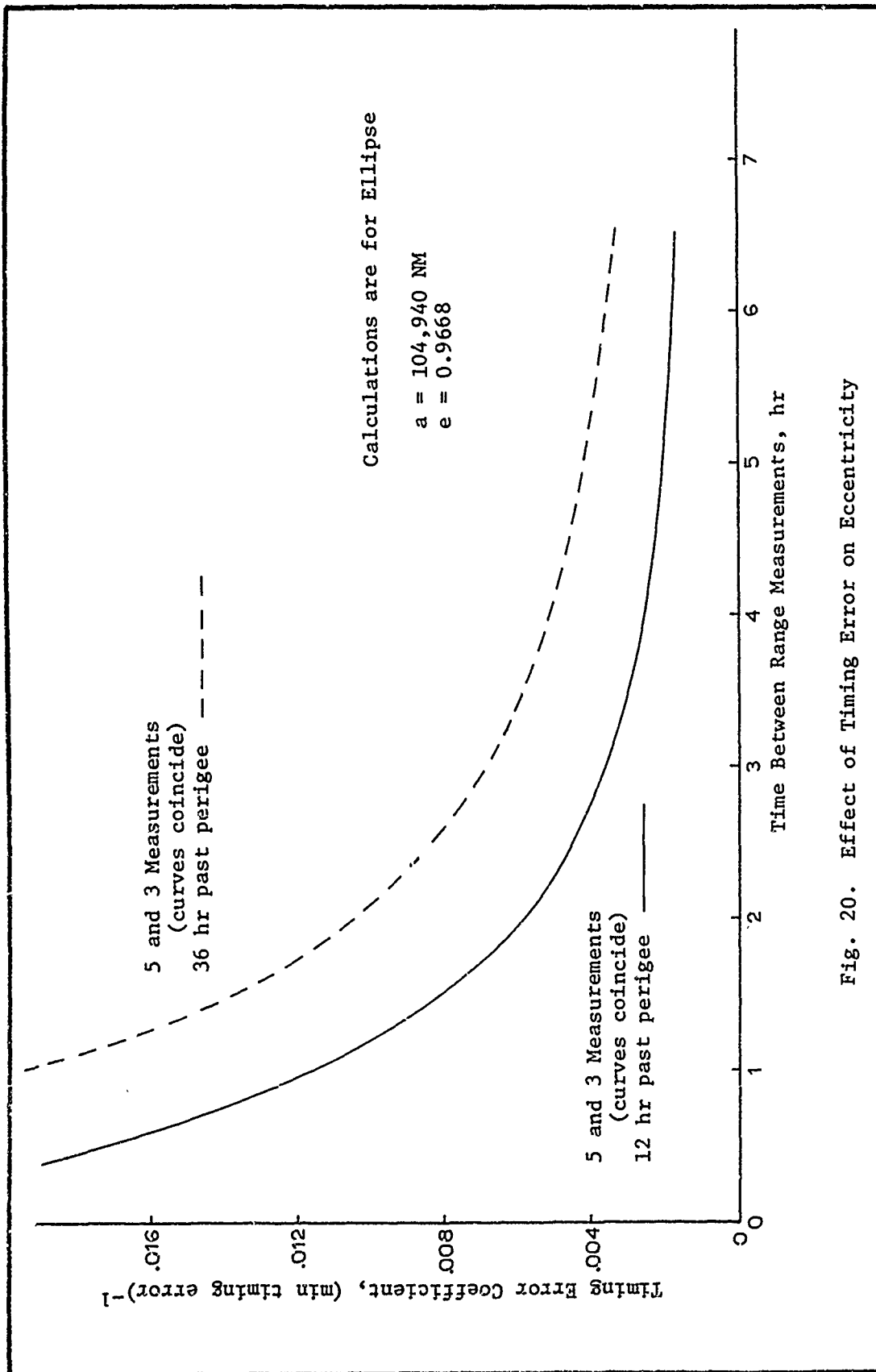
Fig. 20. Effect of Timing Error on Eccentricity

The distance r is given by the equation

$$r = \frac{R_\oplus}{\sin \frac{A}{2}} \tag{3-37}$$

where $R_\oplus$ is the radius of the earth and A is the earth's subtended angle as measured from the spacecraft. Then

$$dr = \frac{- R_\oplus \cos A/2}{2 \sin^2 A/2} dA \tag{3-38}$$

As distance from the earth increases, the angle A becomes smaller--the net result for a given measurement error dA is a decrease in accuracy as distance from the earth increases. Figure 22, from "Space Position Fixing Techniques," (Ref 22:318), is a graph showing the error in distance per minute error in A as a function of distance from the earth. Note that statute, not nautical, miles are presented on the graph.

With proper training, practice, and instrument calibration, sighting measurement error can be held appreciably below one arc minute (Ref 17:5). Therefore, Fig. 22 can be considered to represent the upper bound on range measurement error.

When only a portion of the earth's horizon is visible, the stadimeter, a device which measures the curvature of the horizon, can be used to determine altitude (Ref 17:12). The stadimeter is designed to measure altitudes below 2500 NM. The trajectories considered in this thesis are generally above this altitude.
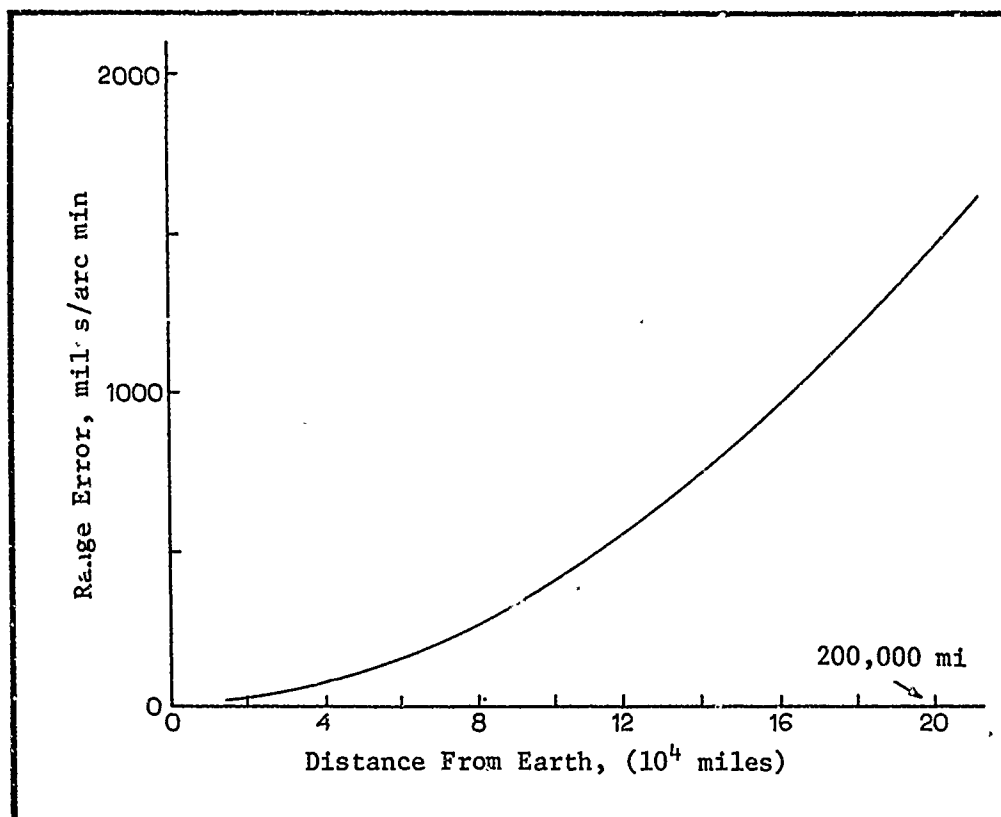
Fig. 22

Range Measurement Error

Summary. In comparison to the severe effect of measurement error, the truncation error resulting from numerical differentiation is negligible. Tables IV and V are tabulations showing specific values of maximum error effects. In all cases, it is seen that measurement error is by far the major culprit in producing erroneous orbital parameter values. Increasing the time interval between measurements decreases the effect of measurement error. This decrease more than offsets the resulting increase in truncation error. For a trajectory of extremely high eccentricity (as those being considered in this thesis), time intervals on the order of hours are necessary.

72

Table IV

Summary of Error Effects

Calculations for Ellipse: a = 104,940 NM
e = .9668
E = 70.434° (12 hr past perigee)

Time between measurements	Orbital Element	three range measurements			five range measurements		
		Truncation Error	Max Error per NM range measurement error	Max Error per minute timing error	Truncation Error	Max Error per NM range measurement error	Max Error per minute timing error
One Hour	a (NM)	27	3845	1676	2	5124	1674
	e	.0004	.0073	.0111	0	.0098	.0110
	E (Deg)	.014	1.70	.450	.002	2.28	.450
Three Hours	a (NM)	243	428	563	32	569	558
	e	.0040	.0007	.0037	.0007	.0011	.0037
	E (Deg)	.110	.190	.150	.009	.250	.150
Five Hours	a (NM)	677	155	343	550	206	342
	e	.0117	.0002	.0023	.0091	.0004	.0022
	E (Deg)	.312	.070	.090	.138	.090	.090
Six Hours	a (NM)	977	108	289	982	144	289
	e	.0176	.0001	.0020	.0215	.0003	.0018
	E (Deg)	.459	.050	.080	.366	.060	.070

Table V

Summary of Error Effects

Calculations for a = 104,940 NM
e = .9668
Ellipse: E = 107.5° (36 hr past perigee)

Time between measurements	Orbital Element	three range measurements			five range measurements		
		Truncation Error	Max Error per NM range measurement error	Max Error per minute timing error	Truncation Error	Max Error per NM range measurement error	Max Error per minute timing error
One Hour	a (NM)	10	7335	789	0	9780	789
	e	.0002	.0579	.0208	0	.0700	.0209
	E (Deg)	.001	4.52	.212	0	6.03	.210
Three Hours	a (NM)	11	815	263	0	1087	263
	e	.0008	.0065	.0069	0	.0080	.0069
	E (Deg)	.012	.503	.070	0	.670	.070
Five Hours	a (NM)	25	293	157	2	391	157
	e	.0023	.0023	.0041	.0001	.0030	.0042
	E (Deg)	.039	.180	.040	.004	.240	.040
Six Hours	a (NM)	65	114	98	21	152	98
	e	.0061	.0009	.0026	.0006	.0012	.0026
	E (Deg)	.105	.070	.020	.012	.090	.020

Another unfortunate situation is also apparent. As distance from the earth increases, the accuracy of range measurement decreases. At the same time, the effect of measurement error on some orbital parameters becomes more severe. It is essential, therefore, to begin orbit determination as near the earth as possible.

It can be safely assumed that timing error can be held to less than five seconds. For the high eccentricity orbits examined and a one hour time interval between readings, five seconds is capable of causing a maximum error in major axis of less than 100 NM. Timing e. rc ; thus not a major drawback in orbit determination using this method.

Conclusions. The conclusions derived from the preliminary error analysis are:

1. Decreasing truncation error by taking five range measurements instead of three is pointless unless extremely accurate range measurements are available.

2. For high eccentricity lunar trajectories, a minimum time interval of five hours between measurements is required to determine the approximate orbit (thus, ten hours are required for orbit determination).

3. Every effort must be directed toward the highest attainable accuracy in range measurements.

4. Timing error of five seconds or less is insignificant.

5. Orbit determination must commence as near the earth as possible.

6. A supplementary correction scheme may be required to further improve the accuracy of the orbital elements.

7. Alternate, more accurate, means of obtaining range, range rate, and radial acceleration should be explored.

8. The use of graphs, slide rule, and/or uninterpolated tabular data is entirely consistent with the degree of accuracy attainable using this orbit determination method.

IV. Differential Correction of Orbital Elements

Introduction

The orbital elements obtained by any means or technique will contain a certain amount of error. For example, in the orbit determination method of Chapter III (orbit determination using range, range rate, and radial acceleration), the orbital elements were found to be increasingly in error as the time interval between range measurements was reduced. This section is a brief discussion of a means to correct the geometric elements of a preliminary orbit to obtain more precise values of a, e, and M_o. The method, however, requires the use of a digital or mechanical analog computer because of the complexity of the computations. The inclusion of such a method in a thesis titled "Manual Astronaut Navigation" can be justified by supposing the eventual development of a hand-held back-up computer.

Differential Correction of Geometric Orbit Parameters

Differential correction of orbits is discussed in most books covering methods of orbit determination. For example, see Ref 6:233 or Ref 3:77. Most applications of differential corrections in the field of celestial mechanics, however, require the simultaneous solution of six equations for the corrections to the six independent elements characterizing an orbit. The computation complexity can be reduced somewhat by the technique of dividing the six parameters into two groups--three parameters (a, e, M_o) describing the size

77

and shape of the orbit, and the remaining three (i, Ω, ω) describing

the orbit orientation. Thus, instead of six equations with six unknown

corrections, there are two groups of three equations in three unknowns.

Differential Correction Equations - Geometric Elements

The conic section equation is

$$r = a(1 - e \cos E) \tag{4-1}$$

The total differential dr is then

$$dr = \frac{\partial r}{\partial a} \, da + \frac{\partial r}{\partial e} \, de + \frac{\partial r}{\partial E} \, dE \tag{4-2}$$

Then, approximately,

$$\Delta r = \frac{\partial r}{\partial a} \, \Delta a + \frac{\partial r}{\partial e} \, \Delta e + \frac{\partial r}{\partial E} \, \Delta E \tag{4-3}$$

The quantity Δr can be obtained by comparing the measured value of r

at a certain time with the corresponding preliminary reference orbit

value at the same time. That is,

$$\Delta r = r_{observed} - r_{preliminary \ orbit} \tag{4-4}$$

The partial derivatives are obtained from the conic section equation

and from Kepler's equation. Three values of Δr, obtained at different

times, yield three equations which can be solved for the corrections

to be applied to the preliminary orbital elements. The partial

derivatives with respect to a, e, and E are, from the conic section

78

equation,

$$\frac{\partial r}{\partial a} = 1 - e \cos E = \frac{r}{a} \qquad (4\text{-}5)$$

$$\frac{\partial r}{\partial e} = - a \cos E \qquad (4\text{-}6)$$

$$\frac{\partial r}{\partial E} = a\, e \sin E \qquad (4\text{-}7)$$

The term dE (to be replaced later by ΔE) is better represented in terms of dM_0, the differential change in mean anomaly. The mean angular velocity n is given by

$$n = \sqrt{\frac{\mu}{a^3}} \qquad (4\text{-}8)$$

then

$$\ell n \; n = \frac{1}{2} \ell n \; \mu - \frac{3}{2} \ell n \; a \qquad (4\text{-}9)$$

and

$$\frac{dn}{n} = - \frac{3}{2} \frac{da}{a} \qquad (4\text{-}10)$$

The mean anomaly $\dot{M}$ is given by

$$M = M_0 + n\,(t - t_0) \qquad (4\text{-}11)$$

where t_0 and t are the times corresponding to M_0 and M respectively.

The differential change in mean anomaly is then

$$dM = dM_0 + dn \, (t - t_0) \tag{4-12}$$

Substituting for dn,

$$dM = dM_0 - \frac{3}{2} n \frac{da}{a} (t - t_0) \tag{4-13}$$

Since

$$n(t - t_0) = M - M_0 \tag{4-14}$$

$$dM = dM_0 - \frac{3}{2} \frac{da}{a} (M - M_0) \tag{4-15}$$

From Kepler's equation, $M = E - e \sin E$

$$dM = dE - e \cos E \, dE - \sin E \, de \tag{4-16}$$

or

$$dM = (1 - e \cos E) \, dE - (\sin E) \, de \tag{4-17}$$

and substituting

$$\frac{r}{a} = 1 - e \cos E, \tag{4-1}$$

$$dM = \frac{r}{a} \, dE - (\sin E) \, de \tag{4-18}$$

and solving for dE

$$dE = \frac{a}{r} \left[dM + (\sin E) \, de \right] \tag{4-19}$$

Now substituting for dM

$$dE = \frac{a}{r} \left[dM_0 - \frac{3}{2} \frac{da}{a} (M - M_0) \right] + \frac{a}{r} (\sin E)\, de \qquad (4\text{-}20)$$

Approximating the differentials with the incremental corrections Δa, Δe, and ΔM_0

$$\Delta r = \frac{r}{a} \Delta a - a(\cos E)\, \Delta e + a\, e(\sin E)\, \Delta E \qquad (4\text{-}21)$$

Substituting for ΔE and simplifying results in

$$\Delta r = \left[\frac{r}{a} - \frac{3(M - M_0)\, a\, e\, \sin E}{2r} \right] \Delta a$$

$$+ \left[\frac{a^2 e}{r} \sin^2 E - a \cos E \right] \Delta e$$

$$+ \left[\frac{a^2 e}{r} \sin E \right] \Delta M_0 \qquad (4\text{-}22)$$

The bracketed coefficients of Δa, Δe, and ΔM_0 are to be evaluated on the preliminary orbit at the times corresponding to the range measurements.

Discussion

Three measurements of Δr obtained at different times provides three equations in the unknowns Δa, Δe, and ΔM_0. The equations can be inverted to yield the values Δa, Δe, and ΔM_0. When the number of readings exceeds three, the number of unknowns, the most probable

values of the corrections can be found by least squares--but this
greatly increases the computational load.

Assuming the availability of a back-up computer, the geometric
parameters can be obtained directly from Eq (4-22) by estimating
values of a, e, and M_0 and then correcting these assumed values in an
iterative process until the orbital elements approach the desired
accuracy. However, such a procedure is of questionable value since
any of a number of iterative techniques could be developed to evaluate
the geometric parameters. Also, a number of iterative techniques
are available which yield all six orbital elements--so why iterate to
obtain only the geometric elements?

A computer program was written to test the effectiveness of the
differential correction procedure. Data generated from previous
computer programs were used to improve an orbit known to be in error.
Only one correction was applied to the erroneous orbit, hence, the
final orbit is still not precise--but further corrections could be
applied to improve the final orbit. Figure 23 is a block diagram
presentation of the results.

Conclusion

The computer makes simple work of the computations involved in
this differential correction scheme. It is out of the question to
consider accomplishing the calculations manually. If a small
back-up computer is available, the differential correction equations
may be of great value because:

    1. The geometric parameters can be refined to more
            accurate values.
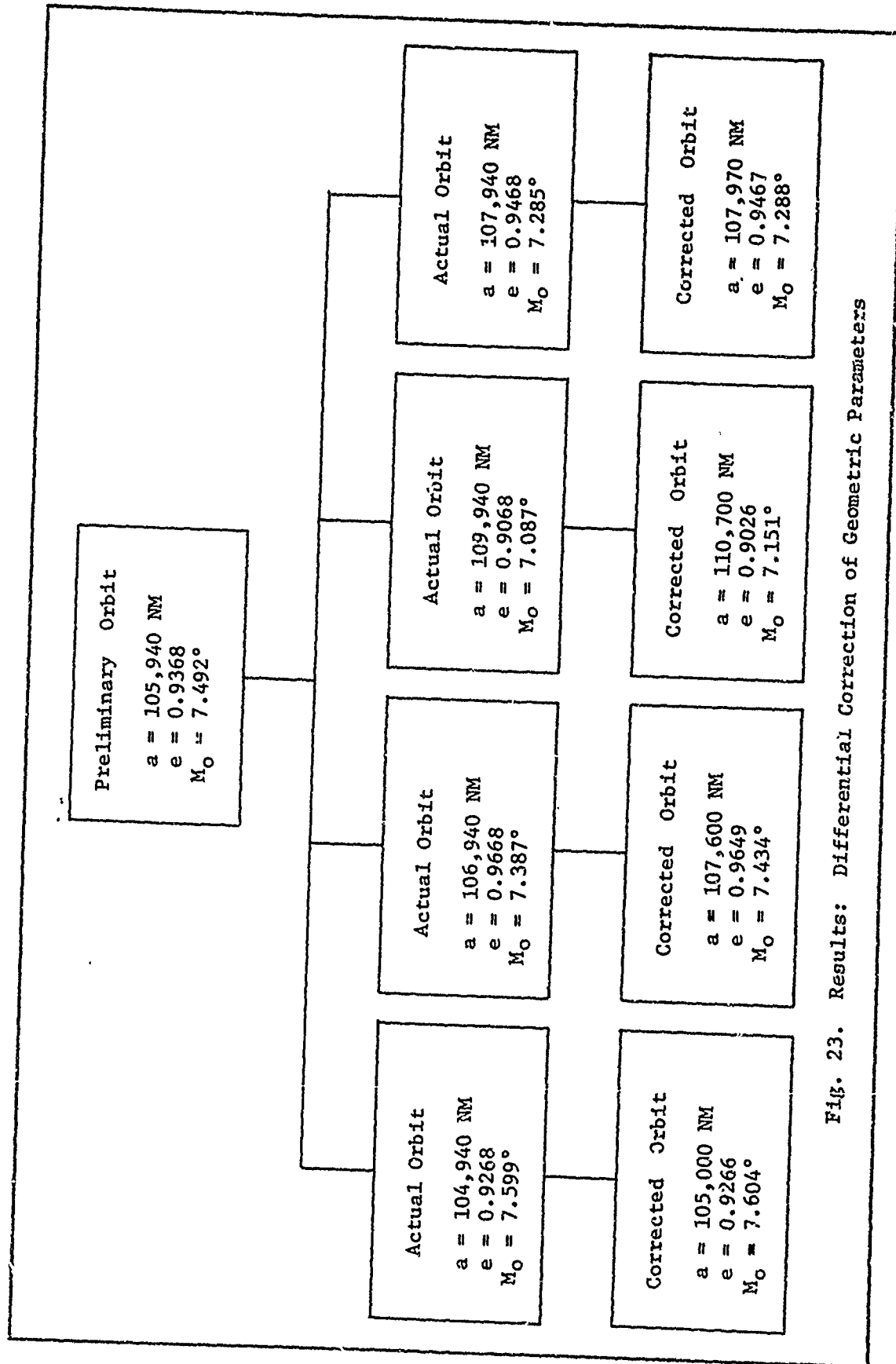
Fig. 23. Results: Differential Correction of Geometric Parameters

Preliminary Orbit

a = 105,940 NM
e = 0.9368
M_O = 7.492°

Actual Orbit

a = 107,940 NM
e = 0.9468
M_O = 7.285°

Corrected Orbit

a. = 107,970 NM
e = 0.9467
M_O = 7.288°

Actual Orbit

a = 109,940 NM
e = 0.9068
M_O = 7.087°

Corrected Orbit

a = 110,700 NM
e = 0.9026
M_O = 7.151°

Actual Orbit

a = 106,940 NM
e = 0.9668
M_O = 7.387°

Corrected Orbit

a = 107,600 NM
e = 0.9649
M_O = 7.434°

Actual Orbit

a = 104,940 NM
e = 0.9268
M_O = 7.599°

Corrected Orbit

a = 105,000 NM
e = 0.9266
M_O = 7.604°

   2. The capability exists to handle redundant data.

The differential correction method will not be considered further

in this thesis. However, the recommendation section will contain a

suggestion for continued study in this area.

V. Orbit Determination Using Position Fixes

Introduction

Two complete three-dimensional fixes in space and knowledge of the time between the two fixes is sufficient for orbit determination using Lambert's theorem (Ref 4:70). Lambert's theorem requires iterative solution and its use is impractical unless a back-up computer is available. By taking another position fix, thus providing three position fixes in space, any of a number of orbit determination methods may be considered (see Ref 3:Ch 1). This section will discuss first a simplified and then a general method of obtaining three-dimensional fixes in space using the hand-held space sextant. These fixes will be used as input to orbit determination methods which will yield both the geometric and orientation orbital elements. Unless otherwise specified, the geocentric equatorial coordinate system is used in this chapter (and succeeding chapters).

Position Vector From Polaris, Earth, 2nd Star

Introduction. The navigation fix in space is discussed in Ref 4:221. In general, a three-dimensional fix requires two star-earth horizon measurements coupled with a means to determine radial distance from the earth. The equations are nonlinear and impractical for manual computations. Considerable simplification results, however, if one of the selected stars is Polaris, the North Star. The development to follow is due, in part, to Mr. L. C. Ragland, of TRW Systems (Ref 14).

Declination From Polaris. Figure 24 is an illustration of two sextant measurements--the earth's angular diameter A and the Polaris-vehicle-earth horizon angle γ_{ns}. Since the lines of sight to Polaris
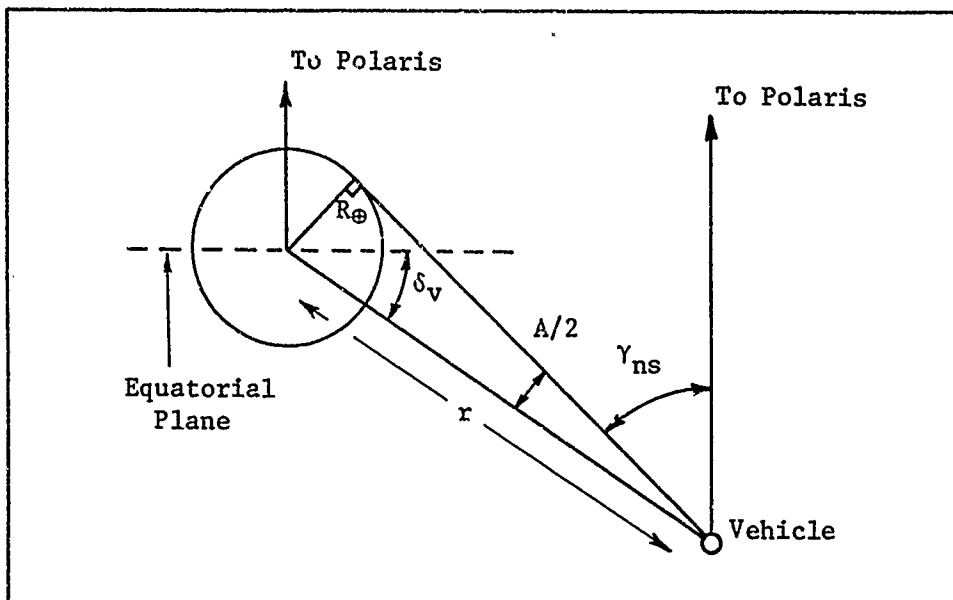
Fig. 24

Sextant Measurements: Polaris
and Earth's Diameter

are parallel, the vehicle declination δ_v is given by

$$- \delta_v + 90° + A/2 + \gamma_{ns} = 180° \qquad (5-1)$$

or

$$\delta_v = (\gamma_{ns} + A/2) - 90° \qquad (5-2)$$

The radial distance from the earth's center, r, is given by

$$r = \frac{R_\oplus}{\sin A/2} \qquad (3-37)$$

86

where $R_{\oplus}$ is the earth's radius.

Right Ascension Determination. Figure 25 shows the geometrical arrangement for finding the right ascension of the vehicle, α_v.

ψ = Star-Earth-Vehicle Angle
δ_v = Vehicle declination
$\Delta\alpha$ = Difference in Right Ascensions of Star and Vehicle
α_s, δ_s = Right Ascension and Declination of Star
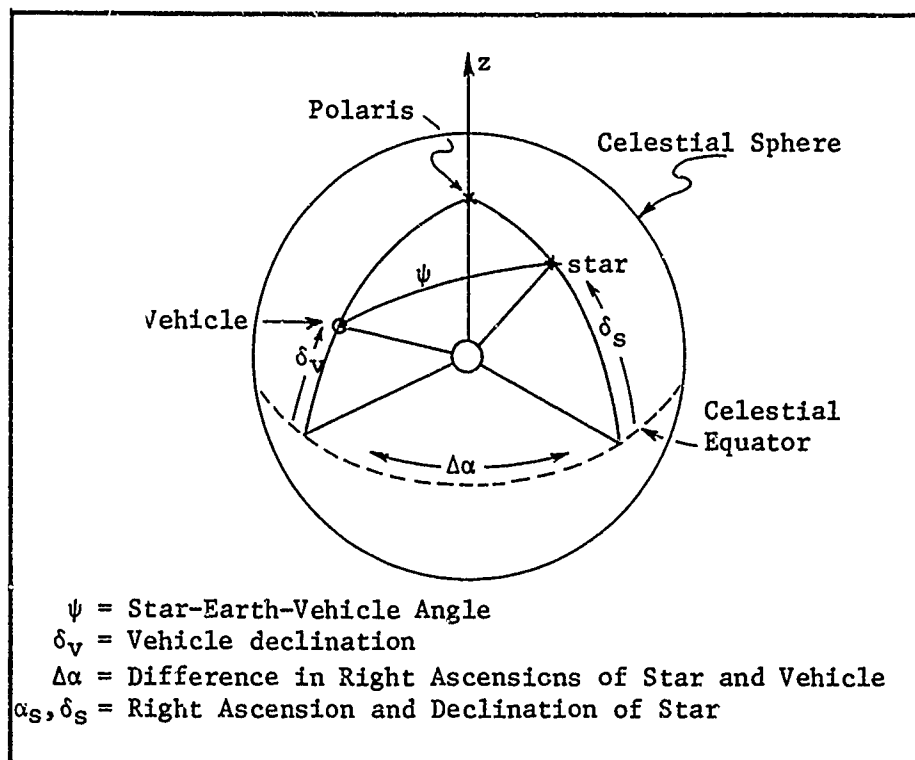
Fig. 25

Geometry for Vehicle Right Ascension

From the spherical triangle star-Polaris-vehicle,

$$\cos \psi = \cos (90 - \delta_s) \cos (90 - \delta_v)$$

$$+ \sin (90 - \delta_s) \sin (90 - \delta_v) \cos \Delta\alpha \qquad (5\text{-}3)$$

or

$$\cos \psi = \sin \delta_s \sin \delta_v + \cos \delta_s \cos \delta_v \cos \Delta\alpha \qquad (5\text{-}4)$$

then

$$\cos \Delta\alpha = \frac{\cos \psi - \sin \delta_S \sin \delta_V}{\cos \delta_S \cos \delta_V} \qquad (5\text{-}5)$$

The terms are defined on Fig. 25. Let $\hat{G}$ be a unit vector normal to the star-earth-vehicle plane. An observer looking down from the tip of this vector toward the earth would see the picture shown in Fig. 26. Again, since the lines of sight to the star are parallel,

$$\psi + \gamma_S + A/2 = 180° \qquad (5\text{-}6)$$

or

$$\psi = 180° - (\gamma_S + A/2) \qquad (5\text{-}7)$$
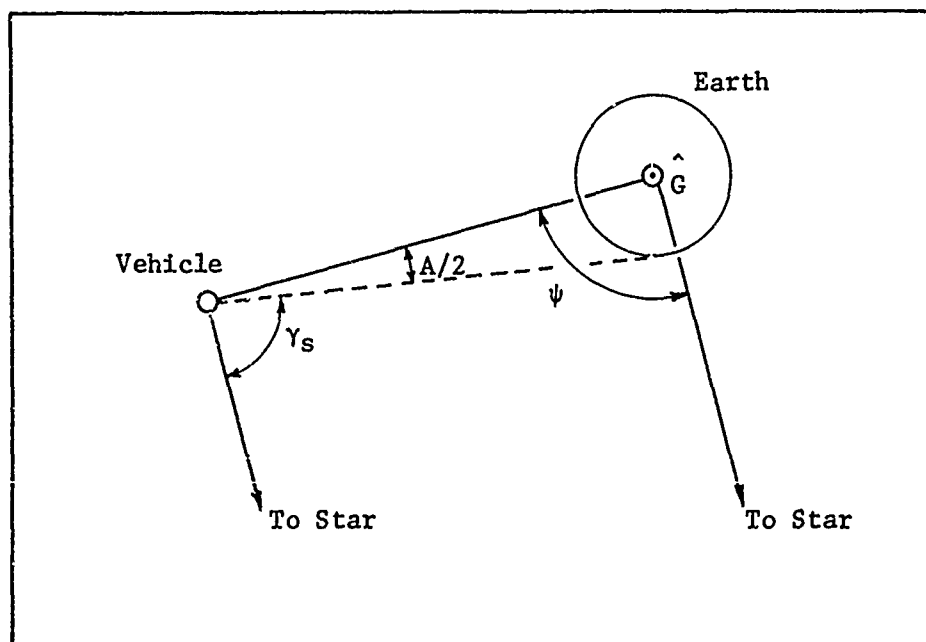
Fig. 26

Geometry of Star-Earth-Vehicle Plane

Substituting ψ into the expression for $\Delta\alpha$ results in

$$\cos \Delta\alpha = \frac{- \cos (\gamma_S + A/2) - \sin \delta_S \sin \delta_V}{\cos \delta_S \cos \delta_V} \qquad (5-8)$$

from which $\Delta\alpha$ can be determined. Note the resulting simplification if a star can be chosen with $\delta_S = 0$. With $\Delta\alpha$ known the right ascension of the vehicle is given by

$$\alpha_V = \alpha_S \pm \Delta\alpha \qquad (5-9)$$

where a simple "right-hand-rule" determines the sign. If the origin, for the moment, is considered at the vehicle, then the sign is plus if the general direction of $\hat{I}_{star} \times \hat{I}_{Polaris}$ is toward the earth. $\hat{I}_{star}$ and $\hat{I}_{Polaris}$ represent unit vectors in the directions of the star and Polaris respectively.

When a star with zero declination can be chosen Eq (5-8) becomes

$$\cos \Delta\alpha = \frac{- \cos (\gamma_S + A/2)}{\cos \delta_V} \qquad (5-10)$$

A number of stars are very close to the celestial equator. (Most of these are closer to the equator than Polaris is to the pole position.) Table VI is a tabulation of some stars with near zero declination. An easily identifiable star is δ Ori (Mintaka) which is in the belt of Orion. With r, α_V, and δ_V known, the coordinates of the vehicle

	Table VI			
	Selected Stars Near Celestial Equator			
Star Name	IAU Abbreviation	Constellation	Right Ascension	Declination
Mintaka	δ Ori	Orion	84.249°	− 0.321°
--	δ Mon	Monoceros	107.557°	− 0.438°
--	δ Vir	Virgo	203.265°	− 0.433°
Sadalmelik	α Aqr	Aquarius	331.035°	− 0.476°

are given by

$$x = r \cos \delta_V \cos \alpha_V$$

$$y = r \cos \delta_V \sin \alpha_V \qquad (5\text{-}11)$$

$$z = r \sin \delta_V$$

Conclusion. The simplified three-dimensional fix presented in this section has as its basis the fact that Polaris is very near the north celestial pole. Of course, Polaris is not exactly at the pole position and this discrepancy must be examined. But even if a detailed error analysis proves the method unsatisfactory, the simplified three-dimensional fix can be of great value to the astronaut. On the earth, Polaris is extremely useful as an instant cross-check of heading and latitude. Its analogous role in space navigation is as a source of vehicle declination. Using another star on the

celestial equator, the astronaut can quickly determine the right

ascension of the vehicle. Therefore, even if eventually deemed

unsatisfactory for manual navigation, the Polaris position fix will

serve as a quick cross-check of more sophisticated fixing means.

General Solution for Position Vector

Introduction. The Polaris-earth-star measurement scheme is the

simplest method known to the authors of obtaining a three-dimensional

fix. This section will attack the more difficult general problem

when, for some reason, Polaris is not observed.

The general formulation of the three-dimensional fix is given

in Ref 4:Ch 7. In general, the three-dimensional fix, using the

minimum number of measurements, requires the simultaneous solution of

the following nonlinear equations

$$\bar{r} \cdot \hat{I}_1 = -r \cos (\gamma_1 + A/2)$$

$$\bar{r} \cdot \hat{I}_2 = -r \cos (\gamma_2 + A/2) \tag{5-12}$$

$$|\bar{r}| = r$$

where $\bar{r}$ is the position vector of the vehicle, $\hat{I}_1$ and $\hat{I}_2$ are unit

vectors in the directions of two selected stars, $\gamma_{1,2}$, the star-

vehicle-earth horizon angles, and A, the earth's subtended angle.

As mentioned previously, the manual solution of these equations for

the components of $\bar{r}$ is impractical. Some simplification results,

however, if an additional star sighting is made. ·

91

The Three Star Fix. The unit position vector of the vehicle is obtained fairly simply by making three star-earth horizon measurements. The set of linear equations

$$\hat{r} \cdot \hat{I}_1 = - \cos (\gamma_1 + A/2)$$

$$\hat{r} \cdot \hat{I}_2 = - \cos (\gamma_2 + A/2) \qquad (5\text{-}13)$$

$$\hat{r} \cdot \hat{I}_3 = - \cos (\gamma_3 + A/2)$$

must be solved for the components of the unit vector $\hat{r}$. The solution for r_x, the x component of the unit vector $\hat{r}$, is

$$r_x = - \cos (\gamma_1 + A/2) \frac{(I_{y2} I_{z3} - I_{y3} I_{z2})}{\Delta}$$

$$+ \cos (\gamma_2 + A/2) \frac{(I_{y1} I_{z3} - I_{y3} I_{z1})}{\Delta} \qquad (5\text{-}14)$$

$$- \cos (\gamma_3 + A/2) \frac{(I_{y1} I_{z2} - I_{y2} I_{z1})}{\Delta}$$

where Δ represents the determinant of coefficients

$$\Delta = \begin{vmatrix} I_{x1} & I_{y1} & I_{z1} \\ I_{x2} & I_{y2} & I_{z2} \\ I_{x3} & I_{y3} & I_{z3} \end{vmatrix} \qquad (5\text{-}14a)$$

The solutions for r_y and r_z are, of course, similar. In general, the solutions take the form

$$r_x = A_{x1} \cos (\gamma_1 + A/2) + B_{x2} \cos (\gamma_2 + A/2)$$

$$+ C_{x3} \cos (\gamma_3 + A/2)$$

$$r_y = A_{y1} \cos (\gamma_1 + A/2) + B_{y2} \cos (\gamma_2 + A/2)$$

$$+ C_{y3} \cos (\gamma_3 + A/2)$$

$$r_z = A_{z1} \cos (\gamma_1 + A/2) + B_{z2} \cos (\gamma_2 + A/2)$$

$$+ C_{z3} \cos (\gamma_3 + A/2) \qquad (5\text{-}15)$$

with the terms defined as follows:

$$A_{x1} = (I_{y3} I_{z2} - I_{y2} I_{z3})/\Delta \qquad C_{y3} = (I_{x1} I_{z2} - I_{x2} I_{z1})/\Delta$$

$$B_{x2} = (I_{y1} I_{z3} - I_{y3} I_{z1})/\Delta \qquad A_{z1} = (I_{x3} I_{y2} - I_{x2} I_{y3})/\Delta$$

$$C_{x3} = (I_{y2} I_{z1} - I_{y1} I_{z2})/\Delta \qquad B_{z2} = (I_{x1} I_{y3} - I_{x3} I_{y1})/\Delta$$

$$A_{y1} = (I_{x2} I_{z3} - I_{x3} I_{z2})/\Delta \qquad C_{z3} = (I_{x2} I_{y1} - I_{x1} I_{y2})/\Delta$$

$$B_{y2} = (I_{x3} I_{z1} - I_{x1} I_{z3})/\Delta \qquad (5\text{-}16)$$

$$\Delta = I_{x1} \left[I_{y2} I_{z3} - I_{y3} I_{z2} \right] - I_{x2} \left[I_{y1} I_{z3} - I_{y3} I_{z1} \right]$$

$$+ I_{x3} \left[I_{y1} I_{z2} - I_{y2} I_{z1} \right]$$

It is a simple computer problem to tabulate the above constants for a considerable number of three-star sets. The astronaut is thus provided some semblance of general capability to manually compute his position in space. Once the unit vector $\hat{r}$ is obtained, the vehicle position vector is given by

$$\bar{r} = r \, \hat{r} \qquad\qquad (5-17)$$

where $r = |\bar{r}|$ and is obtained by semi-diameter or other means.

Manual calculation of position using this procedure will require a publication listing the constants A_{x1} through C_{z3} for selected three-star sets.* Table VII shows a typical format for such a publication. Although the requirement exists for a third star sighting (compared to the nonlinear three-dimensional fix equations), the additional measurement removes the nonlinearity plus the possible ambiguity in the direction of $\bar{r}$ (Ref 4:221). Following Table VII is a sample problem illustrating the manual position fix.

---

* If 25 stars are established as "space navigation stars," there are 2,300 possible three-star sets. Assuming 20 sets per page, the publication would require only 115 pages to cover all possibilities.

Star Set	A_{x1} A_{y1} A_{z1}	B_{x2} B_{y2} B_{z2}	C_{x3} C_{y3} C_{z3}
1 Dubhe	−.90368847	−.29882173	−1.68227200
2 Betelgeuse	.23797789	−.99759279	.16392111
3 Fomalhaut	−1.63183470	−.02032258	−.89050598
1 Pollux	3.16269770	−5.84253850	−3.38404430
2 Betelgeuse	−.19226972	−.28394138	.58373726
3 Rasalague	.78242022	−4.28971420	−3.74551760
1 Capella	−.32702313	.28773730	−.98883642
2 Acrux	−1.67469260	−1.15633370	−.35108396
3 Fomalhaut	.25868869	1.04071820	.52196385
1 Acrux	.22619851	.84496636	−.51440839
2 Arcturus	.28928391	.35811369	.90990474
3 Altair	.99216655	−.44923096	.21120275
1 Dubhe	.25166101	3.02868280	2.96921080
2 Sirus	−.24731313	−.00109432	1.00028020
3 Rasalague	−.97028150	1.56380340	1.39883810
1 Capella	1.76155570	−1.74660870	2.98233530
2 Canopus	−.93319008	−.62009385	−.19967779
3 Acrux	−.84378145	.92195900	−.3816431б
1 Dubhe	−1.69239350	−.52695925	−2.16196100
2 Canopus	−2.39505190	−1.75921190	−1.43748310
3 Fomalhaut	−1.68600160	−.03619068	−.92345019
1 Acrux	.77487909	.90722594	−.64576203
2 Arcturus	−.68124277	.24798659	1.14224790
3 Shaula	.76689250	−.47479314	.26513315

Table VII

Example of Three-Star Position Fix Data

Example Problem 5-1 - Manual Three-Dimensional Fix. Communication failure occurred during the translunar injection burn. Although the navigation computer seems to be working properly, the astronauts suspect the cause of communication failure may have also affected the computer. The astronauts decide to obtain a manual fix and cross-check the manual position with the computer read-out. If the positions cross-check reasonably well, the computer will be relied upon for further navigation. Looking toward the earth, the astronauts can identify the following navigation stars:

Acrux

Arcturus

Altair

The following angular measurements are obtained at TLI (Trans Lunar Injection) plus three hours:

Acrux-vehicle-earth horizon	–	43.970°
Arcturus-vehicle-earth horizon	–	48.011°
Altair-vehicle-earth horizon	–	56.503°
Earth's subtended angle	–	14.018°

The star-vehicle-earth center angles are then

Acrux-vehicle-earth	–	50.979°
Arcturus-vehicle-earth	–	55.020°
Altair-vehicle-earth	–	63.512°

Using data from Table VII, the components of the vehicle's unit position vector are

$$r_x = (.22619) \cos 50.979° + (.84496) \cos 55.020°$$
$$- (.51440) \cos 63.512°$$

$$r_y = (.28928) \cos 50.979° + (.35811) \cos 55.020°$$

$$+ (.90990) \cos 63.512°$$

$$r_z = (.99216) \cos 50.979° - (.44293) \cos 55.020°$$

$$+ (.21120) \cos 63.512°$$

or

$$r_x = (.22619)(.62960) + (.84496)(.57329) - (.51440)(.44600)$$

$$r_y = (.28928)(.62960) + (.35811)(.57329) + (.90990)(.44600)$$

$$r_z = (.99216)(.62960) - (.44923)(.57329) + (.21120)(.44600)$$

and carrying out the operations

$$r_x = .39739$$

$$r_y = .79324$$

$$r_z = .46132$$

The radial distance from the earth is

$$r = \frac{R_\oplus}{\sin \frac{14.018°}{2}} = \frac{3443.93}{0.12201} = 28,226 \text{ NM}$$

so the coordinates of the vehicle are (geocentric equatorial system)

$$x = (.39739)(28226) = 11,216 \text{ NM}$$

$$y = (.79324)(28226) = 22,389 \text{ NM}$$

97

The declination of the vehicle is simply

$$\delta_v = (\gamma_{ns} + A/2) - 90° = 117.467° - 90.000° = 27.467°$$

The expression for $\Delta\alpha$ is

$$\cos \Delta\alpha = \frac{- \cos (\gamma_s + A/2) - \sin \delta_s \sin \delta_v}{\cos \delta_s \cos \delta_v}$$

and substituting values

$$\cos \Delta\alpha = \frac{(-.445937) - (.152698)(.461232)}{(.988273)(.887279)}$$

$$\Delta\alpha = \pm 126.08°$$

The astronauts determine the proper sign as "plus" by looking out the window and establishing the direction of $\hat{I}_{Altair} \times \hat{I}_{Polaris}$ as generally toward the earth. The right ascension of the vehicle is then

$$\alpha_v = \alpha_s + \Delta\alpha$$

The right ascension of Altair is obtained from the ephemiris as 297.305°. Then

$$\alpha_v = 297.305° + 126.08° = 63.38°$$

The polar coordinates of the vehicle are thus

$$\alpha_v = 63.38°$$
$$\delta_v = 27.47°$$
$$r = 28,226 \text{ NM}$$

The rectangular coordinates of the unit position vector are given by

$$r_x = \cos \delta_v \cos \alpha_v$$

$$r_y = \cos \delta_v \sin \alpha_v \qquad (5\text{-}18)$$

$$r_z = \sin \delta_v$$

Substituting values

$$r_x = (.887279)(.448019) = 0.39752$$

$$r_y = (.887279)(.894024) = 0.79325$$

$$r_z = (.461232) = 0.46123$$

The coordinates of the vehicle are

$$x = rr_x = (28226)(.39752) = 11,220 \text{ NM}$$

$$y = rr_y = (28226)(.79325) = 22,390 \text{ NM}$$

$$z = rr_z = (28226)(.46123) = 13,019 \text{ NM}$$

which agree with the values obtained using three-star fix procedures. Note, however, that Polaris was assumed $\underline{at}$ the pole position.

Position Fix Simultaneous Measurement Requirement. The position fix techniques presented require, in the ideal case, simultaneous measurements. Obviously, if only one sextant is available, it is impossible to measure all angles simultaneously. A number of techniques resolving the difficulty are available.

Linear interpolation between an early and late sighting could be used to solve the simultaneous measurement requirement. If linear interpolation is insufficient, more measurements can be obtained for use with a higher order interpolation formula (Ref 24: Ch 10). This procedure is illustrated in the following example:

Example Problem 5-3 - Interpolation for Measurement. The angular measurement of Arcturus-vehicle-earth is desired at time 12:25. The following measurements are obtained:

Reading Number	Time	γ
1	12:10	41.265°
2	12:20	39.271
3	12:30	37.370
4	12:40	35.568

Bessel's interpolation formula (Ref 24:107) reduces to

$$\gamma_{12:25} = \frac{\gamma_2 + \gamma_3}{2} - \frac{\gamma_1 - \gamma_2 - \gamma_3 + \gamma_4}{16} \qquad (5-19)$$

and

$$\gamma_{12:25} = \frac{76.641}{2} - \frac{0.192}{16} = \underline{38.308°}$$

For comparison, linear interpolation for the angle at 12:25 yields

$$\gamma_{12:25} = \frac{\gamma_2 + \gamma_3}{2} = \underline{38.320°}$$

A number of other interpolation formulas are available--see any text on numerical analysis.

The extrapolation of measurements to an earlier or later time can also be achieved using an interpolation formula. Another interesting related technique, which has been used by astronomers for hundreds of years, is also available. The procedure will be illustrated by an example.

Example Problem 5-4 - Early and Late Measurement. The angular measurements of Arcturus-vehicle-earth are desired at 12:00 and 12:50. The measurements of Example Problem 5-3 are to be used.

To obtain the early and late measurement, the set of measurements is used to construct a difference table (Table VIII). First, the difference column of the measurements is obtained by subtracting from each reading the reading immediately preceding it. Then the differences of the differences are tabulated. The table is continued as far as possible. Table VIII is the completed difference array for the set of measurements used in this example.

To extend the table, the last difference is assumed constant and the last column of the difference array is extended. Starting with the extended values in the last column, the table is built "backward" to finally arrive at the desired early and late values. Table IX illustrates the procedure. The underlined values in Table IX represent the extension of the difference array.

The desired values at 12:00 and 12:50 are then:

$$12:00 \quad - \quad 43.346°$$
$$12:50 \quad - \quad 33.871°$$

Table VIII				
Difference Array				
Time	Angle	1st Diff.	2nd Diff.	3rd Diff.
12:10	41.265°			
		−1.994		
12:20	39.271°		.093	
		−1.901		.006
12:30	37.370°		.099	
		−1.802		
12:40	35.568°			

Table IX				
Extended Difference Array				
Time	Angle	1st Diff.	2nd Diff.	3rd Diff.
12:00	43.346			
		−2.081		
12:10	41.265		.087	
		−1.994		.006
12:20	39.271		.093	
		−1.901		.006
12:30	37.370		.099	
		−1.802		.006
12:40	35.568		.105	
		−1.697		
12:50	33.871			

The differencing technique is more fully treated in:

1. Ref 2:135

2. Ref 24:98

3. Ref 6:134

and many others.

The simultaneous measurement problem is also considered in Ref 8:18. The technique employed is to convert measurements to a common time by the use of pre-calculated data on the rate of change of angle with time along a reference trajectory. The method is fully treated in Ref 8 and thus will not be repeated here.

Another possibility is the use of a photograph to obtain the angular sightings--with a photograph, the measurements can indeed be simultaneous.* In any event, the simultaneous measurement requirement represents nothing more than a slight inconvenience to the astronaut.

Graphical Solution – Unit Position Vector

The graphical solution for the unit position vector is straight-forward when the temporary view is taken that the earth is orbiting the spacecraft. The graphical solution solves the equations

$$\hat{r} \cdot \hat{I}_1 = - \cos (\gamma_1 + A/2)$$

$$\hat{r} \cdot \hat{I}_2 = - \cos (\gamma_2 + A/2) \qquad (5\text{-}21)$$

$$|\hat{r}| = 1$$

---

* Additionally, photographs of the stars are in gnomonic projection (Ref 15:81), thus perhaps aiding in the graphical solution for α_v and δ_v discussed later.

and yields the right ascension and declination of the vehicle. A third precision measurement is unnecessary and the only calculation involved is addition or subtraction. The graphical solution is illustrated in Fig. 27. The step-by-step procedure is as follows:

1. Determine the star-vehicle-earth center angle $\gamma + A/2$ for two stars.

2. Find the same two stars on a star chart. The chart projection must be such that a straight line represents a great circle (gnomonic projection).

3. Using Star 1 as a center, lay off an arc of radius $\gamma_1 + A/2$. The angular scale on the equator or a meridian must be used to set the radius.

4. Using Star 2 as a center, lay off an arc of radius $\gamma_2 + A/2$.

5. The arcs intersect at two points. Select the proper point by an eyeball sighting of a third star--an arc drawn using the third star will fall close to the proper point. (Or observe Polaris and roughly determine the earth's declination using $\delta_\oplus = -\delta_v$.)

6. The plotted point represents the apparent position of the earth (the temporary view has been taken that the earth is orbiting the spacecraft).

7. Determine the vehicle coordinates using

$$\alpha_v = \alpha_\oplus \pm 180°$$

$$\delta_v = -\delta_\oplus$$
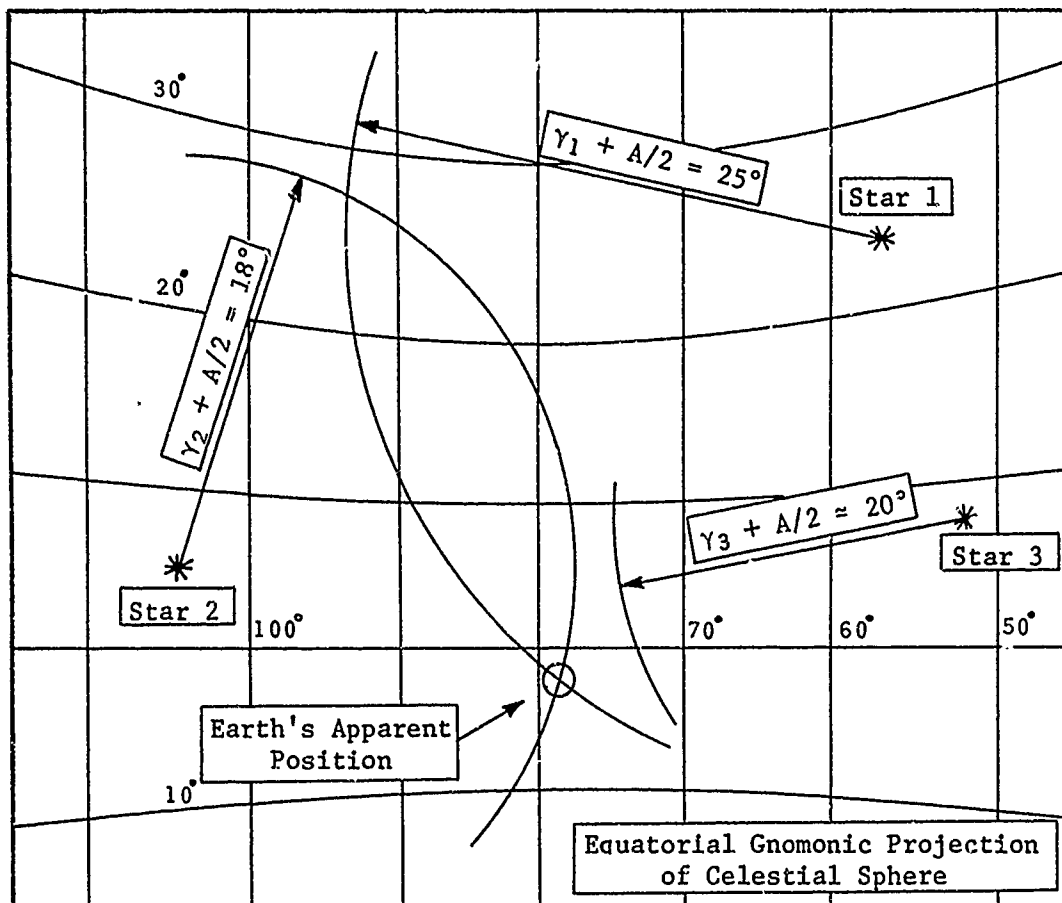
Fig. 27

Graphical Solution For Unit Position Vector

Example Problem 5-5 - Graphical Solution For α_v and δ_v. The situation described in Example Problem 5-1 will be used to illustrate the graphical determination of vehicle right ascension and declination. The angular scale of the star chart (Fig. 28) has been constructed to fit the thesis page--accuracy is therefore sacrificed.

At TLI plus three hours, the astronauts determine the angles

Arcturus-vehicle-earth center   =   55.020°

Rasalhague-vehicle-earth center   =   44.491°

The graphical solution is completed on Fig. 28. Using the star Arcturus as center, an arc of radius 55.0° is drawn. Another arc of radius 44.5° is drawn using Rasalhague as center point. By an eyeball sighting of Polaris, the vehicle declination is around

$$\delta_V \simeq 110° - 90° = +20°$$

so the declination of the earth as viewed from the spacecraft is around -20°. With this knowledge, the proper arc intersection point is read as

$$\alpha_\oplus = 244°$$

$$\delta_\oplus = -27°$$

The coordinates of the vehicle are then

$$\alpha_V = 244° - 180° = 64°$$

$$\delta_V = -(-27°) = +27°$$

Limitations. The surprising simplicity of the graphical solution is marred by the fact that it yields only an approximate angular position. The angular scale of the gnomonic projection varies over the chart, therefore, the intersecting arcs are not truly arcs of circles. However, within a limited range of the chart (the central region of Fig. 28), the scale is fairly uniform; positions obtained within this region will be close to the actual spacecraft coordinates.

Since the chart can only yield an approximate position, the graphical solution is limited to being a cross-check of more

107
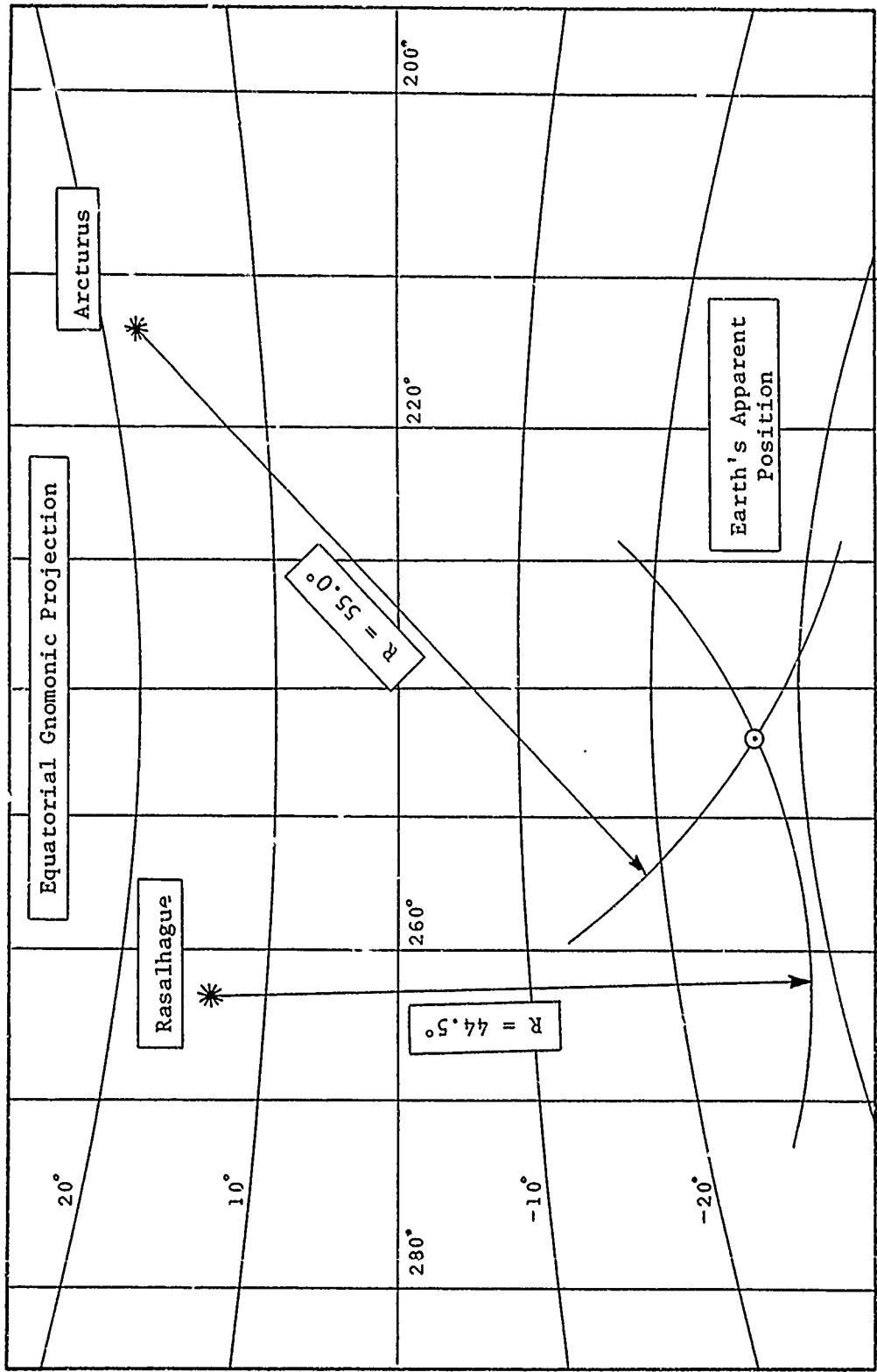
Fig. 28. Example of Graphical Position Fix

sophisticated fixing means. For example, after obtaining α_v and δ_v by other means, the astronauts can quickly check their calculations by determining the vehicle angular position graphically. Gross errors in computation can thus be detected without actually repeating the calculations.

Velocity Determination

An intermediate step before some orbit computation methods is determination of the vehicle's velocity vector. In general, this is an iterative computer problem. Several approximate methods, however, are available.

Numerical Differentiation. Any of the numerical differentiation formulas introduced in Chapter II can be used to obtain velocity. For three position fixes separated by time t

$$\dot{\bar{r}}_2 = \frac{\bar{r}_3 - \bar{r}_1}{2t} \qquad (5\text{-}22)$$

and for four fixes

$$\dot{\bar{r}}_2 = \frac{3(2\bar{r}_3 - \bar{r}_2) - (2\bar{r}_1 + \bar{r}_4)}{6t} \qquad (5\text{-}23)$$

Each vector equation represents three scalar equations. Thus, Eq (5-22) represents three equations, the first of which is

$$\dot{x}_2 = \frac{x_3 - x_1}{2t} \qquad (5\text{-}24)$$

and similar equations for $\dot{y}_2$ and $\dot{z}_2$.

109

Taylor Series. If only two fixes are available, the numerical differentiation technique to obtain velocity fails. However, as suggested in Ref 4:88, a Taylor series expansion about $\bar{r}_1$ will yield an approximate solution for $\dot{\bar{r}}_1$

$$\bar{r}_2 = \bar{r}_1 + \dot{\bar{r}}_1 t + \ddot{\bar{r}}_1 \frac{t^2}{2} + \dddot{\bar{r}}_1 \frac{t^3}{6} + \ldots \quad (5\text{-}25)$$

The series is truncated after the t^3 term. The second derivative is given by

$$\ddot{\bar{r}}_1 = \frac{-\mu\bar{r}_1}{r_1{}^3} \quad (5\text{-}26)$$

The third derivative is obtained, approximately, from an expansion for $\ddot{\bar{r}}_2$

$$\ddot{\bar{r}}_2 = \ddot{\bar{r}}_1 + \dddot{\bar{r}}_1 t + \ldots \quad (5\text{-}27)$$

which is truncated after the second term. Then

$$\dddot{\bar{r}}_1 = \frac{\ddot{\bar{r}}_2 - \ddot{\bar{r}}_1}{t} = \frac{\dfrac{-\mu\bar{r}_2}{r_2{}^3} + \dfrac{\mu\bar{r}_1}{r_1{}^3}}{t} \quad (5\text{-}28)$$

Substituting into Eq (5-25) and simplifying yields

$$\dot{\bar{r}}_1 = \frac{\bar{r}_2 - \bar{r}_1}{t} + \frac{\mu t}{6} \left[\frac{2\bar{r}_1}{r_1{}^3} + \frac{\bar{r}_2}{r_2{}^3} \right] \quad (5\text{-}29)$$

110

Lambert's Theorem. Two vector positions and their time separation
are sufficient for velocity determination using Lambert's theorem
(Ref 4:80). Solution of Lambert's theorem involves a double iteration
process and is thus impractical unless a back-up computer is available.

Orbit Determination From Position and Velocity

Knowledge of position and velocity at a specific time completely
defines an orbit. Methods for computing the orbital elements from
position and velocity are presented in most texts on astrodynamics.
One of the orbit computation methods discussed in Ref 3:Ch 1 is
briefly outlined step-by-step in Table X. The items in Table X
labeled "intermediate steps" are fully derived and discussed in
Ref 3:Ch 1.

Figure 29 shows the orientation unit vectors $\hat{P}$, $\hat{Q}$, and $\hat{W}$ used in
the procedure as well as a pictorial definition of the descriptive
orientation parameters i, Ω, and ω. Two of the unit vectors establish
the orbit orientation—the third unit vector as well as i, Ω, and ω
are not really required.

The computation method of Table X can be extended to include
parabolic and hyperbolic trajectories (Ref 3:Ch 1).

Orbit Determination From Three Position Fixes: Gibbsian Method

An approximate orbit can always be obtained from three fixes by
using numerical differentiation to determine velocity at one of the
positions. But such methods are only approximate. The Gibbsian
method, however, yields the orbit with no need for approximations or
iterations of any kind. The computed orbit using the Gibbsian method

Table X

Orbital Elements From Position and Velocity

Given:

$$\bar{r} = \begin{bmatrix} x \\ y \\ z \end{bmatrix} \qquad \dot{\bar{r}} = \begin{bmatrix} \dot{x} \\ \dot{y} \\ \dot{z} \end{bmatrix}$$

$\bar{r}$ = position vector

$\dot{\bar{r}}$ = velocity vector

Compute $|\bar{r}|$ and $\dot{S}^2$

$$r^2 = (x^2 + y^2 + z^2)$$

$$\dot{S}^2 = \dot{x}^2 + \dot{y}^2 + \dot{z}^2$$

$r = |\bar{r}|$

$\dot{S}^2 = |\dot{\bar{r}}|^2$

Compute a

$$a = \frac{\mu}{(2\mu/r) - \dot{S}^2}$$

Yields semimajor axis a

Compute D

$$D = r\dot{r}/\sqrt{\mu} = \frac{1}{\sqrt{\mu}}(x\dot{x} + y\dot{y} + z\dot{z})$$

D = intermediate step

$\dot{r}$ = radial velocity $\neq |\dot{\bar{r}}|$

Compute $\dot{D}$

$$\dot{D} = \sqrt{\mu}\left[\frac{1}{r} - \frac{1}{a}\right]$$

$\dot{D}$ = intermediate step

$$e\cos E_0 = \frac{r\dot{D}}{\sqrt{\mu}} = 1 - \frac{r}{a}$$

$$e\sin E_0 = \frac{D}{\sqrt{a}} = \frac{r\dot{r}}{\sqrt{\mu a}}$$

Yields e and E_0

$$a_x = (\dot{D}x - \dot{x}D)/\sqrt{\mu}$$

$$a_y = (\dot{D}y - \dot{y}D)/\sqrt{\mu}$$

$$a_z = (\dot{D}z - \dot{z}D)/\sqrt{\mu}$$

$a_{x,y,z}$ = intermediate steps

($a_{x,y,z}$ does not refer to semimajor axis a)

Table X   (Continued)

$$P_x = (a_x/e)$$
$$P_y = (a_y/e)$$
$$P_z = (a_z/e)$$

Yields unit vector $\hat{P}$
(see Fig. 29)

$$\ell = a(1 - e^2)$$
$$H = r - \ell$$
$$\dot{H} = \dot{r} = \frac{\sqrt{\mu}\ D}{r}$$

ℓ = semilatus rectum
H = intermediate step
$\dot{H}$ = intermediate step

$$b_x = (\dot{H}x - \dot{x}H)/\sqrt{\mu}$$
$$b_y = (\dot{H}y - \dot{y}H)/\sqrt{\mu}$$
$$b_z = (\dot{H}z - \dot{z}H)/\sqrt{\mu}$$

$b_{x,y,z}$ = intermediate steps

$$Q_x = b_x/(e\ \sqrt{\ell})$$
$$Q_y = b_y/(e\ \sqrt{\ell})$$
$$Q_z = b_z/(e\ \sqrt{\ell})$$

Yields unit vector $\hat{Q}$
(see Fig. 29)

$$\hat{W} = \hat{P} \times \hat{Q}$$
$$\text{or}$$
$$\hat{W} = (\bar{r} \times \dot{\bar{r}})/|\bar{r} \times \dot{\bar{r}}|$$

Yields unit vector $\hat{W}$
(see Fig. 29)

$$\cos i = W_z \qquad (0 \le i \le \pi)$$
$$\tan \Omega = - (W_x/W_y)$$
$$\sin \Omega = (W_x/\sin i)$$
$$\tan \omega = (P_z/Q_z)$$
$$\cos \omega = (Q_z/\sin i)$$

Yields i, Ω, ω
if desired
(see Fig. 29)

r̄ = vehicle position vector
θ = true anomaly
i = inclination
ω = argument of perifocus
Ω = longitude of ascending node

$\hat{P}$ = unit vector in direction of perifocus

$\hat{W}$ = unit vector in direction of r̄ x ṙ̄

$\hat{Q}$ = unit vector directed such that $\hat{P}$x$\hat{Q}$=$\hat{W}$

Fig. 29

Orientation Parameters and Vectors $\hat{P}$, $\hat{Q}$, $\hat{W}$

is as accurate as the position fix input data.

The Gibbsian method is treated in Ref 3:51. A step-by-step outline of the computation procedure is presented in Table XI. Note that the time interval between fixes is not required. The computation procedure can be extended to include hyperbolic trajectories and variations exist that use redundant data (Ref 3:Ch 1).

114

Table XI

Gibbsian Method: Orbit Determination From Three Position Fixes

Previously determined:
$$\bar{r}_1 = \begin{bmatrix} x_1 \\ y_1 \\ z_1 \end{bmatrix} \quad \bar{r}_2 = \begin{bmatrix} x_2 \\ y_2 \\ z_2 \end{bmatrix} \quad \bar{r}_3 = \begin{bmatrix} x_3 \\ y_3 \\ z_3 \end{bmatrix}$$

$$S = |\bar{r}_1 \times \bar{r}_3|$$

$$\hat{W} = \frac{\bar{r}_1 \times \bar{r}_3}{S}$$

Yields unit vector $\hat{W}$ (see Fig. 29)

$$C_1 = \frac{\ddot{r}_2 \times \bar{r}_3}{S}$$
$$C_3 = \frac{\bar{r}_2 \times \bar{r}_1}{S}$$

$$\ell = \frac{c_1 \, r_1 + c_3 \, r_3 - r_2}{(c_1 + c_3 - 1)}$$

ℓ = semilatus rectum

$$e\hat{Q} = \frac{\bar{r}_3 \, (\ell - r_1) - \bar{r}_1 \, (\ell - r_3)}{S}$$

$$e^2 = e^2 \, Q_x^2 + e^2 \, Q_y^2 + e^2 \, Q_z^2$$

Yields e

115

Table XI (Continued)

$$Q_x = (e\ Q_x/e)$$
$$Q_y = (e\ Q_y/e)$$
$$Q_z = (e\ Q_z/e)$$

→ Yields unit vector $\hat{Q}$
  (see Fig. 29)

$$a = \frac{\ell}{(1 - e^2)}$$

→ Yields a

$$\hat{P} = \hat{Q} \times \hat{W}$$

→ Yields unit vector $\hat{P}$
  (see Fig. 29)

$$\cos E_i = \frac{a - r_i}{ae}$$

$E_i < 180°$ if $|\bar{r}|$ is increasing.

$i = 1, 2, 3$ (or any other known r)

$$t_i - t_o =$$
$$\sqrt{\frac{a^3}{\mu}}\left[E_i - e \sin E_i\right]$$

→ Yields r_i time from
  perifocus

$$\cos i = W_z \quad (0 \le i \le \pi)$$
$$\tan \Omega = - (W_x/W_y)$$
$$\sin \Omega = (W_x/\sin i)$$
$$\tan \omega = (P_z/Q_z)$$
$$\cos \omega = (Q_z/\sin i)$$

→ Yields i, Ω, ω if desired.
  (see Fig. 29)

116
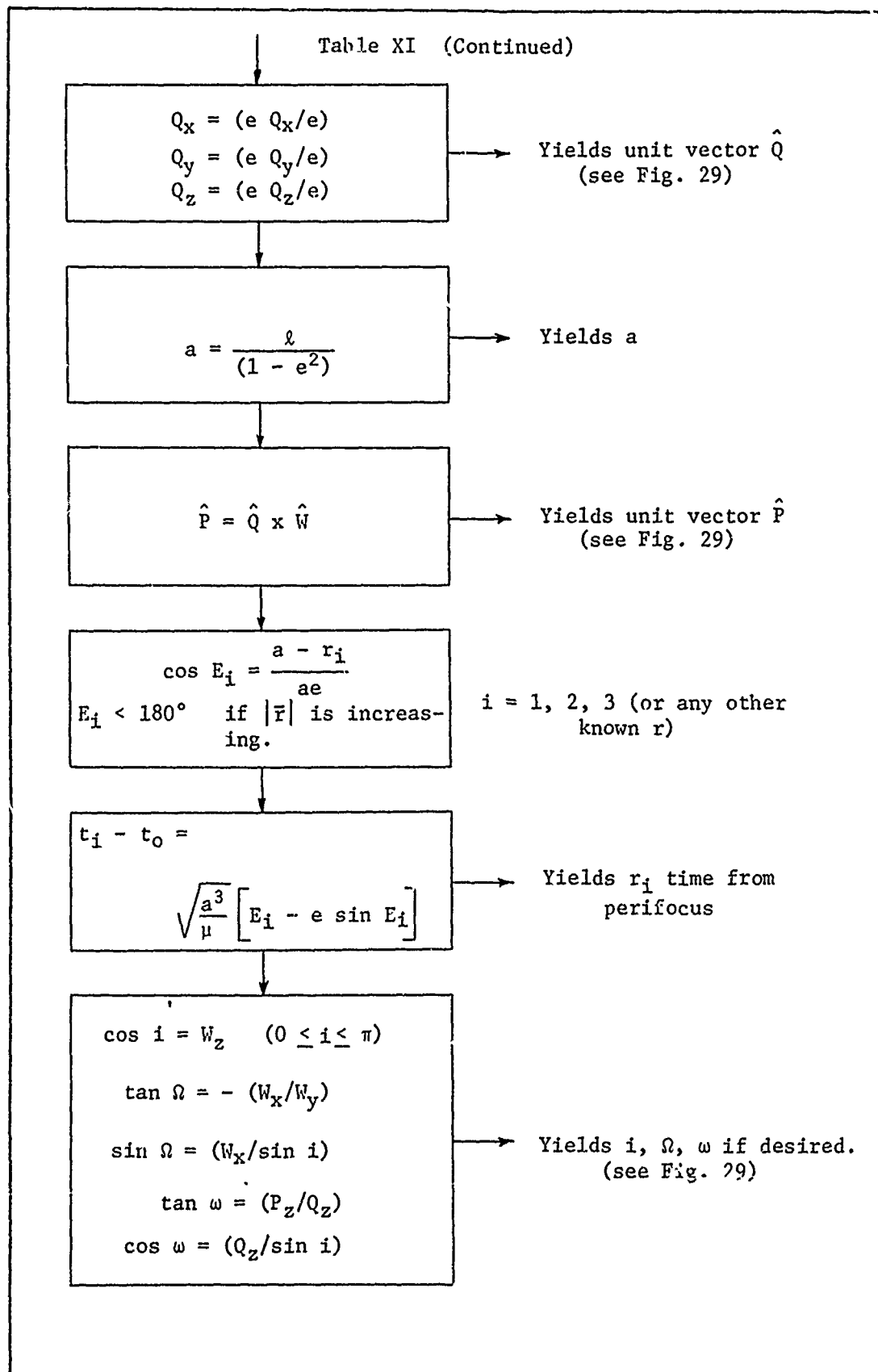
Position in the Orbit - Direct Measurement of True Anomaly

If the orbit orientation is known, the true anomaly difference between two positions can be measured directly. This section will treat a simplified and then general method of measuring true anomaly.

True Anomaly From Star in Orbit Plane. The true anomaly can be measured directly by sighting a star known to be in the orbit plane. Figure 30 illustrates the geometry of the measurement. If the star
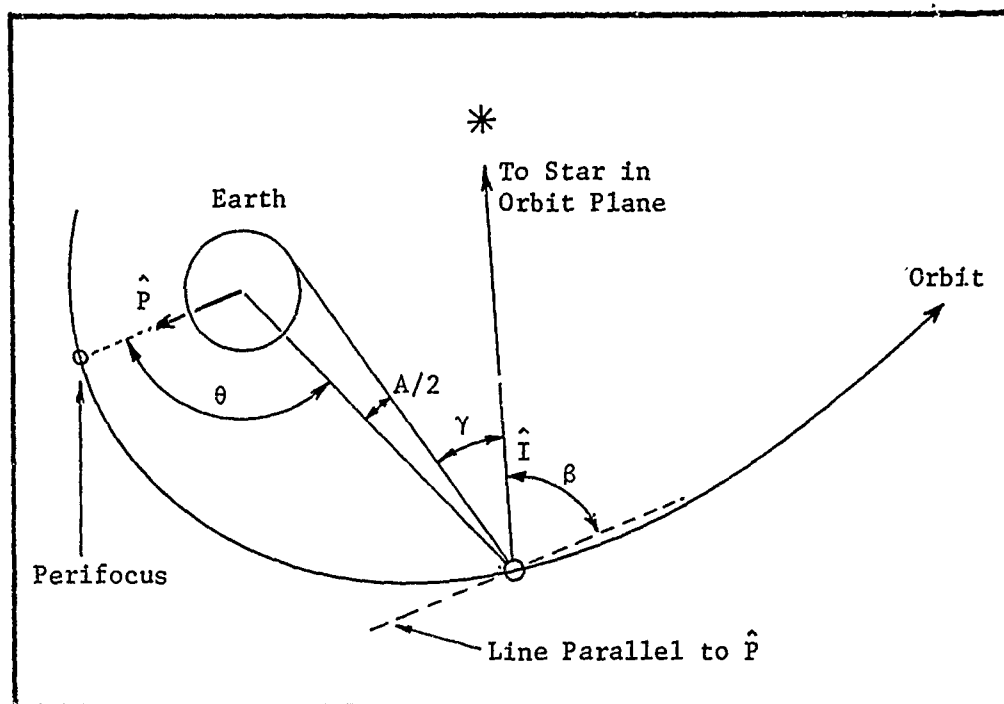
Fig. 30

True Anomaly Measurement

is in the orbit plane, then

$$\theta = \beta + (\gamma + A/2) \tag{5-30}$$

The angle $(\gamma + A/2)$, the star-vehicle-earth center angle, can be

117

measured with the sextant. The angle β, which corresponds to the true anomaly of the orbit plane star, is obtained from

$$\hat{I} \cdot \hat{P} = - \cos \beta \tag{5-31}$$

If only the difference in true anomaly between two positions is needed, then

$$\theta_2 - \theta_1 = (\gamma + A/2)_2 - (\gamma + A/2)_1$$

and there is no need to determine β.

A star in the orbit plane can be found by establishing α and δ of two known orbital points, plotting these points on a properly constructed star chart, and joining them with a straight line. Any star on the line is "in" the orbit plane. The two known points may consist of two unit position vectors or the unit vectors $\hat{P}$ and $\hat{Q}$. Knowledge of i and Ω also establishes the line.

The type of star chart is important since the straight line drawn between the two known points must represent a great circle on the celestial sphere. Projections having this characteristic are:

1. equatorial gnomonic

2. oblique gnomonic

3. polar gnomonic

True Anomaly from any Star. If a star in the orbit plane cannot be found, the situation is more complicated. However, it is possible to sight any star and derive a measure of true anomaly. Preliminary data needed are two angular positions--right ascensions and declinations or the unit position vectors. Complete derivations of

118

the equations to follow may be found in Appendix D.

An illustration of the orbital trace across the celestial sphere is shown in Fig. 31.

$$\psi = 180° - (\gamma_s + A/2)$$
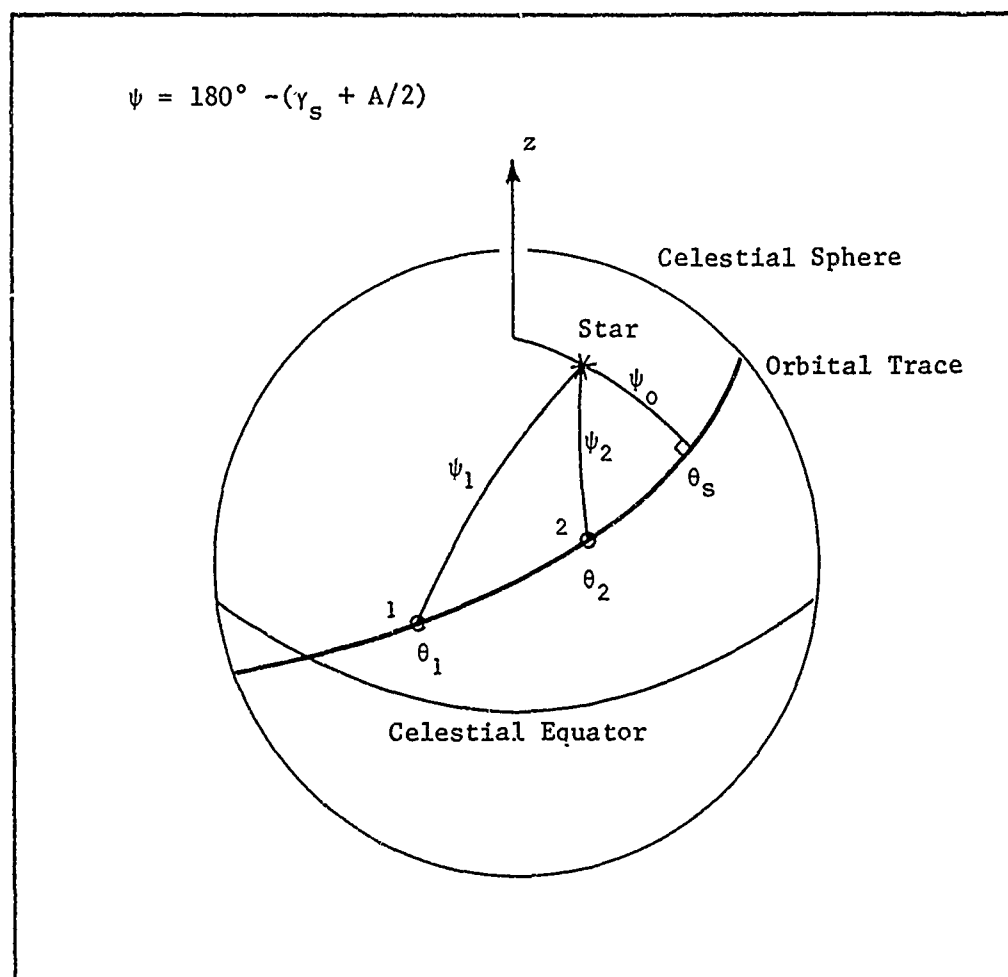
Fig. 31

Orbital Trace on Celestial Sphere

From spherical trigonometry

$$\cos(\theta_s - \theta) = \frac{-\cos(\gamma_s + A/2)}{\cos\psi_o} \qquad (5\text{-}33)$$

119

where

$\gamma_S + (A/2)$ = the measured star-vehicle-earth center angle.

ψ_0 = the <u>minimum possible</u> star-earth-vehicle angle.*

θ = true anomaly of vehicle.

θ_S = true anomaly of star's unit vector as projected into orbit plane.

A = earth's subtended angle.

Note that ψ_0 represents the <u>minimum possible</u> star-earth-vehicle angle. Therefore, if the star and the earth can be observed simultaneously, the vehicle must travel close to 180° before ψ_0 will actually occur.

The angle ψ_0 can be determined from

$$\cos \psi_0 = \left| \frac{- \cos (\gamma_S + A/2)_2}{\cos (\theta_S - \theta_2)} \right| \quad 0 \leq \psi_0 \leq 90° \qquad (5\text{-}34)$$

where $(\gamma_S + A/2)_2$ represents the star-vehicle-earth center angle as measured at position two. The angle $(\theta_S - \theta_2)$ can be determined from

$$\tan (\theta_S - \theta_2) = \cot (\theta_2 - \theta_1)$$

$$- \frac{\cos (\gamma_S + A/2)_1}{\cos (\gamma_S + A/2)_2 \sin (\theta_2 - \theta_1)} \qquad (5\text{-}35)$$

* ψ_0 is called "minimum coaltitude" in Ref 17:46 and is denoted by $\widehat{r}$.

and $(\theta_2 - \theta_1)$ from

$$\cos (\theta_2 - \theta_1) = \cos \delta_1 \cos \delta_2 \cos (\alpha_2 - \alpha_1) + \sin \delta_1 \sin \delta_2$$

(5-36)

The angle ψ_0 for a given star is constant. Therefore, once ψ_0 is established, the true anomaly difference between two positions can be determined through

$$\cos (\theta_s - \theta) = \frac{- \cos (\gamma_s + A/2)}{\cos \psi_0}$$

(5-37)

For the special case when the star is in the orbit plane $\cos \psi_0 = 1$ and Eq (5-37) reduces to the simpler expression treated in the first part of this section.

The angle ψ_0 can also be determined by direct measurement (Ref 13:8). The astronaut simply observes a star passing close by the earth and records the minimum star-vehicle-earth angle. The minimum star-vehicle-earth angle corresponds to ψ_0. Figure 32 is an illustration of this concept.

Conclusion

The manual determination of the three-dimensional fix is within the realm of possibility. With three fixes, the orbit can be obtained using straightforward computations. Although direct manual computation of the orbit will be tedious and time consuming, the capability is there. Simplifying techniques and procedures will become apparent if the method is adopted and analyzed step-by-step.
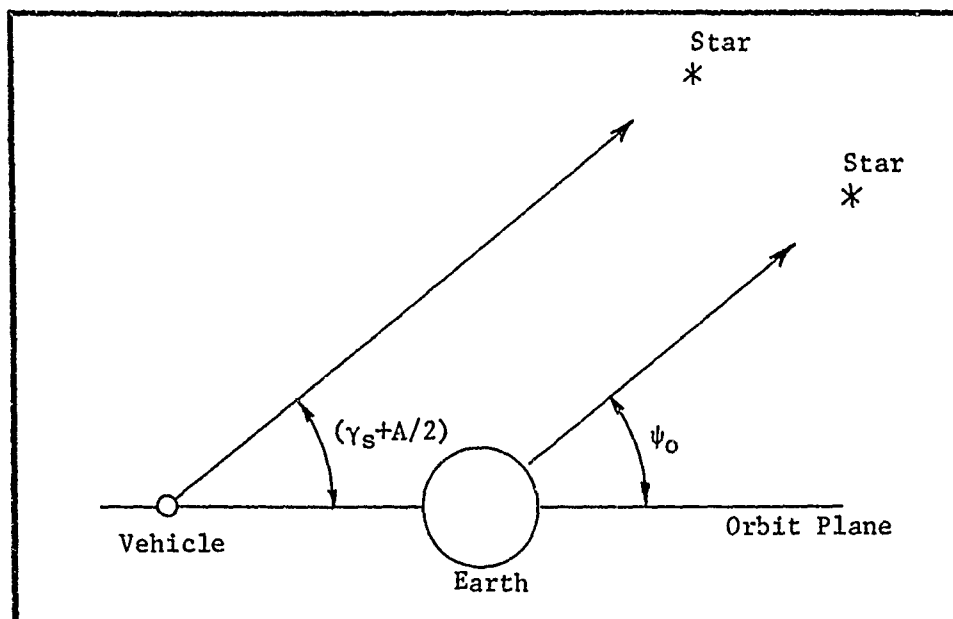
Fig. 32

Star-Vehicle-Earth (SVE) Plane at Instant
of ψ_0 Measurement (Orbit Plane
and SVE Plane Perpendicular)

If a back-up computer is available, several avenues are open:

1. Program the approximate orbit--i.e., obtain velocity
   using numerical differentiation.

2. Solve Lambert's theorem.

3. Program the Gibbsian method.

Programming an approximate orbit is undesirable if better methods are

available. Lambert's theorem involves a double iteration which would

probably exceed a back-up computer's capability. Obviously, the

Gibbsian method, or a variation, should be programmed. Chapter IX will

present such a program. The output of this program will be used as

input to a second program that "projects" position and velocity as a

function of time along the trajectory. This information could be used,

in turn, as input to a back-up guidance scheme.

122

VI. Orientation Parameters - Geometric Elements Known

Summary of Present Manual System

References 12, 17, and 22 present a manual means for determining the orientation parameters i (inclination), Ω (longitude of ascending node), and ω (argument of perifocus). The method consists of determining minimum coaltitudes for a selected star pair (minimum coaltitude is the minimum star-earth-vehicle angle for a given star). Given two minimum coaltitudes, $(\psi_0)_1$ and $(\psi_0)_2$, the following nonlinear set of equations* is solved for the components of $\hat{W}$

$$\hat{W} \cdot \hat{I}_1 = \sin (\psi_0)_1$$

$$\hat{W} \cdot \hat{I}_2 = \sin (\psi_0)_2 \tag{6-1}$$

$$|\hat{W}| = 1$$

where the unit vector $\hat{W}$ is normal to the orbit plane (Fig. 29). $\hat{I}_1$ and $\hat{I}_2$ are unit vectors toward star one and star two respectively. The orientation elements are then determined from knowledge of $\hat{W}$ and presented graphically as a function of $(\psi_0)_1$ and $(\psi_0)_2$. The system is ingenious and works, but there are several disadvantages in determining the orientation parameters using this method.

---

* Notice the similarity of this set of equations to the nonlinear three-dimensional fix (Eq (5-12)).

123

1. The geometric parameters are used in determining $(\psi_o)_1$ and $(\psi_o)_2$. Therefore, any errors in the geometric parameters will be carried over to the computation of each orientation element.

2. The system is dependent upon pre-computations using pre-selected star pairs--star pairs are chosen with regard to the expected orbit and an established range of probable values of i, Ω, and ω. Therefore, the method is not entirely flexible.

3. The solution of the nonlinear set of equations, Eq (6-1), is a disagreeable task even for a ground based computer. Programming a small back-up computer for inflight solution of Eq (6-1) is of questionable practicality.

Alternate methods for determining the orientation parameters are available. The unit vector $\hat{W}$ can be obtained from any two vectors known to be in the orbit plane. For example, if $\bar{r}_1$ and $\bar{r}_2$ represent the vehicle position vector at time one and later time two, then

$$\hat{W} = \frac{\bar{r}_1 \times \bar{r}_2}{\left| \bar{r}_1 \times \bar{r}_2 \right|} \tag{6-2}$$

The position vectors $\bar{r}_1$ and $\bar{r}_2$ can be determined by the methods discussed in Chapter V.

The object in this discussion is not blind criticism of a manual method which works (and quite well - see Ref 12), but is rather an

attempt to start development of a general method of orientation element

computation applicable to any orbit whatsoever--with no requirement

for prior knowledge of what that orbit might be. The following

paragraphs treat the problem of orientation element computation from

partial knowledge of two positions in space.

Orientation Elements From Position Fixes

If the geometric elements are obtained by other means, only two

partial fixes are needed to specify the orientation elements i, Ω,

and ω (defined in Fig. 29). In the development to follow, it is

assumed that two such fixes have been obtained using one of the

methods of Chapter V.

At position one and a later position two, the unit position

vectors are

$$\hat{r}_1 = r_{x1} \hat{i} + r_{y1} \hat{j} + r_{z1} \hat{k}$$

$$\hat{r}_2 = r_{x2} \hat{i} + r_{y2} \hat{j} + r_{z2} \hat{k} \tag{6-3}$$

Then the unit vector $\hat{W}$ (see Fig. 29) is given by

$$\hat{W} = \frac{\hat{r}_1 \times \hat{r}_2}{|\hat{r}_1 \times \hat{r}_2|} \tag{6-4}$$

from which

$$\cos i = W_z \qquad (0 \leq i \leq \pi) \tag{6-5}$$

and

$$\tan \Omega = -\frac{W_x}{W_y} \tag{6-6}$$

The ambiguity for Ω is resolved by noting that

$$\sin \Omega = \frac{W_x}{\sin i} \tag{6-7}$$

Thus, the orbital inclination i and the longitude of ascending node Ω are determined with no requirement for prior knowledge of the geometric parameters.

The solution for ω, the argument of perifocus, requires knowledge of the true anomaly at some position $\bar{r}$. This can be position one, two, or any other known position. Therefore, the geometric elements must be determined before ω can be calculated. The argument of perifocus is given by

$$\omega = \sin^{-1}\left[\frac{r_z}{\sin i}\right] - \theta \tag{6-8}$$

where θ is the true anomaly at the vehicle position $\bar{r}$. The ambiguity for ω can be resolved using

$$\omega = \cos^{-1}\left[\frac{r_x}{\cos \Omega} + \frac{r_z \tan \Omega}{\tan i}\right] - \theta \tag{6-9}$$

Example Problem 6-1 - Orientation Elements. Several spacecraft emergencies have compounded to the point that manual determination

of the orientation elements is necessary. Using the three-star fix
procedures of Chapter V, the astronauts obtain the following unit
position vectors and corresponding radial distances:

$$t = t_1 \qquad\qquad\qquad t = t_1 + 3\ 1/2\ \text{hr}$$

$$r_{x1} = .50837 \qquad\qquad\qquad r_{x2} = .25442$$

$$r_{y1} = .74113 \qquad\qquad\qquad r_{y2} = .83992$$

$$r_{z1} = .43850 \qquad\qquad\qquad r_{z2} = .47937$$

$$r_1 = 21098\ \text{NM} \qquad\qquad\qquad r_2 = \text{unknown--but greater than } r_1$$

The cross-product $\hat{r}_1 \times \hat{r}_2$ is given by

$$\hat{r}_1 \times \hat{r}_2 = \hat{i}\ (r_{y1}\ r_{z2} - r_{z1}\ r_{y2})$$

$$+ \hat{j}\ (r_{x2}\ r_{z1} - r_{x1}\ r_{z2})$$

$$+ \hat{k}\ (r_{x1}\ r_{y2} - r_{y1}\ r_{x2}) \qquad\qquad (6\text{--}10)$$

and substituting values

$$\hat{r}_1 \times \hat{r}_2 = \hat{i}\ (-.01303) + \hat{j}\ (-.13213) + \hat{k}\ (.23843)$$

$$\left| \hat{r}_1 \times \hat{r}_2 \right| = 0.27290$$

The unit vector $\hat{W}$ is then

$$\hat{W} = \hat{i}\ (-.04774) + \hat{j}\ (-.48417) + \hat{k}\ (.87369)$$

from which

$$\cos i \;=\; 0.87369$$

and

$$i \;=\; 29.11°$$

The longitude of the ascending node, Ω, is given by

$$\tan \Omega \;=\; \frac{-W_x}{W_y} \;=\; \frac{(.04774)}{(-.48417)} \;=\; -0.09860$$

from which

$$\Omega \;=\; \begin{bmatrix} 174.36° \\ or \\ 354.36° \end{bmatrix}$$

Since $\sin \Omega = W_x/\sin i$ is negative, the correct value is

$$\Omega \;=\; 354.36° \;=\; -5.64°$$

The true anomaly at one of the positions must be determined before the argument of perifocus, ω, can be calculated. The geometric elements (assumed previously determined) yield the true anomaly at position one through the equation

$$\cos \theta_1 \;=\; \frac{a\,(1 - e^2) - r_1}{er_1} \qquad (6\text{-}11)$$

128

Using the values

$$a = 132,875 \text{ NM}$$

$$e = .9737$$

$$r = 21,098 \text{ NM}$$

the expression for $\cos \theta_1$ is

$$\cos \theta_1 = \frac{(132875)(1 - .9481) - 21098}{(.9737)(21098)} = -0.69132$$

and

$$\theta_1 = 133.73°$$

The true anomaly is less than 180° since the radial distance is increasing. The argument of perifocus is given by

$$\omega = \sin^{-1} \left[\frac{r_{z1}}{\sin i} \right] - \theta_1 = \sin^{-1} \left[\frac{.43850}{.48651} \right] - 133.73°$$

then

$$\omega = \begin{bmatrix} 64.33° \\ \text{or} \\ 115.67° \end{bmatrix} - 133.73° = \begin{bmatrix} -69.40° \\ \text{or} \\ -18.06° \end{bmatrix}$$

The proper angle is determined by a rough calculation of

$$\omega = \cos^{-1} \left[\frac{r_{x1}}{\cos \Omega} + \frac{r_{z1} \tan \Omega}{\tan i} \right] - \theta$$

129

which becomes

$$\omega \simeq \cos^{-1}\left[\frac{(.51)}{(.99)} - \frac{(.44)(.1)}{(.56)}\right] - 134°$$

Then roughly

$$\omega \simeq \begin{bmatrix} 64° \\ \text{or} \\ -64° \end{bmatrix} - 134° = \begin{bmatrix} 70° \\ \text{or} \\ -198° \end{bmatrix}$$

The angle common to both calculations is $-69.40°$ so the argument of perifocus is

$$\omega = -69.40°$$

Orientation Elements from α_v and δ_v

Knowledge of vehicle right ascension and declination at two points coupled with the true anomaly at either point is sufficient to define the orientation elements. Conversion from polar to rectangular coordinates is unnecessary. Figure 33, an illustration of the vehicle's path on the celestial sphere, will be used for some of the derivations to follow.

From the previous section

$$\cos i = W_z = (r_{x1}\, r_{y2} - r_{y1}\, r_{x2})/\left|\hat{r}_1 \times \hat{r}_2\right| \qquad (6\text{-}12)$$

130
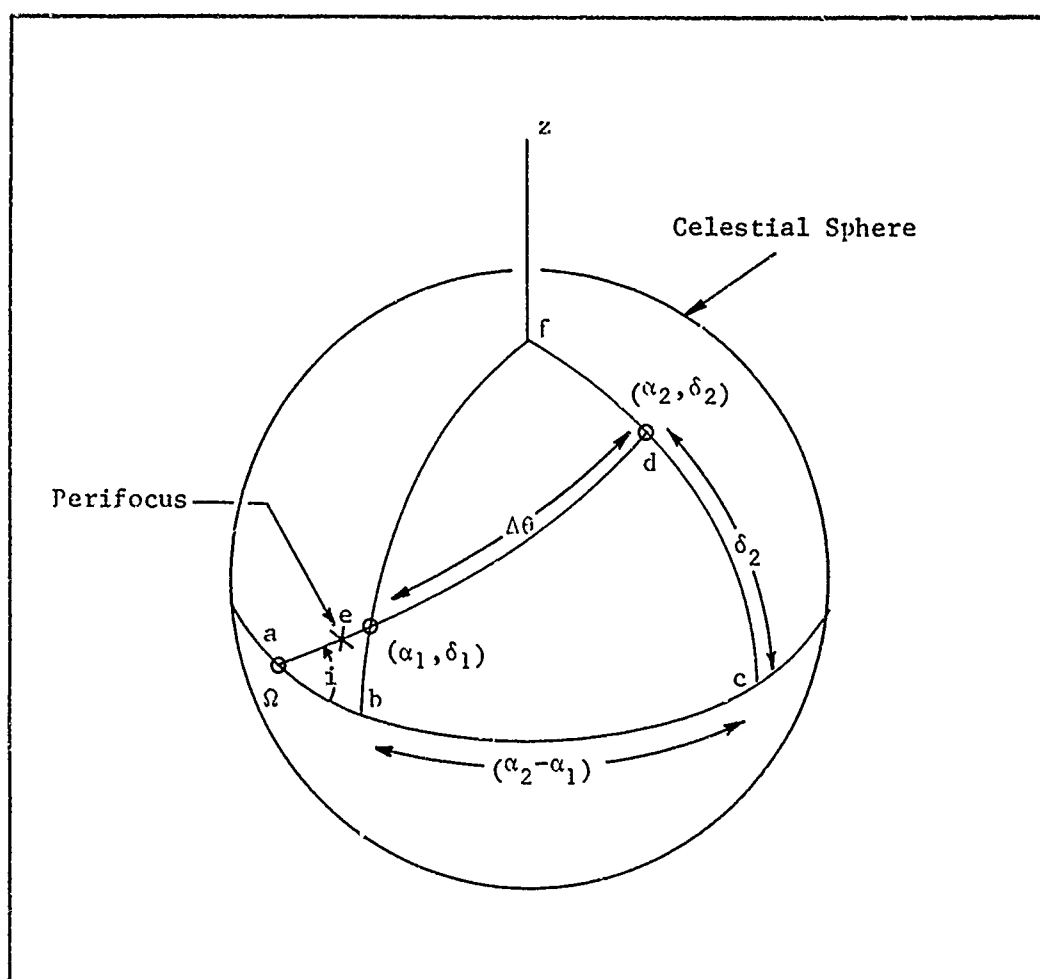
Fig. 33

Orbital Path on Celestial Sphere

Substituting

$$r_x = \cos \delta \cos \alpha$$

$$r_y = \cos \delta \sin \alpha \qquad (5\text{-}18)$$

$$r_z = \sin \delta$$

131

leads to

$$\cos i = \frac{\cos \delta_1 \cos \delta_2 \sin (\alpha_2 - \alpha_1)}{\left| \hat{r}_1 \times \hat{r}_2 \right|} \qquad (6\text{-}13)$$

The cross product of the two unit vectors is

$$\hat{r}_1 \times \hat{r}_2 = \left| \hat{r}_1 \right| \left| \hat{r}_2 \right| \sin \Delta\theta = \sin \Delta\theta \qquad (6\text{-}14)$$

where $\Delta\theta$ is the true anomaly difference between $\hat{r}_1$ and $\hat{r}_2$.

From the spherical triangle def (Fig. 33)

$$\cos \Delta\theta = \sin \delta_1 \sin \delta_2 + \cos \delta_1 \cos \delta_2 \cos (\alpha_2 - \alpha_1) \qquad (6\text{-}15)$$

thus $\Delta\theta$ and $\sin \Delta\theta$ can be determined and the inclination is given by

$$\cos i = \frac{\cos \delta_1 \cos \delta_2 \sin (\alpha_2 - \alpha_1)}{\left| \sin \Delta\theta \right|} \qquad 0 \le i \le \pi \qquad (6\text{-}16)$$

The longitude of the ascending node, Ω, can be found from the spherical triangles abe and acd using

$$\sin (\alpha_2 - \Omega) = \frac{\tan \delta_2}{\tan i} \qquad (6\text{-}17)$$

The ambiguity is resolved using

$$\sin (\alpha_1 - \Omega) = \frac{\tan \delta_1}{\tan i} \qquad (6\text{-}18)$$

The common value of Ω is the solution.

The argument of perifocus requires knowledge of the true anomaly at one of the positions. Assume θ_2 is known. Then, from the spherical triangle acd

$$\sin (\omega + \theta_2) = \frac{\sin \delta_2}{\sin i} \qquad (6\text{--}19)$$

The ambiguity can be resolved using

$$\sin (\omega + \theta_1) = \frac{\sin \delta_1}{\sin i} \qquad (6\text{--}20)$$

and since $\theta_2 = \theta_1 + \Delta\theta$

$$\sin [\omega + (\theta_2 - \Delta\theta)] = \frac{\sin \delta_1}{\sin i} \qquad (6\text{--}21)$$

Example Calculation 6-2 (i, Ω, and ω from α and δ). Using the Polaris fix technique (Chapter V) the astronauts establish the following angular data:

$$t = t_1 \qquad\qquad\qquad t_2 = t_1 + 2 \text{ hr}$$

$$\alpha_1 = 55.55° \qquad\qquad\qquad \alpha_2 = 68.29°$$

$$\delta_1 = 26.01° \qquad\qquad\qquad \delta_2 = 28.15°$$

In addition, the true anomaly at position one is known to be

$$\theta_1 = 133.73°$$

The orientation of the orbit is desired.

133

Solution. The true anomaly difference between position one and two is

$$\cos \Delta\theta = \sin \delta_1 \sin \delta_2 + \cos \delta_1 \cos \delta_2 \cos (\alpha_2 - \alpha_1) \quad (6-15)$$

and substituting values

$$\cos \Delta\theta = (.43851)(.47178) + (.89873)(.88171)(.97541)$$
$$= .97981$$

from which

$$\Delta\theta = 11.53°$$

$$\sin \Delta\theta = .19991$$

The inclination is given by

$$\cos i = \frac{\cos \delta_1 \cos \delta_2 \sin (\alpha_2 - \alpha_1)}{|\sin \Delta\theta|} \quad (6-16)$$

and substituting values

$$\cos i = \frac{(.89873)(.88171)(.22042)}{(.19991)} = .87372$$

Then

$$i = 29.11°$$

The longitude of the ascending node is found from

$$\sin(\alpha_2 - \Omega) = \frac{\tan \delta_2}{\tan i} = \frac{(.53508)}{(.55673)} = .96110$$

$$\alpha_2 - \Omega = \begin{bmatrix} 73.97° \\ \text{or} \\ 106.03° \end{bmatrix} = 68.29° - \Omega$$

Then

$$\Omega = \begin{bmatrix} -5.68° \\ \text{or} \\ -37.74° \end{bmatrix}$$

The ambiguity is resolved by a rough calculation of Ω using the other position. Accordingly

$$\sin(\alpha_1 - \Omega) = \frac{\tan \delta_1}{\tan i} \simeq \frac{.49}{.56} = .87$$

$$\Omega = \begin{bmatrix} -5° \\ \text{or} \\ -65° \end{bmatrix}$$

The angle common to both calculations is near -5° so

$$\Omega = -5.68°$$

The argument of perifocus is determined from

$$\sin(\omega + \theta_1) = \frac{\sin \delta_1}{\sin i} = \frac{(.43851)}{(.48643)} = .90149$$

$$\omega + \theta_1 = \begin{bmatrix} 64.35° \\ \text{or} \\ 115.65° \end{bmatrix} = \omega + 133.73°$$

and

$$\omega \;=\; \begin{bmatrix} -69.38° \\ or \\ -18.08° \end{bmatrix}$$

A rough calculation of ω using the other position yields

$$\sin\,[\omega + (\theta_1 + \Delta\theta)] \;=\; \frac{\sin\,\delta_2}{\sin\,i} \;\approx\; \frac{.47}{.49} \;=\; .96$$

$$\omega + 133.73° + 11.53° \;=\; \begin{bmatrix} 74° \\ or \\ 106° \end{bmatrix}$$

$$\omega \;\approx\; \begin{bmatrix} -71° \\ or \\ -39° \end{bmatrix}$$

The common value is selected, i.e.,

$$\omega \;=\; -69.38°$$

Graphical Solution for i, Ω, and ω.

A graphical solution for the orientation parameters is illustrated in Fig. 34. The graphical solution for i, Ω, and ω consists of the following steps:

1. Plot two known unit position vectors on a properly constructed star chart, i.e., plot $(\alpha_{v1}, \delta_{v1})$ and $(\alpha_{v2}, \delta_{v2})$ where position two is later than position one.

2. Draw a straight line from position two through position one and intersect the equator.

136
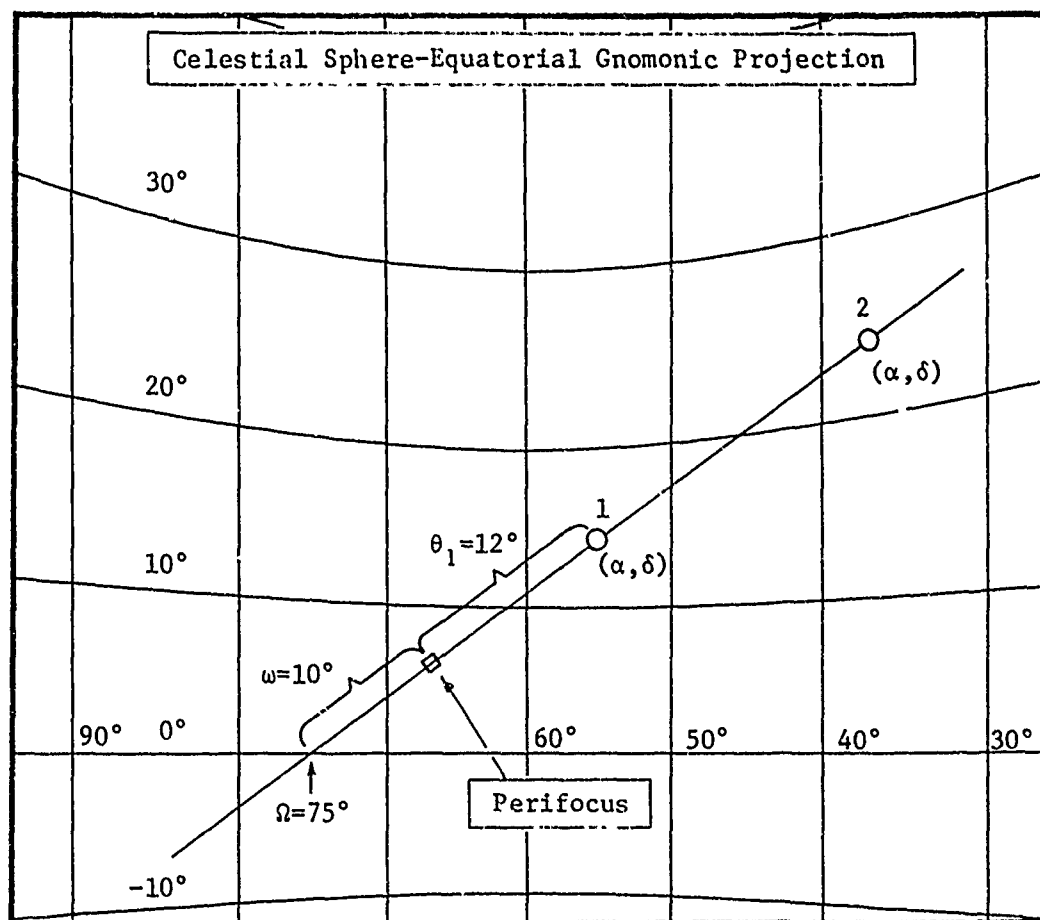
Fig.   34

Graphical Solution - Orientation Elements

3.   The right ascension of the intersection point is Ω.*
    The angle between the orbit plane and the equatorial
    plane is the inclination--but the angle i cannot be
    measured directly from the chart. Instead, the
    inclination must be calculated using the right

* The intersection will yield the descending node if the line is
  drawn from position one to two to the equator.

137

spherical trigonometry relationship

$$\tan i = \frac{\tan \delta_v}{\sin (\alpha_v - \Omega)} \qquad (6\text{-}22)$$

4. Assume the true anomaly of position one is known.
Plot the point representing perifocus by measuring
backward on the constructed line (i.e., in direction
of point two to point one) from point one an angular
distance equal to the true anomaly (the angular
scale on the equator or a meridian must be used).
The angular distance from the equator to perifocus,
measured on the constructed line, is ω.

The star chart must be constructed such that a straight line repre-
sents a portion of a great circle. Projections having this
characteristic are:

        1. equatorial gnomonic

        2. oblique gnomonic

        3. polar gnomonic

The scale distortion of the gnomonic projection does not
appreciably affect the accuracy of the graphical determination of Ω
and i. However, the distorted scale must be used to determine
ω—therefore, ω can only be determined approximately.

Example 6-3 (Graphical Solution for i and Ω). Using the
Polaris fix techniques (Chapter V), the astronauts establish the

following angular data:

$$t = t_1 \qquad\qquad\qquad t_2 = t_1 + 2 \text{ hr}$$

$$\alpha_1 = 39.12° \qquad\qquad\qquad \alpha_2 = 63.39°$$

$$\delta_1 = 21.40° \qquad\qquad\qquad \delta_2 = 27.47°$$

The inclination of the orbital plane and the longitude of the ascending node is desired.

Solution. Figure 35 represents an equatorial gnomonic projection of the celestial sphere. The two angular positions are plotted and a straight line is drawn from position two through position one. The line intersects the equator at $\alpha = -5.5°$, therefore

$$\Omega = -5.5°$$

The inclination is given by

$$\tan i = \frac{\tan \delta_2}{\sin (\alpha_2 - \Omega)} = \frac{\tan 27.47°}{\sin (63.39° + 5.5°)}$$

$$\tan i = \frac{.51983}{.93285} = .55725$$

from which

$$i = 29.1°$$

The solution for ω is not shown since, for the example orbit selected, the construction lies outside the range of the chart.

Fig. 35. Graphical Solution for Ω
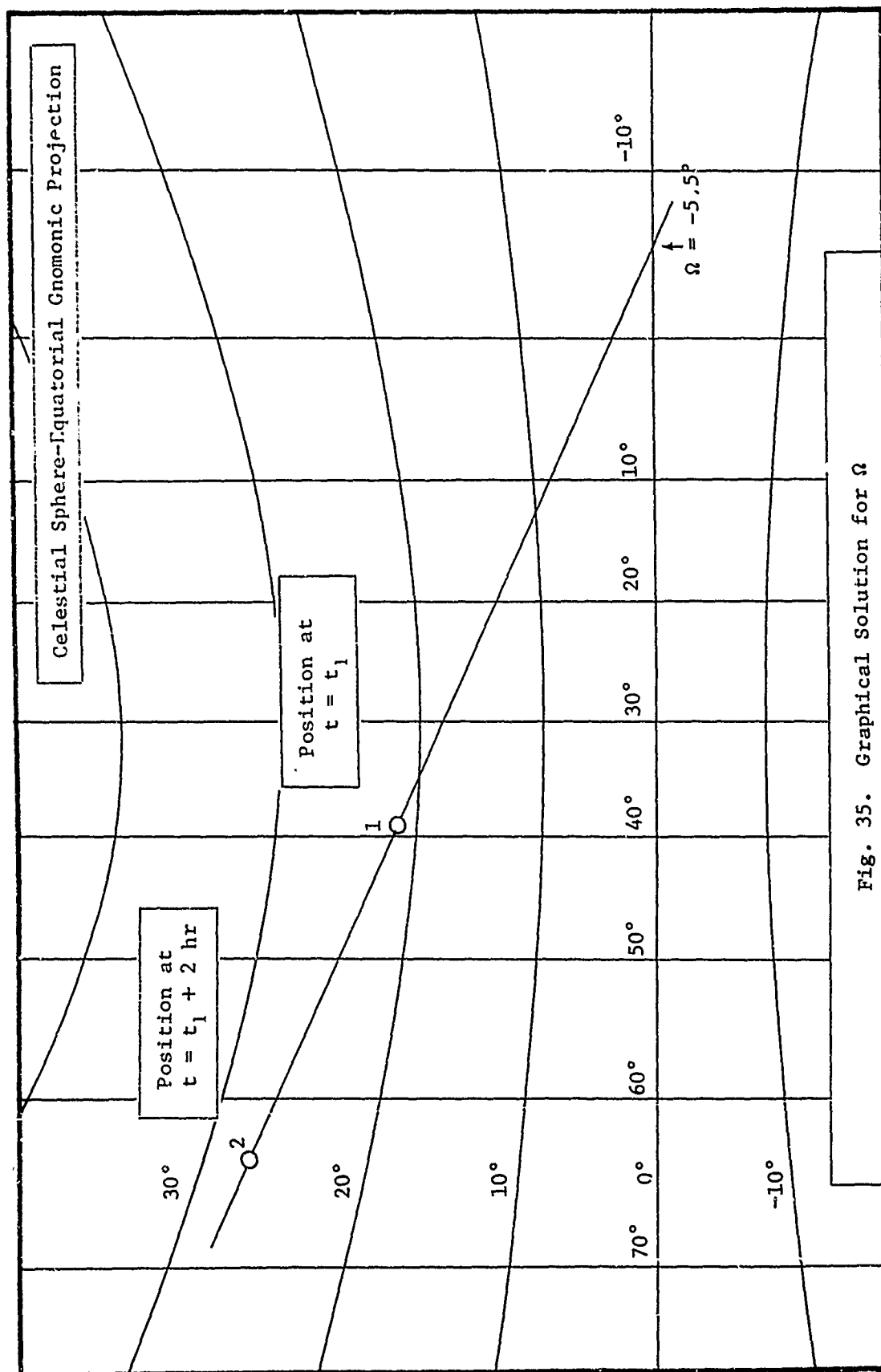
Orientation Elements From Minimum Coaltitudes

This section is an outline of an alternate method for determining the unit vector $\hat{W}$ (Fig. 29). The scheme is related to the present minimum coaltitude method used in Refs 12, 17, and 23. The present method was briefly summarized at the opening of this chapter.

Three minimum coaltitudes can yield the unit vector $\hat{W}$ through the equations

$$\hat{W} \cdot \hat{I}_1 = \sin (\psi_o)_1$$

$$\hat{W} \cdot \hat{I}_2 = \sin (\psi_o)_2$$

$$\hat{W} \cdot \hat{I}_3 = \sin (\psi_o)_3 \tag{6-23}$$

Eq (6-23) is the same form as the three-dimensional fix equations of Chapter V, Eq (5-13). Solution for the components of the unit vector $\hat{W}$ leads to

$$W_x = - A_{x1} \sin (\psi_o)_1 - B_{x2} \sin (\psi_o)_2 - C_{x3} \sin (\psi_o)_3$$

$$W_y = - A_{y1} \sin (\psi_o)_1 - B_{y2} \sin (\psi_o)_2 - C_{y3} \sin (\psi_o)_3$$

$$W_z = - A_{z1} \sin (\psi_o)_1 - B_{z2} \sin (\psi_o)_2 - C_{z3} \sin (\psi_o)_3 \tag{6-24}$$

The constants A_{x1} through C_{z3} are the same quantities defined by Eq (5-16) and used in the three star fix procedure of Chapter V. The same publication tabulating the constants can therefore be used either for three star fix procedures or for directly determining the unit vector $\hat{W}$. The orientation elements can be derived from knowledge

of $\hat{W}$.

The minimum coaltitudes can be determined geometrically using spherical trigonometry if the geometric elements are known (Ref 17:45). Minimum coaltitude can also be observed directly--the geometry is shown in Fig. 32 in Chapter V.

Other than eliminating the simultaneous measurement requirement of the three-dimensional fix, the minimum coaltitude method offers little advantage over the position fix technique. Indeed, since similar equations must be solved for either method, the position fix is preferred. A position fix in space yields more information the astronaut can use directly in solving the navigation and guidance problem.

Summary - Orientation Elements

Compared to the geometric elements, the solution for the orientation parameters is simple. The exact solution for the geometric elements from a set of range measurements involves a set of nonlinear equations. The orientation elements, with the exception of ω which depends on true anomaly, can be obtained using simpler equations. There is no need to toil over nonlinear interative techniques to obtain the orientation elements. Notice that the solutions for i and Ω do not require knowledge of the vehicle's distance from the earth--a plus feature since the range measurement is the most difficult to obtain accurately,

VII. Orbit Determination - No Range Measurements

Most of the orbit determination methods presented in this thesis require one or more measurements of range (range is radial distance from the center of the earth). In general, the range measurement is the most difficult to obtain accurately. For this reason, it seems logical to seek an orbit determination scheme that does not require any range measurement whatsoever. One such method will be briefly described. Time permits the presentation of only the bare details-- the recommendation section of this thesis will suggest further analysis of this orbit determination scheme.

Orbit Determination - No Range Measurements

One possible method of computing an orbit without knowledge of radial distance is briefly presented.

1. Determine the orbit plane--two angular positions are required from which i and Ω can be determined.

2. Find a star in the orbit plane. This can be done using procedures described in Chapter V.

3. Obtain three values of $\dot{\theta}$. $\dot{\theta}$ might be determined using numerical differentiation. For three measurements

$$\dot{\theta}_2 = \frac{\theta_3 - \theta_1}{2t} \tag{7-1}$$

143

The quantity $(\theta_3 - \theta_1)$ can be measured directly by sighting the orbit-plane star. Chapter V outlines the procedure.

4. Compute e and θ_1 using*

$$e \cos \theta_1 = \tilde{Q}/\tilde{S} \tag{7-2}$$

$$e \sin \theta_1 = \tilde{R}/\tilde{S} \tag{7-3}$$

where

$$\tilde{Q} = (\dot{\theta}_2)^{1/2} \sin \Delta\theta_{13} - (\dot{\theta}_3)^{1/2} \sin \Delta\theta_{12}$$
$$+ (\dot{\theta}_1)^{1/2} [\sin \Delta\theta_{12} - \sin \Delta\theta_{13}] \tag{7-4}$$

$$\tilde{R} = - (\dot{\theta}_3^{1/2} - \dot{\theta}_1^{1/2}) \cos \Delta\theta_{12}$$
$$+ (\dot{\theta}_2^{1/2} - \dot{\theta}_1^{1/2}) \cos \Delta\theta_{13}$$
$$- (\dot{\theta}_2^{1/2} - \dot{\theta}_3^{1/2}) \tag{7-5}$$

$$\tilde{S} = \dot{\theta}_1^{1/2} \sin (\Delta\theta_{13} - \Delta\theta_{12})$$
$$+ \dot{\theta}_3^{1/2} \sin \Delta\theta_{12} - \dot{\theta}_2^{1/2} \sin \Delta\theta_{13} \tag{7-6}$$

$$\Delta\theta_{ij} = \theta_j - \theta_i \tag{7-7}$$

* These equations are presented in Ref 20:697.

144

Note that if a suitable measurement schedule is

followed, a number of terms can be pre-calculated.

5. Compute ℓ (semilatus rectum) from

$$\ell = \left[\frac{\mu(1 + e \cos \theta_1)^4}{\dot{\theta}_1^2} \right]^{1/3} = a(1 - e^2) \qquad (7-8)$$

Summary

Only the bare essentials of a "no range" orbit determination method

have been presented. Other orbit determination schemes that involve

indirect measurements of distance are also available--the classical

Laplacian method (Ref 3:36) is one example. Intuitively, it seems

that an orbit determination scheme of this type would be highly

advantageous because:

1. To date, the accuracy of range determination is
   marginal.

2. Angular measurements can be obtained more directly
   and probably with greater accuracy.

3. The semi-diameter method of obtaining range is
   limited to close earth orbits. Range in deep space
   requires the solution of a more complex equation
   (Ref 4:222).

4. Range determination methods using a reference trajectory
   are useless if the reference trajectory is invalidated
   (this topic is treated in Chapter VIII).

VIII. An Improved Optical Method of
Range Measurement

Introduction

As has been seen in the previous chapters, accurate range or
altitude measurement is essential in most manual navigation schemes.
Optical measurement using the planet angular diameter is subject to
large errors as the distance from the measured body increases.
Therefore, other optical ranging techniques have been investigated.
Harold A. Hamer, of the NASA Langley Research Center, has proposed a
method based upon linear perturbations from a pre-computed reference
trajectory (Ref 8). This chapter deals with Mr. Hamer's approach to
accurate optical range measurement.

The Method

The geometry of the measurement procedure is depicted in Fig. 36.
The angle D, which can vary between 0 degrees and 180 degrees, lies in
the instantaneous earth-moon-vehicle plane. If Fig. 36 represents the
vehicle on a reference trajectory at a given time, then the incremental
range Δr_{ev} (actual range minus reference range) at that time is obtained
as follows:

$$r_{ev} = \frac{r_{em}}{\sin A} \sin C = \frac{r_{em}}{\sin A} \sin (A + B) \qquad (8\text{-}1)$$

or

$$r_{ev} = r_{em} \cos B + r_{em} \sin B \cot A \qquad (8\text{-}1a)$$

146
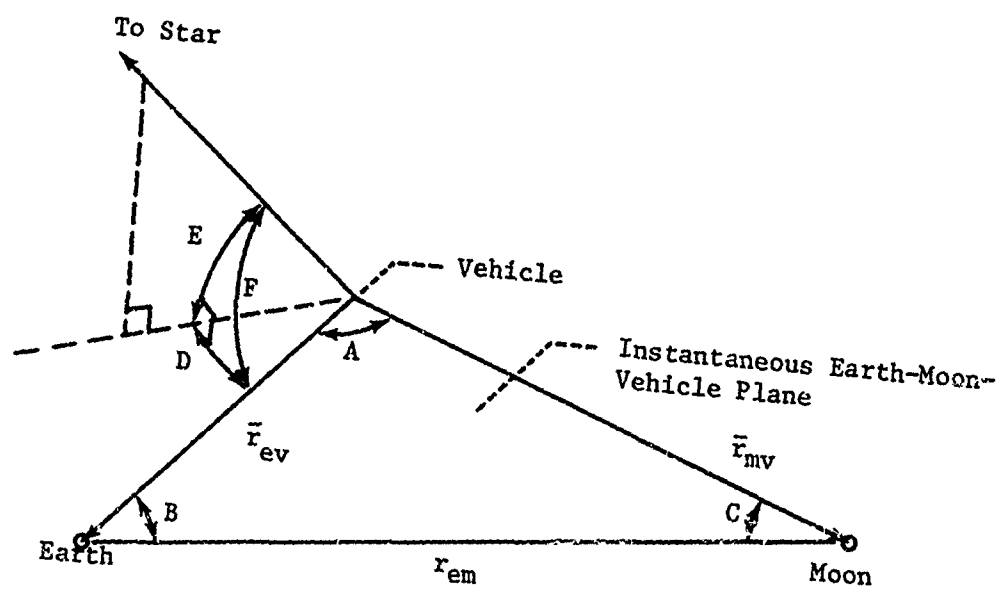
Fig. 36

Geometry of The Hamer Method (From Ref 8:6)

As shown in Eq (8-1a), the variables which define r_{ev} at a given time are the angles A and B; therefore

$$dr_{ev} = \frac{\partial r_{ev}}{\partial A} dA + \frac{\partial r_{ev}}{\partial B} dB \qquad (8-2)$$

From Eq (8-1a)

$$\frac{\partial r_{ev}}{\partial A} = - r_{em} \sin B \csc^2 A \qquad (8-3)$$

but

$$\sin B = \frac{r_{mv}}{r_{em}} \sin A \qquad (8-4)$$

so that

$$\frac{\partial r_{ev}}{\partial A} = - \frac{r_{mv}}{\sin A} \qquad (8-5)$$

where

$$\cos A = \frac{r_{ev}^2 + r_{mv}^2 - r_{em}^2}{2r_{ev} r_{mv}} \qquad (8-6)$$

Further, from Eq (8-1a)

$$\frac{\partial r_{ev}}{\partial B} = r_{em} (\cos B \cot A - \sin B) \qquad (8-7)$$

where angle B is given by Eq (8-4) and angle A is given by Eq (8-6). The values of r_{ev}, r_{mv}, and r_{em} are known for the reference trajectory.

148

The variables A and B in Eq (8-2) refer to angular measurements
which must be made onboard the vehicle. Angle B cannot be measured
from the vehicle. Therefore, a related angle which can be measured
must be substituted. As shown in Fig. 36, the angle F, measured
between a star and the earth's center, can be used in the following
manner. For the case in which the star is in the instantaneous
earth-moon-vehicle plane, $dD/dB = \pm 1$, (this is true because r_{em}
and the line-of-sight to the star are fixed in direction for the
instant being considered), where the sign is determined by the
relative directions of the earth and the star. Equation (8-2),
therefore, can be written

$$dr_{ev} = \frac{\partial r_{ev}}{\partial A} \, dA + k \, \frac{\partial r_{ev}}{\partial B} \, dD \qquad (8-8)$$

where dD represents the change in the star-to-earth angle and k is
plus or minus one. (The equation for determining k is derived in
Appendix E.) If the star is not in the instantaneous plane, as
shown in Fig. 36, dD can be determined from the right spherical
trigonometric relationship

$$\cos F = \cos D \cos E \qquad (8-9)$$

or

$$D = \cos^{-1}\left(\frac{\cos F}{\cos E}\right) \qquad (8-9a)$$

Thus

$$dD = \left(\frac{\sin^2 F}{\cos^2 E - \cos^2 F} \right)^{1/2} dF \qquad (8\text{-}10)$$

or

$$dD = \left(\frac{1 - \cos^2 F}{\cos^2 E - \cos^2 F} \right)^{1/2} dF \qquad (8\text{-}11)$$

Therefore, in terms of two angles which can be measured from the vehicle (earth center to moon center and star-to-earth center), Eq (8-8) can be written

$$dr_{ev} = \frac{\partial r_{ev}}{\partial A} dA + k \frac{\partial r_{ev}}{\partial B} \left(\frac{1 - \cos^2 F}{\cos^2 E - \cos^2 F} \right)^{1/2} dF \qquad (8\text{-}12)$$

or, for the region in which a change in r_{ev} is linear with changes in A and B

$$\Delta r_{ev} = \frac{\partial r_{ev}}{\partial A} \Delta A + k \frac{\partial r_{ev}}{\partial B} \left(\frac{1 - \cos^2 F}{\cos^2 E - \cos^2 F} \right)^{1/2} \Delta F \qquad (8\text{-}13)$$

where

$$\Delta A = A_{actual} - A_{reference} \qquad (8\text{-}14)$$

$$\Delta F = F_{actual} - F_{reference} \qquad (8\text{-}15)$$

The incremental range Δr_{ev}, then, is determined by the two measurements A(actual) and F(actual), and by the pre-calculated values of

A(reference), F(reference), $\partial r_{ev}/\partial A$, $\partial r_{ev}/\partial B$, and $k\left[(1 - \cos^2 F)/\right.$ $\left.(\cos^2 E - \cos^2 F)\right]^{1/2}$. Equations for calculating F, E, and k, which pertain to the reference trajectory, are derived in Appendix E.

Linearity Characteristics. Mr. Hamer's investigation of the variations of Δr_{ev} with ΔA and ΔB for a typical lunar trajectory showed that at a given time the partials $\partial r_{ev}/\partial A$ and $\partial r_{ev}/\partial B$ can be considered to be essentially constant over a wide region, as indicated in Fig. 37. (Note that the kilometer is used as the unit of distance in this chapter.) The reference trajectory used was selected from Ref 7. In Fig. 37, the curve for ΔB was determined from the relations

$$\sin C = \frac{r_{ev}}{r_{em}} \sin A \qquad (8\text{-}16)$$

and

$$B = 180° - (A + C) \qquad (8\text{-}17)$$

where A is held constant at the reference value and is given by Eq (8-6). The curve for ΔA was determined from the relation

$$\sin A = \frac{r_{em}}{r_{mv}} \sin B \qquad (8\text{-}18)$$

where

$$r_{mv} = (r_{ev}^2 + r_{em}^2 - 2 r_{em} r_{ev} \cos B)^{1/2} \qquad (8\text{-}19)$$

and B is held constant at the reference value, and is determined by Eqs (8-16) and (8-17). The curves shown in Fig. 37 are for a
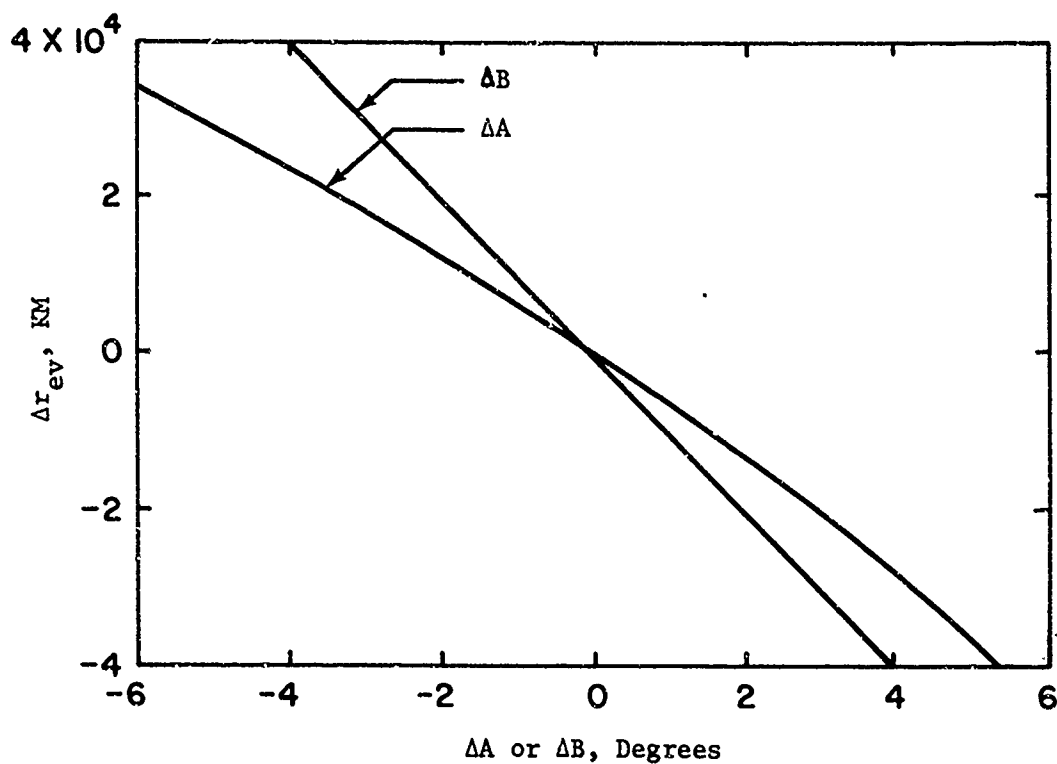
Fig. 37

Linearity Characteristics of the Hamer Method for a Reference
Distance of 162,000 KM From Earth (Ref 8:10)

reference time from injection (perigee) of 16.125 hours. (Here, r_{ev} is approximately 162,000 kilometers.) At this time, a two hour difference at injection from the reference injection time would represent a difference in range from the earth of about 13,000 kilometers. The data in Fig. 37 show that this difference can be considered to be within the linear region. Several reference trajectories, therefore, could suffice for range determination for a given launch window.

The linearity characteristics of $\partial r_{ev}/\partial A$ and $\partial r_{ev}/\partial B$ illustrated in Fig. 37 are representative of those over most of the earth-moon distance. Actually, the linear approximation for $\partial r_{ev}/\partial A$ improves as the moon is approached, as shown by the derivative of Eq (8-5), which is

$$\frac{\partial^2 r_{ev}}{\partial A^2} = r_{mv} \frac{\cos A}{\sin^2 A} \tag{8-20}$$

The angle A approaches 90 degrees as the moon is approached. From the derivative of Eq (8-7)

$$\frac{\partial^2 r_{ev}}{\partial B^2} = - r_{em} (\cot A \sin B + \cos B) \tag{8-21}$$

it can be determined that the linear approximation for $\partial r_{ev}/\partial B$ will also improve as the moon is approached.

Effect of Proximity to the Earth-Moon Line. The values of $\partial r_{ev}/\partial A$ and $\partial r_{ev}/\partial B$ which are pre-calculated and supplied to the

astronaut in the form of charts or tables are shown in Fig. 38 for

vehicle positions along the translunar portion of the reference

trajectory. The partials $\partial r_{mv}/\partial A$ and $\partial r_{mv}/\partial C$ required to determine

range from the moon are also shown. These values will approach those

shown for $\partial r_{ev}/\partial A$ and $\partial r_{ev}/\partial B$ at distances near the earth. It is to

be noted that for a position fix near the moon, higher accuracy is

obtained by measuring range from the earth rather than from the moon,

inasmuch as the geometry gives lower values for $\partial r_{ev}/\partial A$ and $\partial r_{ev}/\partial B$.

It will be seen that the error in determining the incremental range,

Δr_{ev}, is proportional to the magnitudes of the partials.

In Fig. 38, the large values shown for $\partial r_{ev}/\partial A$ and $\partial r_{ev}/\partial B$ near

the earth occur because of the close proximity to the earth-moon line

(angle A approaches 180 degrees). Thus, range determination using

Eq (8-13) would be inaccurate for about the first five hours (or

75,000 KM) from injection. These results would be typical for any

method based upon earth-moon measurements. The accuracy of angular

diameter measurements is much better for the first five hours, as

shown in Fig. 39. The dashed curve represents the error in the range

for an angular diameter measurement σ error of 10 arc-seconds.

For times along the reference trajectory except for the first

five hours, the error in determining range by Eq (8-13) is relatively

small, as shown by the solid curve in Fig. 39. This curve represents

the error in the incremental range along the translunar portion of

the reference trajectory where the angular measurements A and F are

considered to have random uncorrelated errors, each with a standard
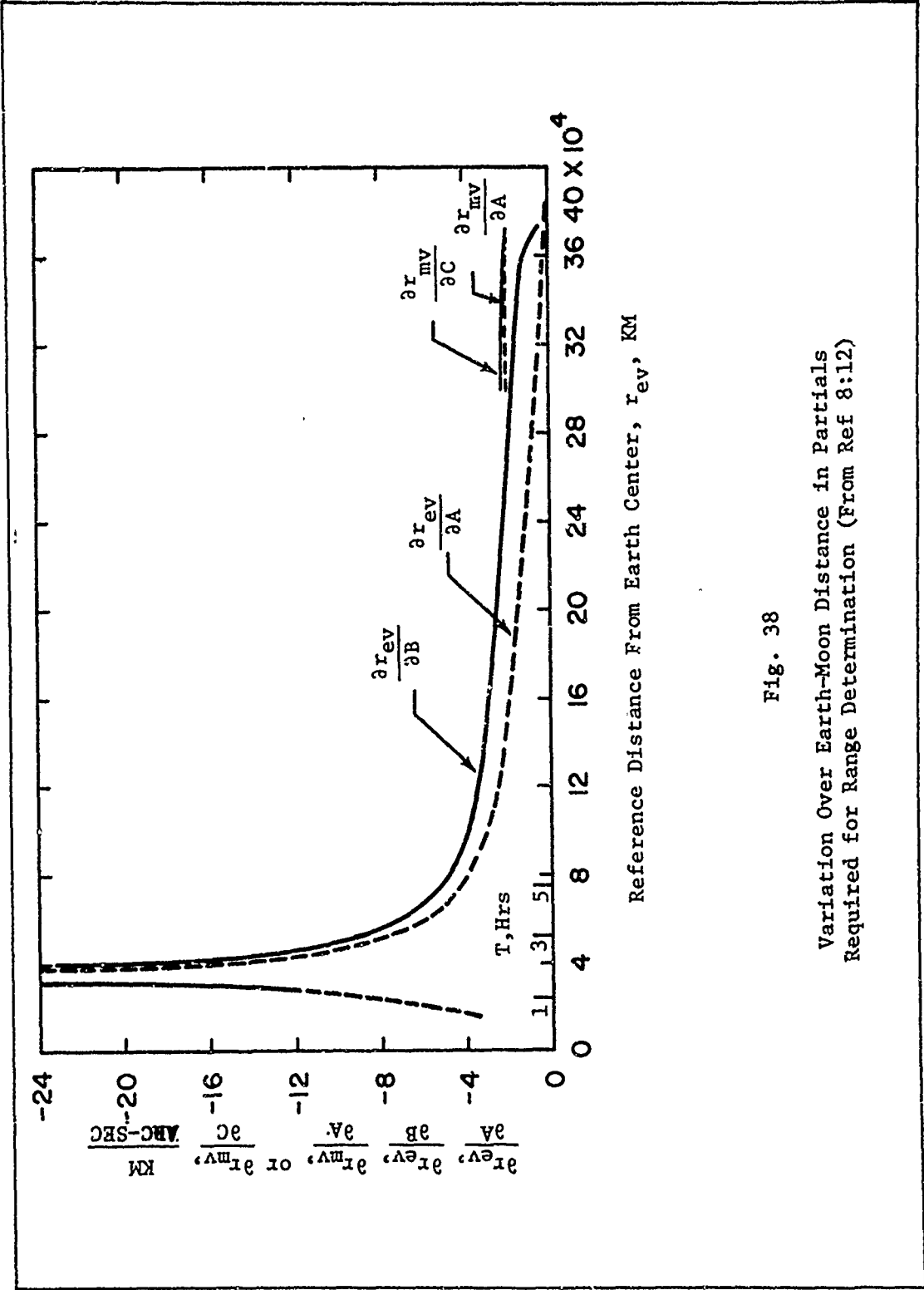
Fig. 38

Variation Over Earth-Moon Distance in Partials
Required for Range Determination (From Ref 8:12)
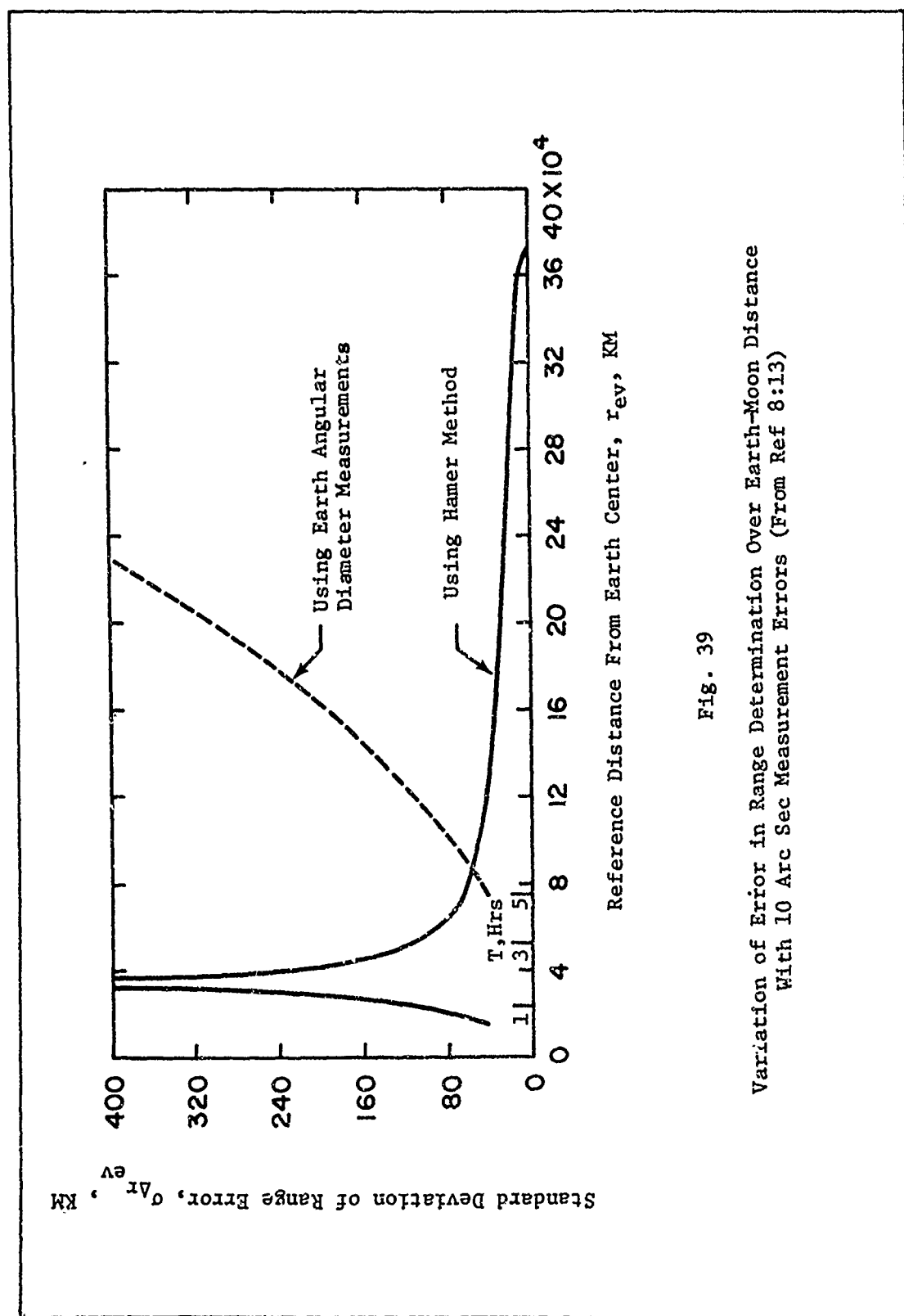
Fig. 39

Variation of Error in Range Determination Over Earth-Moon Distance
With 10 Arc Sec Measurement Errors (From Ref 8:13)

deviation σ of 10 arc-seconds, such that

$$\sigma_{\Delta r_{ev}} = \left[\left(\frac{\partial r_{ev}}{\partial A} \ \sigma_A \right)^2 + \left(\frac{\partial r_{ev}}{\partial F} \ \sigma_F \right)^2 \right]^{1/2} \qquad (8\text{-}22)$$

where

$$\frac{\partial r_{ev}}{\partial F} = k \left(\frac{1 - \cos^2 F}{\cos^2 E - \cos^2 F} \right)^{1/2} \frac{\partial r_{ev}}{\partial B} \qquad (8\text{-}22a)$$

In Fig. 39, the star which is used to measure F is assumed to lie in (or near) the instantaneous earth-moon-vehicle plane so that the value of the term $[(1 - \cos^2 F)/(\cos^2 E - \cos^2 F)]^{1/2}$ in Eq (8-13) is one, and $\partial r_{ev}/\partial B = \pm \ \partial r_{ev}/\partial F$.

Effect of the Star Selected for Measurement. The value of the quantity $[(1 - \cos^2 F)/(\cos^2 E - \cos^2 F)]^{1/2}$ can vary from one to infinity, depending on the reference trajectory and the star selected for the measurement of F. The effect of star position on the error in Δr_{ev} is shown in Fig. 40. The error in Δr_{ev} is a minimum when the quantity $[(1 - \cos^2 F)/(\cos^2 E - \cos^2 F)]^{1/2}$ is a minimum. This quantity has its minimum with respect to F at F = 90 degrees and rises rapidly as the extreme values, F = E and F = 180 degrees minus E, are approached. The extreme values of F occur when the star position is in the plane containing the vehicle-earth line and the vertical to the earth-moon-vehicle plane. The desired stars, therefore, are those that lie near the earth-moon-vehicle plane (E within about plus or minus 30 degrees) with projections in that plane away from the
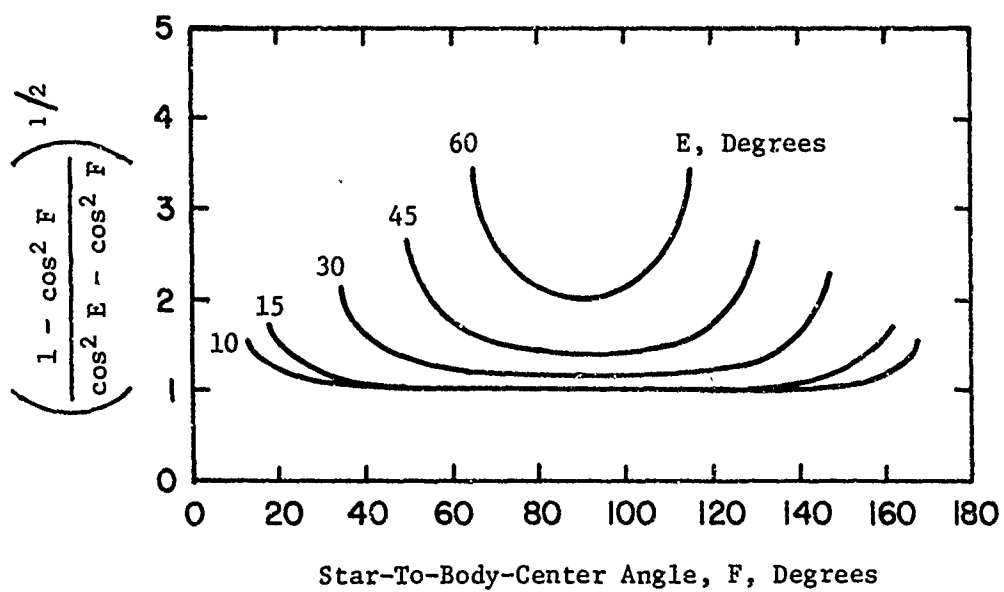
Fig. 40

Effect of Star Position on Accuracy of
Range Determination (From Ref 8:14)

vehicle-earth line.

Corrections for Nonsimultaneous Measurements. In the equation for range determination, Eq (8-13), both measurements are assumed to have been made simultaneously. Since simultaneous measurements are not usually possible, errors would be introduced in the results unless the measurements were corrected or converted to some common time. This time could be either before or after the actual time of the measurements. If the time corresponding to one of the measurements is made the common time, only one measurement would have to be converted.

The measurements can be converted to a common time (small time increments only) by use of pre-calculated data on the rate of change of angle with time along the reference trajectory. These data would be practically the same for any other trajectory reasonably near the reference, so that they would apply for making corrections when off the reference trajectory. Equations for calculating dA/dt and dF/dt along a reference trajectory are given in Appendix B of Ref 8.

In converting a measurement to a common time, the corresponding value of dA/dt or dF/dt at the given range multiplied by the time increment would be sufficient to calculate the incremental angle to be added algebraically to the measured angle. The range would have to be known only approximately. For trajectories launched near nominal injection time, the nominal range at the time of the measurements would be adequate, whereas for trajectories not launched near the nominal injection time, the approximate range could be determined according to the time from actual injection time.

Measurements of the Center of a Body

Throughout this discussion, it has been assumed that optical measurements to the center of the earth and moon are possible. The USAF Hand-held Space Sextant has been qualified for star-horizon measurements only. It is felt by the authors of this thesis that this sextant could be adapted to measure star-earth center and moon-earth center angles. The incorporation of an attachment such as a filter enscribed with concentric circles and centering cross-hairs has been suggested to the Air Force Avionics Laboratory, sponsors of the sextant's development and testing. Their response has been favorable, and this idea may be investigated with possible operational testing in the D-009 Apollo experiment.

Discussion

Mr. Hamer points out that the range measurement method he has proposed could be used just as easily with the Sun and a planet as with the earth and the moon. Also, he has determined that after the first five hours from injection on a translunar trajectory, the uncertainty in range is relatively constant at about 35 kilometers as long as the star used is within plus or minus 30 degrees of the earth-moon-vehicle plane.

These results are very encouraging. With range measurements of this accuracy, the manual navigation techniques described in this thesis are of much greater utility in cislunar and, indeed, in interplanetary space than they would have been if angular diameter measurements were used exclusively to determine range. The linearity

characteristics of the method allow large deviations from the reference trajectory. Thus, barring a catastrophic failure such as an uncontrollable propulsion system, this method is flexible enough to be incorporated in a manual navigation scheme. The only equipment necessary would be the space sextant with attachment for body center measurements, a time history of the reference trajectory (or trajectories, if several sets of data are carried for greater flexibility), and a computational tool for use in the solution of Eq (8-13).

Summary

The precomputations necessary for the Hamer method of range determination are:

1. $\bar{r}_{ev}$, $\bar{r}_{mv}$, r_{em}, A, B, and F as functions of time on the reference trajectory

2. $$\frac{\partial r_{ev}}{\partial A} = -\frac{r_{mv}}{\sin A}$$

3. $$\frac{\partial r_{ev}}{\partial B} = r_{em} (\cos B \cot A - \sin B)$$

4. $\bar{h} = \bar{r}_{ev} \times \bar{r}_{mv}$ (See Appendix E)

5. $$\sin E = \left| \frac{\ell\, h_x + m\, h_y + n\, h_z}{h} \right|$$ (See Appendix E)

6. $\bar{b} = \bar{r}_{ev} \times \bar{h}$ (See Appendix E)

7. $k = \dfrac{\ell\, b_x + m\, b_y + n\, b_z}{\left|\ell\, b_x + m\, b_y + n\, b_z\right|}$ (See Appendix E)

All of these values must be precomputed before flight. Inflight, the astronaut is required to solve only

$$\Delta r_{ev} = C_1\, \Delta A + C_2\, \Delta F \qquad (8\text{-}13a)$$

where C_1 and C_2 are constants which are precomputed for the reference trajectory, i.e.,

$$C_1 = \frac{\partial r_{ev}}{\partial B} \qquad (8\text{-}23)$$

and

$$C_2 = k\, \frac{\partial r_{ev}}{\partial B}\, \left(\frac{1 - \cos^2 F}{\cos^2 E - \cos^2 F}\right)^{1/2} \qquad (8\text{-}24)$$

Sample Problem. The following is a sample calculation of distance from the earth using the Hamer method. The reference values were taken from Ref 8.

At 31.125 hours from injection (about halfway to the moon), the reference trajectory values are:

$$x_{ev} = -\,9233.1921$$

$$y_{ev} = 211785.18$$

$$z_{ev} = 116836.74$$

$$r_{ev} = 242051.73$$

162

$$x_{mv} = -\ 113475.61$$

$$y_{mv} = -\ 101136.23$$

$$z_{mv} = -\ 49059.589$$

$$r_{mv} = 159725.06$$

$$r_{em} = 369198.98$$

$$A = 132.4675 \text{ degrees}$$

$$B = 18.0877 \text{ degrees}$$

$$F = 82.4794 \text{ degrees (the star chosen is}$$
$$\text{Algenib)}$$

The precomputation yields

$$C_1 = -\ 212234.26$$

and

$$C_2 = -\ 450855.29$$

An actual position was __assumed__ at

$$x_{ev} = -\ 15000$$

$$y_{ev} = 220000$$

$$z_{ev} = 122000$$

163

So that

$$r_{ev} = 252010$$

which is approximately 10000 kilometers off the reference value. (This position was chosen to test the linearity characteristics of the Hamer method.) At this position, the actual angular measurements would be, assuming 10 arc-seconds error in each:

$$A_{actual} = 127.2446 \text{ degrees}$$

$$F_{actual} = 83.6540 \text{ degrees}$$

Applying Eq (8-13a)

$$\Delta r_{ev} = C_1 \Delta A + C_2 \Delta F$$

or

$$r_{actual} = r_{ref} + C_1 \Delta A + C_2 \Delta F$$

yields

$$r_{actual} = 252155 \text{ kilometers}$$

This value is in error by 145 kilometers, since the precise assumed value is 252010 kilometers. This represents a .06 per cent error. An angular diameter measurement would have been in error by more than 500 kilometers. It is probable that the error in the Hamer

estimate of the actual range is primarily due to nonlinearity at such

a large distance off the reference trajectory. The coefficients

C_1 and C_2 are fairly large also, and this magnifies the measurement

error introduced. In any case, the Hamer method is a vast improvement

over the angular diameter method.

IX. Aids to Manual Navigation

As progress is made in the exploration of space, operational manual navigation and guidance systems will become a necessity. The authors of this thesis believe that as this requirement makes itself felt certain "aids" will be developed to enhance the performance of these systems.

To date, no concerted effort has been made to develop a general manual system. Those who have worked on the idea have been limited by the constraints of the hardware available at the present time. (The sum total of this hardware consists of the USAF Hand-held Space Sextant and the USAF Space Stadimeter.) The manual navigation techniques developed thus far are inflexible due to these constraints. Many of the methods described in this thesis are impractical when viewed from the standpoint of current equipment. The authors feel that no promising method or approach should be discarded on this basis. Indeed, the equipment must be designed to fit the best approach, and not vice versa.

It is, therefore, the purpose of this chapter to explore the utility of three categories of "aids" to manual navigation; the back-up inertial platform, the hand-held mechanical calculator, and the hand-held, battery operated, digital computer.

The Back-up Inertial Platform

A back-up inertial platform would be invaluable in determining spacecraft position. An instrument such as a theodolite mounted on an inertial platform is capable of measuring directly the right ascension and declination of the vehicle by simply sighting the earth, sun, or any other body whose coordinates are known. No computations would be necessary to obtain this information. The space sextant could be used to align the platform by sighting two known stars. Since the lines-of-sight define a plane, the platform can be oriented so as to be parallel to any desired reference plane. The power source could be electrical (batteries) or mechanical (hand-crank).

The Hand-held Mechanical Calculator

Many of the manual navigation techniques described in this report involve several computation steps. It would be difficult to achieve consistent accuracy with a slide rule. Reducing the equations to graphical form is not always practical because of the volume of graphs necessary for flexible operation. A better approach may lie in the use of a small, highly accurate mechanical calculator. Such a device is manufactured by the Curta Corporation, of Van Nuys, California. Figure 41 is a photograph of the Curta Calculator. This machine is capable of performing addition, subtraction, multiplication, and division. It also squares, cubes, and extracts square roots. The accuracy of the Curta Calculator is an amazing eight significant figures! (This is based upon the limit imposed by division. Multiplication can be carried to fifteen figures.) The diameter of

Fig. 41

The Curta Calculator

the machine is 2 9/16 inch, and the height is 3 5/8 inch. Most

importantly, the weight of the Curta Calculator is but 12 1/2 ounces.

This hand-held mechanical calculator combines the accuracy of a desk

calculator with the portability of a slide rule. The authors feel

that such a computational tool is ideally suited as an aid to manual

navigation.

The Hand-held, Battery Operated, Digital Computer

The hand-held, battery operated, digital computer is, in the opinion of the authors, the most important tool in the future of manual navigation in space. With the proper measuring equipment, such a device could be capable of solving explicitly the manual navigation problem. The most promising methods explored in this thesis are ideally suited to being programmed into a small computer. The proper use of such a tool is paramount in determining its true utility. Memory space is the prime limitation. It would be unreasonable to attempt "brute force" techniques that require excessive iterations. The hand-held computer should not be used to duplicate the functions of the primary system computers. It should not be pre-programmed with inflexible routines that cannot be altered as needed. It should be designed so that the astronaut, who is obviously familiar with astro-dynamics and celestial mechanics, can program the equations he needs under any circumstances. Several small computers are in existence today. The most promising investigated is the Hewlett-Packard 9100A. This computer is capable of performing at least as well as the IBM 1620. It can be programmed with magnetic "credit cards" to solve problems up to and including numerical integration. The present weight of the 9100A is 40 pounds. There is no reason to believe that this couldn't be reduced for manual navigation and guidance applications.

To demonstrate the utility of a small, hand-held computer in manual navigation, the Gibbs method of orbit determination (see Chapter V) was programmed in Fortran II and run on the IBM 1620. This program would easily fit into the Hewlett-Packard 9100A.

169

Figure 42 is a reproduction of the Gibbs program with output. This program is totally flexible in that it may be applied to elliptic and hyperbolic trajectories. The output includes the type of trajectory, the eccentricity, the semimajor axis, the time past perifocus to the third fix, the $\hat{P}$, $\hat{Q}$, and $\hat{W}$ orientation vectors, and the velocity components at the third fix. The three input fixes were obtained from a precision trajectory in Ref 8. All of the output values are within .01 per cent of the quoted precision (translunar) trajectory values. Since the program is written in general form, it is applicable to any inverse-square field, as long as the gravitational constant for the attracting body is known. This constant must be input with the three fixes. The output, then, is in the units of the gravitational constant and the position fixes. For example, in Fig. 42, the gravitational constant and fixes are in the kilometer-second system of units. Therefore, the output distances are in kilometers and the velocities are in KM/SEC.

Since position and velocity are known at fix three, the position and velocity at any time thereafter can be projected. Figure 43 is a reproduction of a program which uses the universal formulas developed by Battin in Ref 4. The output is position and velocity at hourly intervals past the third fix. Again, a general form is used for flexibility, and the units of the input determine the units of the output. (Since the output of the Gibbs program is input to this program, its output is in kilometers and KM/SEC.) This information could be used to initiate a guidance scheme.

```
C   C   GIBBS METHOD OF ORBIT DETERMINATION--HORRIGAN AND WALSH
        PI=3.1415927
        READ,X1,Y1,Z1,X2,Y2,Z2,X3,Y3,Z3,EMU
        A=SQRT((Y1*Z3-Y3*Z1)**2+(Z1*X3-X1*Z3)**2+(X1*Y3-Y1*X3)**2)
        B=SQRT((Y2*Z3-Y3*Z2)**2+(Z2*X3-X2*Z3)**2+(X2*Y3-Y2*X3)**2)
        C=SQRT((Y2*Z1-Y1*Z2)**2+(Z2*X1-X2*Z1)**2+(X2*Y1-Y2*X1)**2)
        C1=B/A
        C3=C/A
        R1=SQRT(X1**2+Y1**2+Z1**2)
        R2=SQRT(X2**2+Y2**2+Z2**2)
        R3=SQRT(X3**2+Y3**2+Z3**2)
        P=(C1*R1+C3*R3-R2)/(C1+C3-1.)
        WX=(Y1*Z3-Y3*Z1)/A
        WY=(Z1*X3-X1*Z3)/A
        WZ=(X1*Y3-Y1*X3)/A
        EQX=(X3*(P-R1)-X1*(P-R3))/A
        EQY=(Y3*(P-R1)-Y1*(P-R3))/A
        EQZ=(Z3*(P-R1)-Z1*(P-R3))/A
        E=SQRT(EQX**2+EQY**2+EQZ**2)
        QX=EQX/E
        QY=EQY/E
        QZ=EQZ/E
        AXIS=P/(1.-E**2)
        PX=QY*WZ-QZ*WY
        PY=QZ*WX-QX*WZ
        PZ=QX*WY-WX*QY
        YW3=QX*X3+QY*Y3+QZ*Z3
        IF(AXIS)1,1,2
2       COSE3=(AXIS-R3)/(AXIS*E)
        SINE3=YW3/(AXIS*SQRT(1.-E**2))
        GAMMA=ATAN((E/(SQRT(1.-E**2)))*SINE3)
        PUNCH 100
100     FORMAT(26HTHE TRAJECTORY IS ELLIPTIC,//)
        IF(COSE3)5,5,3
5       EANOM=ATAN(SINE3/COSE3)+PI
        GO TO 11
3       EANOM=ATAN(SINE3/COSE3)
11      EN=EMU/(AXIS**1.5)
        DELTT=((EANOM-E*SINE3)/EN)/3600.
        GO TO 15
1       SINHF=-YW3/(AXIS*SQRT(E**2-1.))
        GAMMA=SQRT((P**2)/(R3*(2.*P+R3*(E**2-1.))))
        PUNCH 101
101     FORMAT(28HTHE TRAJECTORY IS HYPERBOLIC,//)
        F=LOG(SINHF+SQRT((SINHF**2)+1.))
        EN=EMU/((-AXIS)**1.5)
        DELTT=((E*SINHF-F)/EN)/3600.
15      RTDOT=(EMU/R3)*SQRT(AXIS*ABS(1.-E**2))
        RDOT=RTDOT*SIN(GAMMA)/COS(GAMMA)
        VX=(RDOT*X3+RTDOT*(WY*Z3-WZ*Y3))/R3
        VY=(RDOT*Y3+RTDOT*(WZ*X3-WX*Z3))/R3
        VZ=(RDOT*Z3+RTDOT*(WX*Y3-WY*X3))/R3
        PUNCH 102,E
102     FORMAT(20HTHE ECCENTRICITY IS ,F7.4,//)
        PUNCH 103,AXIS
103     FORMAT(23HTHE SEMI-MAJOR AXIS IS ,F12.4,//)
        PUNCH 104,DELTT
```

Fig. 42

Typical Gibbs Method Program

171

```
104 FORMAT(40HTHE TIME PAST PERIFOCUS TO FIX THREE IS ,F12.4,//)
    PUNCH 105
105 FORMAT(16HPX,PY,AND PZ ARE)
    PUNCH 106,PX,PY,PZ
106 FORMAT(3F12.4,//)
    PUNCH 107
107 FORMAT(16HQX,QY,AND QZ ARE)
    PUNCH 106,QX,QY,QZ
    PUNCH 108
108 FORMAT(16HWX,WY,AND WZ ARE)
    PUNCH 106,WX,WY,WZ
    PUNCH 109
109 FORMAT(54HTHE X,Y,AND Z VELOCITY COMPONENTS AT THE THIRD FIX ARE)
    PUNCH 106,VX,VY,VZ
    STOP
    END
17000.141  13826.706  8591.5583  20284.239  66965.325  38219.273
 15797.195  106257.19  59747.541  631.35093
```

THE TRAJECTORY IS ELLIPTIC

THE ECCENTRICITY IS   .9739

THE SEMI-MAJOR AXIS IS   247285.1800

THE TIME PAST PERIFOCUS TO FIX THREE IS   10.5060

PX,PY,AND PZ ARE
        .2694   -.8485   -.4555

CX,QY,AND QZ ARE
        .9619   .2136   .1709

WX,WY,AND WZ ARE
       -.0478   -.4842   .8737

THE X,Y,AND Z VELOCITY COMPONENTS AT THE THIRD FIX ARE
       -.3010   1.9199   1.0475

Fig. 42 (Continued)

```
C   C   PROJECTED POSITION AND VELOCITY--HORRIGAN AND WALSH
        READ,X,Y,Z,VX,VY,VZ,EMU
        TT=3600.
        B=1.
    4   XX=1.
        DIST=SQRT(X*X+Y*Y+Z*Z)
        VSQR=VX*VX+VY*VY+VZ*VZ
        ALPHA=2./DIST-VSQR/(EMU**2)
    1   IF(ALPHA)8,7,2
    8   D=SQRT(-ALPHA*(XX**2))
        S=((EXP(D)-EXP(-D))/2.-D)/(D**3)
        C=((EXP(D)+EXP(-D))/2.-1.)/(D**2)
        GO TO 3
    7   S=1./6.
        C=.5
        GO TO 3
    2   E=SQRT(ALPHA*(XX**2))
        S=(E-SIN(E))/(E**3)
        C=(1.-COS(E))/(E**2)
    3   T1=((X*VX+Y*VY+Z*VZ)*(XX**2)*C)/(EMU**2)
        T2=((1.-ALPHA*DIST)*(XX**3)+S)/EMU+(DIST*XX)/EMU
        T=T1+T2
        IF(ABS(TT-T)-.01)6,6,5
    5   Q=(X*VX+Y*VY+Z*VZ)/(EMU**2)
        DERIV=Q*(XX-ALPHA*(XX**3)*S)+((1.-DIST*ALPHA)*(XX**2)*C+DIST)/EMU
        XX=XX-(T-TT)/DERIV
        GO TO 1
    6   RX=(1.-((XX**2)/DIST)*C)*X+(TT-(XX**3)*S/EMU)*VX
        RY=(1.-((XX**2)/DIST)*C)*Y+(TT-(XX**3)*S/EMU)*VY
        RZ=(1.-((XX**2)/DIST)*C)*Z+(TT-(XX**3)*S/EMU)*VZ
        R=SQRT(RX*RX+RY*RY+RZ*RZ)
        A=EMU
        VXX=((1./(R*DIST))*(ALPHA*(XX**3)*S-XX))*X*A+(1.-((XX**2)/R)*C)*VX
        VYY=((1./(R*DIST))*(ALPHA*(XX**3)*S-XX))*Y*A+(1.-((XX**2)/R)*C)*VY
        VZZ=((1./(R*DIST))*(ALPHA*(XX**3)*S-XX))*Z*A+(1.-((XX**2)/R)*C)*VZ
        TTT=B
        PUNCH 100,TTT
  100   FORMAT(38HPOSITION AND VELOCITY COMPONENTS AT T=,F7.4,//)
        PUNCH 101,RX,RY,RZ
  101   FORMAT(3F12.4,//)
        PUNCH 101,VXX,VYY,VZZ
        B=B+1.
        X=RX
        Y=RY
        Z=RZ
        VX=VXX
        VY=VYY
        VZ=VZZ
        GO TO 4
        END
15797.195 106257.19 59747.541 -.3010 1.9199 1.0475 631.35093
```

Fig. 43

Projected Position and Velocity Program

```
C  C  PROJECTED POSITION AND VELOCITY

POSITION AND VELOCITY COMPONENTS AT T= 1.0000

   14693.4090 113027.0500  63438.8700

         -.3118       1.8426       1.0041

POSITION AND VELOCITY COMPONENTS AT T= 2.0000

   13555.2520 119533.5600  66982.3800

         -.3202       1.7733        .9652

POSITION AND VELOCITY COMPONENTS AT T= 3.0000

   12390.1440 125803.2800  70393.1990

         -.3268       1.7108        .9302

POSITION AND VELOCITY COMPONENTS AT T= 4.0000

   11203.8160 131858.2800  73683.8680

         -.3320       1.6539        .8984

POSITION AND VELOCITY COMPONENTS AT T= 5.0000

   10000.7620 137717.1100  76864.9120

         -.3362       1.6017        .8693

POSITION AND VELOCITY COMPONENTS AT T= 6.0000

    8784.5643 143395.5600  79945.2750

         -.3394       1.5536        .8424

POSITION AND VELOCITY COMPONENTS AT T= 7.0000

    7558.1158 148907.2500  82932.6660

         -.3419       1.5090        .8176

POSITION AND VELOCITY COMPONENTS AT T= 8.0000

    6323.7722 154263.9600  85833.7390

         -.3438       1.4674        .7944
```

Fig. 43 (Continued)

```
C  C   ORBIT GEOMETRY FROM ANGULAR RATE DATA--HORRIGAN AND WALSH
       READ,DT12,DT13,TD1,TD2,TD3,EMU
       STD1=SQRT(TD1)
       STD2=SQRT(TD2)
       STD3=SQRT(TD3)
       Q=STD2*SIN(DT13)-STD3*SIN(DT12)+STD1*(SIN(DT12)-SIN(DT13))
       R=-(STD3-STD1)*COS(DT12)+(STD2-STD1)*COS(DT13)-(STD2-STD3)
       S=STD1*SIN(DT13-DT12)+STD3*SIN(DT12)-STD2*SIN(DT13)
       E=SQRT((R/S)**2+(Q/S)**2)
       T1=ATAN(R/Q)+3.1415927
       P=((EMU*((1.+E*COS(T1))**4))/(TD1**2))**.33333333
       A=P/ABS(1.-E**2)
       RDOT=E*SQRT(EMU/(A*ABS(1.-E**2)))*SIN(T1)
       R1=((EMU*P)**.25)/STD1
       T1=T1*57.2957795
       RTDOT=R1*TD1
       IF(A)1,1,2
   1   PUNCH 100
 100   FORMAT(28HTHE TRAJECTORY IS HYPERBOLIC,//)
       GO TO 3
   2   PUNCH 101
 101   FORMAT(26HTHE TRAJECTORY IS ELLIPTIC,//)
   3   PUNCH 1C2,E
 102   FORMAT(20HTHE ECCENTRICITY IS ,F7.4,//)
       PUNCH 103,A
 103   FORMAT(23HTHE SEMI-MAJOR AXIS IS ,F12.4,//)
       PUNCH 104,T1
 104   FORMAT(39HTHE TRUE ANOMALY AT ANGULAR FIX ONE IS ,F12.4,//)
       PUNCH 105,RDOT
 105   FORMAT(42HTHE RADIAL VELOCITY AT ANGULAR FIX ONE IS ,F12.4,//)
       PUNCH 106,RTDOT
 106   FORMAT(45HTHE TRANSVERSE VELOCITY AT ANGULAR FIX ONE IS,F12.4,//)
       PUNCH 107,R1
 107   FORMAT(42HTHE RADIAL DISTANCE AT ANGULAR FIX ONE IS ,F12.4,//)
       STOP
       END
.138862 .2271076 .000010214764 .0000059230245 .00000040938722 62750.717




THE TRAJECTORY IS ELLIPTIC

THE ECCENTRICITY IS    .9068

THE SEMI-MAJOR AXIS IS  104948.6000

THE TRUE ANOMALY AT ANGULAR FIX ONE IS   138.3645

THE RADIAL VELOCITY AT ANGULAR FIX ONE IS      1.1051

THE TRANSVERSE VELOCITY AT ANGULAR FIX ONE IS      .5911

THE RADIAL DISTANCE AT ANGULAR FIX ONE IS   57870.6980
```

Fig. 44

Orbit Determination Program Using Angular Rate Data

If a complete position fix is not available, the trajectory may be determined by knowledge of the angular position of the vehicle and three true anomaly rates (see Chapter VII). Figure 44 is a reproduction of a program which utilizes angular rate data. In this case, only the true anomaly rates and differences in true anomaly are known. The orbit geometry can, therefore, be determined; but not the inertial orientation. The program can be altered to provide this information if angular position data is available. The units of the input and output are nautical miles and NM/SEC.

Discussion

This chapter has been a discussion of some important aids to manual navigation. This, by no means, exhausts the list of possibilities. Total commitment to the development of manual navigation and guidance systems will bring forth many more new ideas. Flexibility and accuracy are the bywords for the future. Equipment must be designed with this in mind. Methods cannot be limited just because hardware is not available. It must be made available.

X. Conclusions and Recommendations

Introduction

This chapter completes the theoretical development of this report with general conclusions and recommendations for follow-on research. Many interesting possibilities remain to be examined and some of these topics are listed under "Recommendations." The "Conclusions" paragraph lists some of the important determinations resulting from research associated with this thesis.

Conclusions

The following conclusions are offered as the result of experience gained in preparing this report:

1. The ΔH method, a graphical method of obtaining eccentricity, is feasible for high eccentricity elliptical trajectories. A major drawback is the need for prior knowledge of the semimajor axis.

2. The numerical differentiation approach for computing the geometric elements is sensitive to measurement accuracy. But the method is simple, explicit, and entirely adequate if accurate values of range are available. The method appears to be especially well suited for near earth orbits.

3. Differential correction procedures are impractical unless a back-up computer is available. If such a

computer is provided, the differential correction method
should be exploited.

4. Position fixes can be obtained using straightforward
   procedures. The simultaneous measurement requirement,
   frequently cited as a major problem in obtaining a
   three-dimensional fix, can be resolved using procedures
   similar to those presently used in astronomy and
   celestial aircraft navigation. With position fixing
   capability, the astronaut possesses a powerful and
   flexible tool that can be used for:

   (a) orbit determination

   (b) cross-check of the primary navigation
        computer

   (c) manual guidance procedures (yet to be
        developed)

5. The orientation elements are much easier to obtain
   than the geometric elements. Two angular positions
   and knowledge of true anomaly at some point of the
   orbit are all that is required to completely define
   the orientation parameters.

6. Range can be determined optically with much better
   precision than previously thought. The accuracy
   of the Hamer method of measuring range (Chapter VIII)
   is far better than the semi-diameter method.

7. Manual navigation aids such as small mechanical
   calculators and back-up computers that can be

178

programmed in fligh. are practical necessities.

Recommendations for Follow-on Theses

The following areas are suggested as worthy endeavors for future research:

1. Further study of graphical methods for obtaining orbital parameters. Extend the ΔH method to hyperbolic trajectories. Study the behavior of the ΔH plots around an entire high-eccentricity ellipse (perigee to perigee). Examine other graphical solutions to the orbit determination problem.

2. Extended study of methods for determining range. The range measurement accuracy is considerably improved using the methods of Chapter VIII. However, if a suitable reference trajectory is not available, other range measurement procedures must be provided. Several alternate methods are discussed in Ref 4:223.

3. Continued study and development of orbit determination methods. Many of the classical orbit determination methods are simplified by the fact that the observer is on the spacecraft and not on the surface of the earth. Several excellent orbit determination schemes are suggested in Ref 20:683, Ref 13, and Ref 3:Ch 1. All of the published methods should be investigated. The goal should be to assemble new orbit computation methods using the good points of previous schemes.

Special attention should be given to methods that
require no direct measurement of distance (such as
the method of Chapter V$^\tau$I).

4. Error Analyses. A number of methods discussed in
   this thesis require comprehensive error analysis.
   For example, the Polaris fixing procedure must be
   investigated to see what corrections, if any, are
   required to compensate for the fact that Polaris
   deviates from the pole position. Other topics of
   the thesis require error analysis before final
   adoption as manual navigation procedures.

5. Back-up Computer Techniques. A small back-up computer
   will greatly enhance manual navigation capability.
   But the capability of such a computer can be easily
   wasted on needless iterative techniques. Several
   short programs were presented in this thesis. Other
   programs and procedures should be devised--the purpose
   being the most efficient use of a limited memory
   computer.

6. Application of Differential Correction. The differential
   correction equations are complex but extremely useful
   if a back-up computer is available. It appears that
   a navigation scheme incorporating redundant data could
   be constructed using the differential correction concept.
   The use of redundant data is desirable since the effect
   of measurement error is reduced considerably.

180

7. <u>Systematized</u> <u>Navigation</u> <u>Procedures</u>. After the suitability of a navigation scheme is established, the astronaut must be provided systematic procedures in flight manual form. The flight manual should consist of charts, worksheets, and operational procedures arranged to render the solution of the navigation problem to step-by-step form. Compilation of such a flight manual is suggested as a follow-on thesis project.

8. <u>Manual</u> <u>Guidance</u>. After the orbit is known, the astronaut must have the capability to determine what corrections are required to make the spacecraft go where he wants to go. The problem of a manual abort after translunar injection is of prime concern. At first glance, it appears the Gibbsian procedure (Chapter V) could be molded into an explicit guidance scheme. In any event, the guidance problem is complex and could well support several thesis topics.

XI. Concluding Remarks

As stated in Chapter I, the purpose of this thesis is to lay a foundation for the development of an operational manual navigation system. Several independent methods of obtaining the necessary orbital parameters have been presented. The combination of procedures selected for use in an operational system depends upon several factors, and most importantly upon the answers to the four questions posed in the Introduction (Chapter I:4). The authors believe that these questions should be answered as follows:

1. What computational tools are available?

> Answer - A hand-held, battery operated, computer capable of flexible operation, and a hand-held mechanical calculator for incidental computations.

2. What types of measurements are possible?

> Answer - Equipment and procedures will be made available to allow complete position fixing using star-body and range measurements.

3. How much time is allowable for the completion of the procedures?

> Answer - At least five hours for highly eccentric trajectories, and correspondingly less for lower eccentricity orbits.

4. What is the required accuracy?

> Answer - This depends upon the use to which the
> orbital parameters are put. Different
> requirements will exist for re-entry
> navigation and guidance than for mid-
> course navigation and guidance. The
> best accuracy attainable should be a
> goal, however, since the same manual
> system will probably be used throughout
> the mission.

If the above answers are acceptable, the manual navigation problem
is solved. An operational system consisting of position fixes input to
the Gibbs method of orbit determination programmed into a back-up
computer is, in the author's opinion, the most promising combination
devised to date. It is completely flexible; it involves no approxi-
mations or iterations; and it provides direct input to a manual guidance
system.

Bibliography

1. Apollo Mission Planning Task Force: Design Reference Mission II A: Mission Description. MSC Report No. PM3/M-171/66. Houston: National Aeronautics and Space Administration Manned Spacecraft Center, 1966.

2. Baker, R. M. L., and M. W. Makemson. An Introduction to Astrodynamics. New York: Academic Press Inc., 1967.

3. Baker, Robert M. L. Astrodynamics--Applications and Advanced Topics. New York: Academic Press Inc., 1967.

4. Battin, Richard H. Astronautical Guidance. New York: McGraw-Hill Book Co., 1964.

5. Bielkowicz, Peter. "Lecture Notes, Aerospace Trajectories, AE 6.60, AE 6.61." Wright-Patterson Air Force Base, Ohio: Air Force Institute of Technology, 1967.

6. Brouwer, D., and G. M. Clemence. Methods of Celestial Mechanics. New York: Academic Press Inc., 1961.

7. Gapcynski, J. P., and D. S. Woolston. Characteristics of Three Precision Circumlunar Trajectories for the Year 1968. NASA Technical Note D-1028. Washington: National Aeronautics and Space Administration, March 1962.

8. Hamer, H. A. Manual Procedures for Determining Position in Space from Onboard Optical Measurements. NASA Technical Note No. D-1852. Washington: National Aeronautics and Space Administration, 1964.

9. Havill, C. Dewey. An Emergency Midcourse Navigation Procedure for a Space Vehicle Returning from the Moon. NASA Technical Note No. D-1765. Washington: National Aeronautics and Space Administration, 1963.

10. Jorris, T. R., and A. E. Barth. "The USAF Manned Space Navigation Experiment on Apollo and its Implications on Advanced Manned Spacecraft." (Unpublished Paper.) Wright-Patterson Air Force Base, Ohio: Air Force Avionics Laboratory, 1967.

11. Martin Company. Orbital Flight Manual. Prepared for the George C. Marshall Space Flight Center, Washington, D. C., Office of Scientific and Technical Information, NASA, 1963.

12. Mills, J. G., and Robert M. Silva. Analytic Development of Optimum Astronaut Procedures for use of the Air Force Space Navigation System in the Manual Mode. Technical Report No. AFAL-TR-69-14. Wright-Patterson Air Force Base, Ohio: Air Force Avionics Laboratory, Research and Technology Division, 1969.

13. Nordvedt, Kenneth, Jr. A Theory of Manual Space Navigation. NASA Contractor Report No. 841. Washington: National Aeronautics and Space Administration, 1967.

14. Ragland, L. C. A Brief Error Study of an Onboard Backup Procedure for Orbit Determination. Unpublished Memo Redondo Beach, California: TRW Systems, 1966.

15. Raisz, Erwin J. General Cartography. New York: McGraw-Hill Book Co., 1948.

16. Scheid, F. Schaum's Outline of Theory and Problems of Numerical Analysis. New York: McGraw-Hill Book Co., 1968.

17. Schehr, Richard R., and Patrick J. Smith. Manual Astronaut Navigation: Apollo Mission Applications. Unpublished Thesis. Wright-Patterson Air Force Base, Ohio: Air Force Institute of Technology, June 1968.

18. Shchigolev, Boris M. Mathematical Analysis of Observations. Translated by Scripta Technica Inc., edited by H. Eagle. New York: American Elsevier Publishing Co., 1965.

19. Silva, Robert M., et al. The Air Force Space Navigation Experiment on Gemini (DOD/NASA Gemini Experiment D-9, Gemini IV and VII Flights). Technical Report No. AFAL-TR-66-289. Wright-Patterson Air Force Base, Ohio: Air Force Avionics Laboratory, Research and Technology Division, 1966.

20. Szebehely, Victor G. Progress in Astronautics and Aeronautics: Celestial Mechanics and Astrodynamics. New York: Academic Press Inc, 1964.

21. U. S. Naval Observatory. American Ephemeris and Nautical Almanac for the Year 1968. Washington: Government Printing Office, 1968.

22. Webber, A., et al. Space Position Fixing Techniques, Phase II. Technical Documentary Report No. AFAL-RTD-ITR-1. Wright-Patterson Air Force Base, Ohio: Air Force Avionics Laboratory, Research and Technology Division, 1967.

23. -----. Space Position Fixing Techniques, Phase IIIa. Technical
Report No. AFAL-TR-67-5. Wright-Patterson Air Force Base, Ohio:
Air Force Avionics Laboratory, Research and Technology Division,
1967.

24. Willers, F. A. Practical Analysis. New York: Dover Publica-
tions Inc., 1948.

Appendix A

The Computer Program

This Appendix consists of a reproduction of the double-precision computer program developed to investigate the Delta-H method of eccentricity determination and to provide accurate data for use throughout this thesis. A listing of the variables is included to aid the reader in following the logic involved.

List of Variables

EMU = (gravitational constant)$^{1/2}$

RPLAN = earth's radius in NM

AXSS = semimajor axis of ellipse in NM

AXI = (AXSS)$^{1.5}$

EN = mean motion

TAU = orbital period in hours

ETAU = number of 2.5 minute increments

ELC = eccentricity

TEE = time in seconds from perigee

ECAN = eccentric anomaly in radians

RAD1 = perigee radius

VEL = velocity magnitude in NM/SEC

ALT = altitude

EMAN = mean anomaly

RAD = radial distance

CONT = time in minutes from perigee

DELTA = $\Delta H1$

DELTB = $\Delta H2$

ECA = eccentric anomaly in degrees

VELO = ratio of velocity to perigee velocity

The program that follows generates data for high eccentricity ellipses with a five minute timing interval for $\Delta H1$ and $\Delta H2$. A portion of the resulting output is also included. Total running time on the IBM 7094 digital computer is approximately two minutes.

189

```
$ JOB            0,3,5000       68-514   WALSH,RC   AFIT-SE
$IBJOB
$IBFTC MAIN
C      GEOCENTRIC 5 MINUTE DELTA-H FOR HIGH ECCENTRICITY
       DOUBLE PRECISION ECAN,ALT,VEL,EMU,TAU,ECC,RAD1,RIGHT,CONT,
      1VELO,RPLAN,AXI,ETAU,EMAN,RAD,DELTA,ECA,AXSS,EN,TEE,ALEFT,DELTB
       DIMENSION ECAN(85),ALT(85),VEL(85)
       EMU=DSQRT(62750.717)
       RPLAN=3440.1728
       AXSS=105000.00
       DO 12 I=1,7
       AXI=DSQRT(AXSS*AXSS*AXSS)
       EN=EMU/AXI
       TAU=6.28318530/(EN*3600.)
       ETAU=210./2.5
       N=ETAU
       ECC=0.9068
       DO 11 J=1,7
       TEE=150.0
       WRITE(6,1)
1      FORMAT(1H1,9X,4HAXIS,13X,12HECCENTRICITY,7X,6HPERIOD,//)
       WRITE(6,2) AXSS,ECC,TAU
2      FORMAT(1X,3F17.4,//)
       ECAN(1)=0.
       RAD1=AXSS-AXSS*ECC
       VEL(1)=EMU*DSQRT((2./RAD1)-(1./AXSS))
       ALT(1)=RAD1-RPLAN
       DO 10 K=2,N
       EMAN=EN*TEE
       ECAN(K)=ECAN(K-1)
14     ALEFT=DSIN(ECAN(K))
       RIGHT=(1./ECC)*(ECAN(K)-EMAN)
       IF(ABS(ALEFT-RIGHT)-.0000001)6,6,9
9      ECAN(K)=ECAN(K)-(ALEFT-RIGHT)/(DCOS(ECAN(K))-1./ECC)
       GO TO 14
6      RAD=AXSS-AXSS*ECC*DCOS(ECAN(K))
       ALT(K)=RAD-RPLAN
       VEL(K)=EMU*DSQRT((2./RAD)-(1./AXSS))
10     TEE=TEE+150.0
       WRITE(6,3)
3      FORMAT(2X,4HTIME,5X,8HALTITUDE,5X,8HDELTA H1,5X,8HDELTA H2,3X,
      111HECC ANOMALY,7X,4HV/VP,//)
       M=N-4
       CONT=0.0
       DO 13 L=1,M
       DELTA=ALT(L)-ALT(L+2)
       DELTB=ALT(L+2)-ALT(L+4)
       ECA=ECAN(L)*57.2957795D0
       VELO=VEL(L)/VEL(1)
       WRITE(6,4) CONT,ALT(L),DELTA,DELTB,ECA,VELO
4      FORMAT(F6.1,5F13.3)
13     CONT=CONT+2.5
11     ECC=ECC+0.01
12     AXSS=AXSS+1000.00
30     STOP
       END
$EOF
```

190

	AXIS	ECCENTRICITY		PERIOD	
	105000.0000	0.9068		237.0566	
TIME	ALTITUDE	DELTA H1	DELTA H2	ECC ANOMOLY	V/VP
0.	6345.827	-26.688	-79.475	0.	1.000
2.5	6352.508	-53.228	-105.291	0.679	1.000
5.0	6372.515	-79.475	-130.547	1.357	0.999
7.5	6405.737	-105.291	-155.128	2.033	0.997
10.0	6451.991	-130.547	-178.933	2.703	0.994
12.5	6511.028	-155.128	-201.875	3.375	0.991
15.0	6582.538	-178.933	-223.884	4.041	0.988
17.5	6666.156	-201.875	-244.906	4.701	0.983
20.0	6761.471	-223.884	-264.902	5.356	0.978
22.5	6868.031	-244.906	-283.850	6.004	0.973
25.0	6985.355	-264.902	-301.739	6.644	0.967
27.5	7112.937	-283.850	-318.570	7.278	0.961
30.0	7250.257	-301.739	-334.355	7.903	0.955
32.5	7396.787	-318.570	-349.115	8.521	0.948
35.0	7551.996	-334.355	-362.878	9.130	0.941
37.5	7715.356	-349.115	-375.677	9.730	0.933
40.0	7886.350	-362.878	-387.550	10.321	0.926
42.5	8064.471	-375.677	-398.539	10.903	0.918
45.0	8249.228	-387.550	-408.686	11.476	0.911
47.5	8440.148	-398.539	-418.035	12.039	0.903
50.0	8636.778	-408.686	-426.630	12.594	0.895
52.5	8838.687	-418.035	-434.517	13.140	0.887
55.0	9045.464	-426.630	-441.737	13.676	0.879
57.5	9256.722	-434.517	-448.334	14.204	0.872
60.0	9472.094	-441.737	-454.347	14.723	0.864
62.5	9691.239	-448.334	-459.816	15.233	0.856
65.0	9913.832	-454.347	-464.778	15.735	0.848
67.5	10139.572	-459.816	-469.268	16.228	0.841
70.0	10368.178	-464.778	-473.320	16.714	0.833
72.5	10599.388	-469.268	-476.964	17.191	0.826
75.0	10832.956	-473.320	-480.231	17.660	0.819
77.5	11068.656	-476.964	-483.148	18.122	0.812
80.0	11306.276	-480.231	-485.740	18.576	0.804
82.5	11545.620	-483.148	-488.032	19.023	0.798
85.0	11786.507	-485.740	-490.045	19.463	0.791
87.5	12028.767	-488.032	-491.802	19.896	0.784
90.0	12272.246	-490.045	-493.321	20.322	0.777
92.5	12516.799	-491.802	-494.620	20.741	0.771
95.0	12762.292	-493.321	-495.715	21.155	0.765
97.5	13008.601	-494.620	-496.622	21.562	0.758
100.0	13255.613	-495.715	-497.356	21.962	0.752

Appendix B

Derivation of Equations for Geometric Elements Using $\dot{\bar{r}}$ and $\ddot{\bar{r}}$

The following notation is used in the derivation:

$\bar{r}$ = vehicle position vector

x, y, z = coordinates of vehicle

$r = |\bar{r}|$

$\dot{r}$ = radial velocity

$\ddot{r}$ = radial acceleration

$\hat{i}, \hat{j}, \hat{k}$ = unit vectors in x, y, z directions

μ = earth gravitational constant

$\dot{S} = |\dot{\bar{r}}|$ = magnitude of vehicle velocity

a = semimajor axis

E = eccentric anomaly

e = eccentricity

θ = true anomaly

ℓ = semilatus rectum

h = angular momentum

192

Starting with

$$r^2 = x^2 + y^2 + z^2 \qquad (B-1)$$

and differentiating with respect to time obtain

$$r\dot{r} = x\dot{x} + y\dot{y} + z\dot{z} \qquad (B-2)$$

Taking the derivative of $r\dot{r}$ leads to

$$\dot{r}^2 + r\ddot{r} = (x\ddot{x} + y\ddot{y} + z\ddot{z}) + (\dot{x}^2 + \dot{y}^2 + \dot{z}^2) \qquad (B-3)$$

Now $\dot{x}^2 + \dot{y}^2 + \dot{z}^2 = \dot{S}^2$ and

$$\ddot{x} = -\mu r/r^3 \ , \quad \ddot{y} = -\mu y/r^3 \ , \quad \ddot{z} = -\mu z/r^3 \qquad (B-4)$$

then

$$\dot{r}^2 + r\ddot{r} = \dot{S}^2 - \left[\frac{x^2\mu}{r^3} + \frac{y^2\mu}{r^3} + \frac{z^2\mu}{r^3} \right]$$

$$= \dot{S}^2 - \frac{\mu}{r^3}(x^2 + y^2 + z^2)$$

$$= \dot{S}^2 - \frac{\mu}{r} \qquad (B-5)$$

From the energy equation

$$\dot{S}^2 = \mu\left[\frac{2}{r} - \frac{1}{a} \right] \qquad (B-6)$$

$$\dot{r}^2 + r\ddot{r} = \frac{2\mu}{r} - \frac{\mu}{a} - \frac{\mu}{r} \qquad (B-7)$$

$$\dot{r}^2 + r\ddot{r} = \frac{\mu}{r} - \frac{\mu}{a} \qquad (B-8)$$

Therefore

$$a = \frac{\mu}{\frac{\mu}{r} - \dot{r}^2 - \_\ddot{r}} \tag{B-9}$$

a relatively simple expression for the semimajor axis a.

Two more expressions are required to obtain the eccentricity and eccentric anomaly. The first expression is the equation of the conic section

$$r = a (1 - e \cos E) \tag{B-10}$$

from which

$$e \cos E = 1 - \frac{r}{a} \tag{B-11}$$

The second expression is derived from the conic section equation involving the true anomaly θ

$$r = \frac{\ell}{1 + e \cos \theta} \tag{B-12}$$

where ℓ is the semilatus rectum.

The first derivative yields $\dot{r}$

$$\dot{r} = \frac{\ell e (\sin \theta) \dot{\theta}}{(1 + e \cos \theta)^2} \tag{B-13}$$

194

then multiplying and dividing by ℓ

$$\dot{r} = \frac{\ell^2 e (\sin \theta) \dot{\theta}}{\ell (1 + e \cos \theta)^2} = \frac{r^2 \dot{\theta} e \sin \theta}{\ell} \qquad \text{(B-14)}$$

However, $r^2 \dot{\theta}$ is the angular momentum per unit mass, i.e.,

$$h = r^2 \dot{\theta} = \sqrt{\mu \ell} \qquad \text{(B-15)}$$

so

$$\dot{r} = \frac{\sqrt{\mu \ell} e \sin \theta}{\ell} = \sqrt{\frac{\mu}{\ell}} e \sin \theta \qquad \text{(B-16)}$$

from which

$$\sin \theta = \frac{\dot{r} \sqrt{\frac{\ell}{\mu}}}{e} \qquad \text{(B-17)}$$

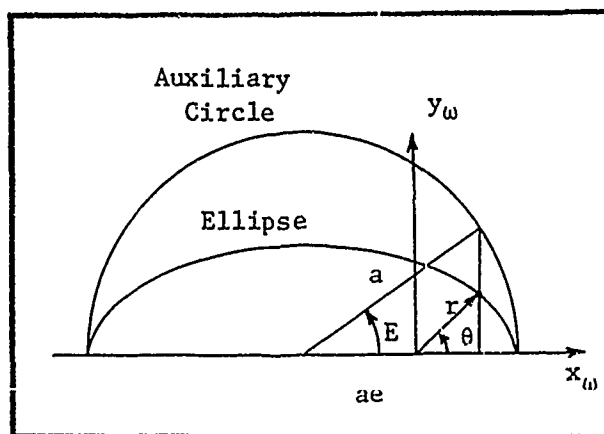The orbit plane coordinate system is shown in Fig. 45. In this

Fig. 45

Orbit Plane Coordinate System

coordinate system

$$y_\omega = r \sin \theta = \frac{r \, \dot{r} \sqrt{\frac{\ell}{\mu}}}{e} \qquad \text{(B-18)}$$

and als,

$$y_\omega = a \sqrt{1 - e^2} \sin E \qquad \text{(B-19)}$$

then

$$a \sqrt{1 - e^2} \sin E = \frac{r \, \dot{r} \sqrt{\frac{\ell}{\mu}}}{e} \qquad \text{(B-20)}$$

For an ellipse, $\ell = a(1 - e^2)$, therefore

$$a \sqrt{1 - e^2} \sin E = \frac{r \, \dot{r} \sqrt{a} \sqrt{1 - e^2}}{e \sqrt{\mu}} \qquad \text{(B-21)}$$

then

$$e \sin E = \frac{r \, \dot{r}}{\sqrt{\mu a}} \qquad \text{(B-22)}$$

The two equations for e and E are

$$e \sin E = \frac{r \, \dot{r}}{\sqrt{\mu a}} \qquad \text{(B-23)}$$

$$e \cos E = 1 - \frac{r}{a} \qquad \text{(B-24)}$$

Dividing

$$\tan E = \frac{r \, \dot{r} \sqrt{a}}{\sqrt{\mu} \, (a - r)} \qquad \text{(B-25)}$$

196

from which E can be determined. Note that if $\dot{r}$ is positive, the radial velocity is away from the focus and E is less than 180°. Knowing E, the eccentricity may be determined from either Eq (B-23) or (B-24).

The expression for $\cos \theta$ for the parabolic case is easily derived. Since the total velocity can be determined, i.e.,

$$\dot{S}^2 = \frac{\mu}{r} + \dot{r}^2 + r\ddot{r} \tag{B-26}$$

and the radial velocity $\dot{r}$ is known, the transversal velocity $r\dot{\theta}$ must be

$$(r\dot{\theta})^2 = \dot{S}^2 - \dot{r}^2 = \frac{\mu}{r} + r\ddot{r} \tag{B-27}$$

The angular momentum h is then

$$h = r(r\dot{\theta}) = r\sqrt{\frac{\mu}{r} + r\ddot{r}} \tag{B-28}$$

$$h^2 = r\mu + r^3\ddot{r} \tag{B-29}$$

Since $h^2 = \mu\ell$

$$\ell = r + \frac{r^3\ddot{r}}{\mu} \tag{B-30}$$

The general equation of the parabola

$$r = \frac{\ell}{1 + \cos\theta} \tag{B-31}$$

yields

$$\cos \theta = \frac{\ell}{r} - 1 \qquad \text{(B-32)}$$

and substituting the expression for ℓ

$$\cos \theta = \frac{r^2 \ddot{r}}{\mu} \qquad \text{(B-33)}$$

Appendix C

The Error Involved in Functions
of Several Variables

Suppose that $U = f(x,y)$ is a continuously differentiable function on some set of values of the arguments x and y. Suppose x and y are replaced by their approximate values a and b. Then the approximate value of the function is

$$u = f(a,b) \tag{C-1}$$

Let Δ_a and Δ_b be the errors in the arguments, i.e.,

$$A = a + \Delta_a \quad , \quad B = b + \Delta_b \tag{C-2}$$

where A and B are the exact values of the arguments. The exact value of the function is then

$$U = f(a + \Delta_a \quad , \quad b + \Delta_b) \tag{C-3}$$

Using Taylor's theorem for functions of two variables

$$U = f(a,b) + \Delta_a \left[\frac{\partial f}{\partial x}\right]_{\substack{x=a \\ y=b}} + \Delta_b \left[\frac{\partial f}{\partial y}\right]_{\substack{x=a \\ y=b}}$$

$$+ \frac{1}{2!} \left[\Delta_a \frac{\partial}{\partial x} + \Delta_b \frac{\partial}{\partial y}\right]^2 f(x,y)_{\substack{x=a \\ y=b}} + \ldots \tag{C-4}$$

Assuming the errors are small and dropping the terms containing squares of errors

$$\Delta_u = U - f(a,b) = \left[\frac{\partial f}{\partial x}\right]_{\substack{x=a \\ y=b}} \Delta_a + \left[\frac{\partial f}{\partial y}\right]_{\substack{x=a \\ y=b}} \Delta_b \qquad (C-5)$$

where Δ_u represents an approximate value of the error (since only the first two terms of the expansion were retained). Then

$$|\Delta_u| \leq \left|\frac{\partial f}{\partial x}\right|_{\substack{x=a \\ y=b}} |\Delta_a| + \left|\frac{\partial f}{\partial y}\right|_{\substack{x=a \\ y=b}} |\Delta_b| \qquad (C-6)$$

Now let E_u, E_a, and E_b be the maximum absolute values of error. Then

$$E_u = \left|\frac{\partial f}{\partial x}\right|_{\substack{x=a \\ y=b}} E_a + \left|\frac{\partial f}{\partial y}\right|_{\substack{x=a \\ y=b}} E_b \qquad (C-7)$$

Given the maximum errors of the arguments of a function, the maximum error in the value of the function can be obtained. If E_a and E_b are unknown, the conditions necessary to minimize the total error can still be obtained by examining the partial derivatives $\partial f/\partial x$ and $\partial f/\partial y$. The derivation can be extended to functions of more than two variables with analogous results. This derivation and further supporting material may be found in Ref 20:34.

200

Appendix D

Derivation of Equations for True Anomaly Determination

Figure 46, an illustration of the vehicle's path across the celestial sphere, will be used in the derivation to follow.
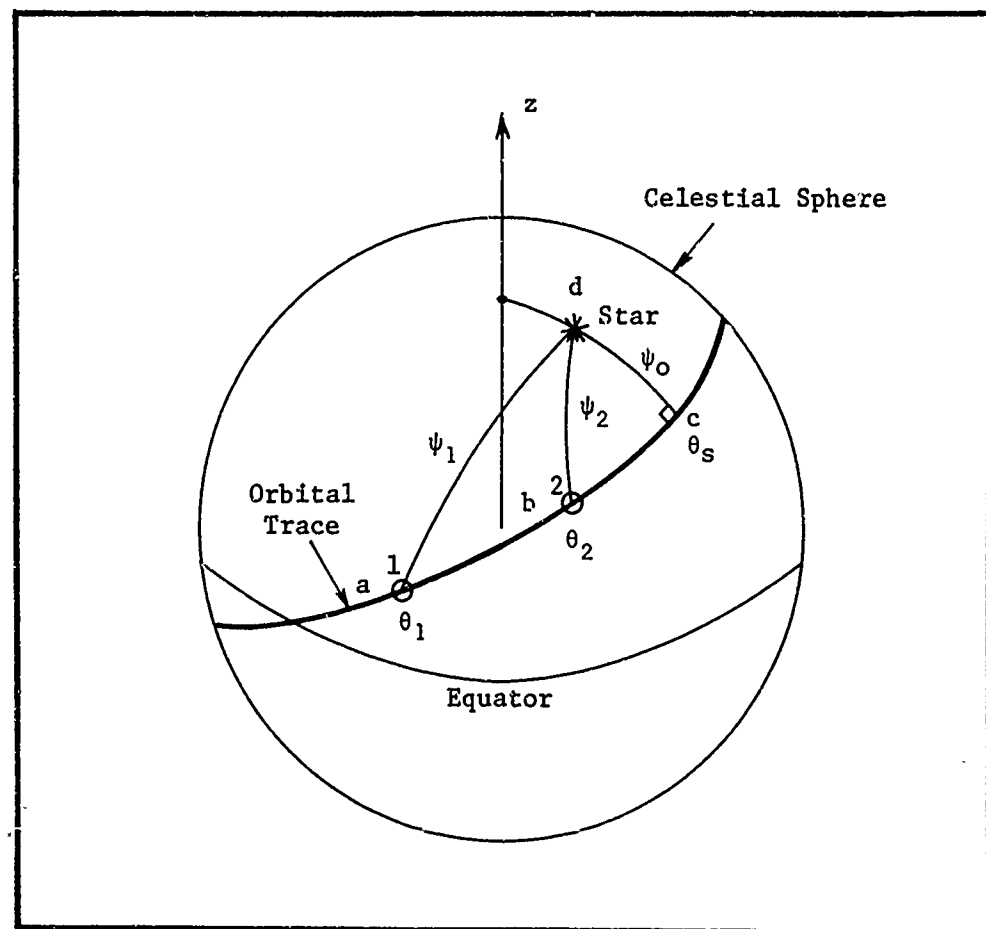

Fig. 46

Vehicle Path on Celestial Sphere

From the spherical triangles bcd and acd

$$\cos \psi_2 = \cos \psi_0 \cos (\Delta\theta_s)* \qquad \text{(D-1)}$$

$$\cos \psi_1 = \cos \psi_0 \cos (\Delta\theta + \Delta\theta_s)* \qquad \text{(D-2)}$$

where $\Delta\theta_s = \theta_s - \theta_2$ and $\Delta\theta = \theta_2 - \theta_1$.

Dividing the above equations yields

$$\frac{\cos \psi_1}{\cos \psi_2} = \frac{\cos (\Delta\theta_s + \Delta\theta)}{\cos \Delta\theta_s} \qquad \text{(D-3)}$$

which reduces to

$$\tan \Delta\theta_s = \cot \Delta\theta - \cos \psi_1 \sec \psi_2 \csc \Delta\theta \qquad \text{(D-4)}$$

The angles ψ_1 and ψ_2 can be obtained by direct measurement or by the vector dot products

$$\hat{I} \cdot \hat{r}_1 = \cos \psi_1$$

$$\hat{I} \cdot \hat{r}_2 = \cos \psi_2 \qquad \text{(D-5)}$$

In polar coordinates, the dot products become

$$\cos \psi_1 = \cos \delta_1 \cos \delta_s \cos (\alpha_1 - \alpha_s) + \sin \delta_1 \sin \delta_s$$

$$\cos \psi_2 = \cos \delta_2 \cos \delta_s \cos (\alpha_2 - \alpha_s) + \sin \delta_2 \sin \delta_s \qquad \text{(D-6)}$$

* ψ_0 is termed "minimum coaltitude" in Ref 17:46.

202

By direct measurement, the angles ψ_1 and ψ_2 can be determined from

$$\psi = 180° - (\gamma_s + A/2) \qquad \text{(D-7)}$$

as can be seen from Fig. 26.

The angle $\Delta\theta$ represents the true anomaly difference between $\hat{r}_1$ and $\hat{r}_2$. The vector dot product yields

$$\cos \Delta\theta = r_{x1} \, r_{x2} + r_{y1} \, r_{y2} + r_{z1} \, r_{z2} \qquad \text{(D-8)}$$

or

$$\cos \Delta\theta = \cos \delta_1 \cos \delta_2 \cos (\alpha_2 - \alpha_1) + \sin \delta_1 \sin \delta_2 \qquad \text{(D-9)}$$

All of the quantities appearing in Eq (D-4) can therefore be evaluated and $\Delta\theta_s$ can be determined. With $\Delta\theta_s$ known for one position, the angle ψ_0 can be calculated from

$$\cos \psi_0 = \frac{\cos \psi_2}{\cos \Delta\theta_s} \qquad 0 \leq \psi_0 \leq 90° \qquad \text{(D-10)}$$

and this angle remains constant. Then for any subsequent measurement using the same star

$$\cos \Delta\theta_s = \frac{\cos \psi}{\cos \psi_0} = \frac{- \cos (\gamma_s + A/2)}{\cos \psi_0} \qquad \text{(D-11)}$$

Appendix E

Equations for Calculating E, F, and k

This Appendix gives the equations for calculating E, F, and k for use in the Hamer method of range determination.

The angles E and F (see Fig. 47), as well as the value k, pertaining to a reference trajectory can be pre-calculated for any given star with known direction cosines ℓ, m, and n.
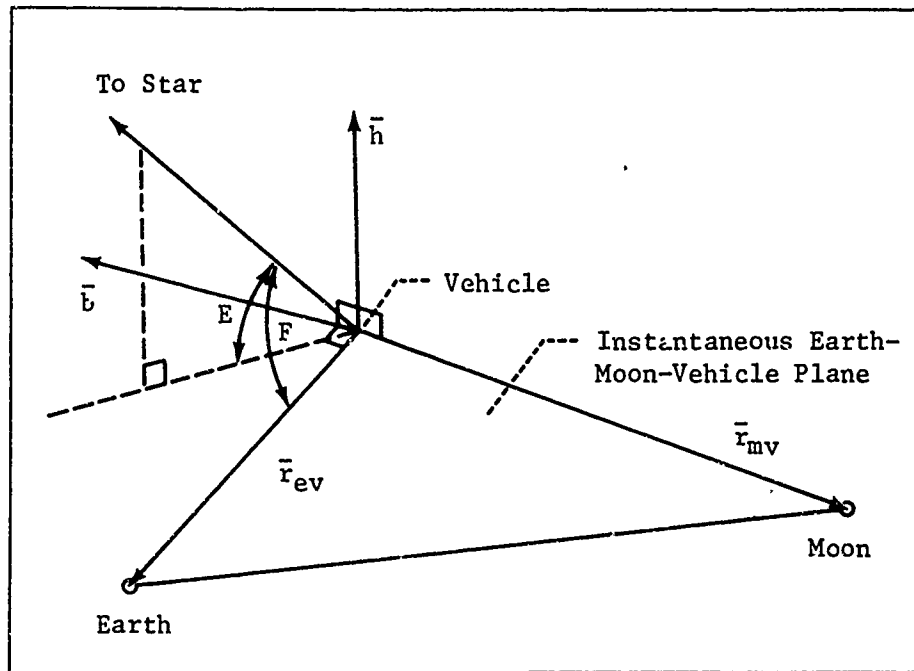

Fig. 47

Illustration Showing Vectors
$\bar{b}$ and $\bar{h}$ (From Ref 8:23)

The angle F, which is the angle measured from the vehicle between the lines-of-sight to a star and a body center (earth, for example), is obtained from the dot product of the position vectors of the earth center and star so that

$$\cos F = \frac{\ell\, x_{ev} + m\, y_{ev} + n\, z_{ev}}{r_{ev}} \qquad (0° \leq F \leq 180°) \qquad (E\text{-}1)$$

By defining a vector $\bar{h}$ perpendicular to the instantaneous earth-moon-vehicle plane, the angle E, which is the angle between the line-of-

205

sight to a star and its projection in this plane, is obtained from the

dot product of the vector $\bar{h}$ and the unit position vector of the star

giving

$$\sin E = \left| \frac{\ell\, h_x + m\, h_y + n\, h_z}{h} \right| \qquad \text{(E-2)}$$

where the absolute value can be used such that $0° \le E \le 90°$ and where

the values for h_x, h_y, and h_z are obtained from the cross product of

the position vectors of the earth and moon centers. Thus,

$$h_x = y_{ev}\, z_{mv} - z_{ev}\, y_{mv}$$

$$h_y = z_{ev}\, x_{mv} - x_{ev}\, z_{mv}$$

$$h_z = x_{ev}\, y_{mv} - y_{ev}\, x_{mv} \qquad \text{(E-3)}$$

and

$$h = (h_x{}^2 + h_y{}^2 + h_z{}^2)^{1/2} \qquad \text{(E-4)}$$

The sign of the quantity k in Eq (8-19) is determined by the

position of the star with respect to the earth-vehicle line, r_{ev}.

The sign is positive (negative) if, as viewed from the direction of

$\bar{h}$, the projection of the line to the star in the instantaneous

earth-moon-vehicle plane is to the right (left) of the earth-vehicle

line. As shown in Fig. 47, the relative directions of these two

lines at a given time along a reference trajectory can be determined

by first defining a vector $\bar{b}$ which is perpendicular to the plane

containing the vectors $\bar{r}_{ev}$ and $\bar{h}$.

The vector $\bar{b}$ is obtained from the cross product of the vectors $\bar{r}_{ev}$ and $\bar{h}$ such that the components of $\bar{b}$ are given by

$$b_x = y_{ev} h_z - z_{ev} h_y$$

$$b_y = z_{ev} h_x - x_{ev} h_z$$

$$b_z = x_{ev} h_y - y_{ev} h_x \tag{E-5}$$

where the values of h_x, h_y, and h_z are given in Eq (E-3). Next, the dot product of the unit position vector of the star and the vector $\bar{b}$ will yield the component of the star vector along the vector $\bar{b}$ which is given by the term $(\ell b_x + m b_y + n b_z)/b$. If this term is positive, the projection of the unit star vector in the instantaneous earth-moon-vehicle plane is to the right of the earth-vehicle line so that the quantity k is given as

$$k = \frac{\ell b_x + m b_y + n b_z}{\left| \ell b_x + m b_y + n b_z \right|} \tag{E-6}$$

The quantity k is, of course, always either plus or minus one.

VITA

Roger Charles Horrigan was born ████████████ in ███████████, ██████. He graduated from Brooklyn High School, Brooklyn, Iowa in 1953 and entered Iowa State University where he majored in Mechanical Engineering. After graduating with a Bachelor of Science degree in 1957, he was employed by General Telephone Laboratories, Chicago, Illinois, before entering the United States Air Force in 1958. After completing pilot training, he was assigned to B-47 aircraft at Lake Charles, Louisiana. Before coming to the Air Force Institute of Technology, he served as an Aircraft Commander in B-52 aircraft at Ellsworth Air Force Base, South Dakota. He is a member of the following societies: Phi Eta Sigma, Pi Tau Sigma, Phi Kappa Phi, and Tau Beta Pi.

       Permanent address: ███████ ██████████████

This thesis was typed by Mrs. Mary E. Mahaffey

VITA

Richard C. Walsh was born on ███████████ in ██████████ ████████ He graduated from Lowrey High School, Dearborn, Michigan in 1959 and entered the Detroit Institute of Technology where he majored in Electrical Engineering until June 1960, when he entered the United States Air Force Academy, at Colorado Springs, Colorado. He graduated with a Bachelor of Science degree in International Affairs in June 1964. He was stationed at Williams Air Force Base, Arizona from that time until his entry into the Air Force Institute of Technology. He served as Executive Officer of the 3525th Organizational Maintenance Squadron while at Williams Air Force Base. He is a member of Tau Beta Pi.

Permanent address: ████████████ ████████████

This thesis was typed by Mrs. Mary E. Mahaffey

DOCUMENT CONTROL DATA - R&D

(Security classification of title, body of abstract and indexing annotation must be entered when the overall report is classified)

1. ORIGINATING ACTIVITY (Corporate author)	2a. REPORT SECURITY CLASSIFICATION
Air Force Institute of Technology Wright-Patterson Air Force Base, Ohio, 45433	Unclassified
	2b GROUP

3. REPORT TITLE

Manual Astronaut Navigation

4. DESCRIPTIVE NOTES (Type of report and inclusive dates)

AFIT Thesis

5. AUTHOR(S) (Last name, first name, initial)

Roger C. Horrigan and Richard C. Walsh
Major USAF Captain USAF

6. REPORT DATE	7a. TOTAL NO. OF PAGES	7b. NO. OF REFS
June 1969	229	24

8a. CONTRACT OR GRANT NO.	9a. ORIGINATOR'S REPORT NUMBER(S)
b. PROJECT NO.	GA/AE/69-1
c. N/A	9b. OTHER REPORT NO(S) (Any other numbers that may be assigned this report)
d.	

10. AVAILABILITY/LIMITATION NOTICES This document is subject to special export controls and each transmittal to foreign governments or foreign nationals may be made only with prior approval of the Dean of Engineering, Air Force Institute of Technology (AFIT-SE), Wright-Patterson Air Force Base, Ohio, 45433.

11. SUPPLEMENTARY NOTES	12. SPONSORING MILITARY ACTIVITY

13. ABSTRACT

This report presents selected methods, procedures, and equipment that form a basis for the development of a flexible manual space navigation system. These include a graphical method of eccentricity determination, geometric element determination by numerical differentiation of range measurements, differential correction of orbital elements, manual position fix, orientation elements determination, improved optical ranging, and the possible uses of back-up inertial platforms, hand-held mechanical calculators, and hand-held, battery operated, computers. Numerical examples and error analyses are also presented.

14.		LINK A		LINK B		LINK C	
	KEY WORDS	ROLE	WT	ROLE	WT	ROLE	WT
Manual Space Navigation							
Space Navigation							
Orbit Determination							
Manual Orbit Determination							

INSTRUCTIONS

1. ORIGINATING ACTIVITY: Enter the name and address of the contractor, subcontractor, grantee, Department of Defense activity or other organization (*corporate author*) issuing the report.

2a. REPORT SECURITY CLASSIFICATION: Enter the overall security classification of the report. Indicate whether "Restricted Data" is included. Marking is to be in accordance with appropriate security regulations.

2b. GROUP: Automatic downgrading is specified in DoD Directive 5200.10 and Armed Forces Industrial Manual. Enter the group number. Also, when applicable, show that optional markings have been used for Group 3 and Group 4 as authorized.

3. REPORT TITLE: Enter the complete report title in all capital letters. Titles in all cases should be unclassified. If a meaningful title cannot be selected without classification, show title classification in all capitals in parenthesis immediately following the title.

4. DESCRIPTIVE NOTES: If appropriate, enter the type of report, e.g., interim, progress, summary, annual, or final. Give the inclusive dates when a specific reporting period is covered.

5. AUTHOR(S): Enter the name(s) of author(s) as shown on or in the report. Enter last name, first name, middle initial. If military, show rank and branch of service. The name of the principal author is an absolute minimum requirement.

6. REPORT DATE: Enter the date of the report as day, month, year; or month, year. If more than one date appears on the report, use date of publication.

7a. TOTAL NUMBER OF PAGES: The total page count should follow normal pagination procedures, i.e., enter the number of pages containing information.

7b. NUMBER OF REFERENCES: Enter the total number of references cited in the report.

8a. CONTRACT OR GRANT NUMBER: If appropriate, enter the applicable number of the contract or grant under which the report was written.

8b, 8c, & 8d. PROJECT NUMBER: Enter the appropriate military department identification, such as project number, subproject number, system numbers, task number, etc.

9a. ORIGINATOR'S REPORT NUMBER(S): Enter the official report number by which the document will be identified and controlled by the originating activity. This number must be unique to this report.

9b. OTHER REPORT NUMBER(S): If the report has been assigned any other report numbers (*either by the originator or by the sponsor*), also enter this number(s).

10. AVAILABILITY/LIMITATION NOTICES: Enter any limitations on further dissemination of the report, other than those imposed by security classification, using standard statements such as:

(1) "Qualified requesters may obtain copies of this report from DDC."

(2) "Foreign announcement and dissemination of this report by DDC is not authorized."

(3) "U. S. Government agencies may obtain copies of this report directly from DDC. Other qualified DDC users shall request through

_____ ."

(4) "U. S. military agencies may obtain copies of this report directly from DDC. Other qualified users shall request through

_____ ."

(5) "All distribution of this report is controlled. Qualified DDC users shall request through

_____ ."

If the report has been furnished to the Office of Technical Services, Department of Commerce, for sale to the public, indicate this fact and enter the price, if known.

11. SUPPLEMENTARY NOTES: Use for additional explanatory notes.

12. SPONSORING MILITARY ACTIVITY: Enter the name of the departmental project office or laboratory sponsoring (*paying for*) the research and development. Include address.

13. ABSTRACT: Enter an abstract giving a brief and factual summary of the document indicative of the report, even though it may also appear elsewhere in the body of the technical report. If additional space is required, a continuation sheet shall be attached.

It is highly desirable that the abstract of classified reports be unclassified. Each paragraph of the abstract shall end with an indication of the military security classification of the information in the paragraph, represented as (TS), (S), (C), or (U)

There is no limitation on the length of the abstract. However, the suggested length is from 150 to 225 words.

14. KEY WORDS: Key words are technically meaningful terms or short phrases that characterize a report and may be used as index entries for cataloging the report. Key words must be selected so that no security classification is required. Identifiers, such as equipment model designation, trade name, military project code name, geographic location, may be used as key words but will be followed by an indication of technical context. The assignment of links, rules, and weights is optional.

AFLC–WPAFB–OCT 66 6M